Molecular Analysis of Proteins Involved in Certain Eye Diseases

Thesis submitted for the degree of

DOCTOR OF PHILOSOPHY

To

THE DEPARTMENT OF BIOCHEMISTRY
SCHOOL OF LIFE SCIENCES
UNIVERSITY OF HYDERABAD
HYDERABAD – 500 046
INDIA

By

Venu Talla

Hyderabad Eye Research Foundation
L. V. Prasad Eye Institute
Hyderabad – 500 034

April 2008

Enrolment No: 02LBPH03

Dedicated to beloved Balu sir and my parents

UNIVERSITY OF HYDERABAD

School of Life Sciences

Department of Biochemistry

Hyderabad - 500 046 (India)

DECLARATION

The research work embodied in this thesis entitled, "**Molecular Analysis of Proteins Involved in Certain Eye Diseases**", has been carried out by me at the L. V. Prasad Eye Institute, Hyderabad, under the guidance of Prof. D. Balasubramanian and Prof. T. Suryanarayana. I hereby declare that this work is original and has not been submitted in part or full for any other degree or diploma of any other university.

Venu Talla

Prof. D. Balasubramanian
Supervisor
Director, Research
L. V. Prasad Eye Institute
Hyderabad

Prof. T. Suryanarayana
Co-supervisor
Dept. Biochemistry
School of Life Sciences
University of Hyderabad

UNIVERSITY OF HYDERABAD

School of Life Sciences

Department of Biochemistry

Hyderabad - 500 046 (India)

CERTIFICATE

This is to certify that this thesis entitled, "**Molecular Analysis of Proteins Involved in Certain Eye Diseases**", submitted by **Venu Talla** for the degree of **Doctor of Philosophy** to the University of Hyderabad is based on the work carried out by him at the L. V. Prasad Eye Institute, Hyderabad, under our supervision. This work has not been submitted for any diploma or degree of any other University or Institution.

Prof. D. Balasubramanian
Supervisor
Director, Research
L. V. Prasad Eye Institute
Hyderabad

Prof. T. Suryanarayana
Co-supervisor
Department of Biochemistry
School of Life Sciences
University of Hyderabad

ACKNOWLEDGEMENTS

I'm very much indebted to my mentor **Prof. Dorairajan Balasubramanian** for guiding me for PhD, and words cannot express my gratitude to him. He has been a constant source of inspiration through out my PhD and life. He gave me the independence in work and think on my own which provoked the scientific instinct and more importantly self-confidence. I thank him for providing me constant encouragement and continued support.

I would like to thank **Prof. T. Suryanarayana,** University of Hyderabad, for having agreed to be my co-supervisor.

I am thankful to **Dr. G. N. Rao**, Chairman, L. V. Prasad Eye Institute, for his encouragement, support and providing the necessary infrastructure and a congenial research atmosphere. I thank all research faculty LVPEI who have constantly encouraged and supported me through out my PhD.

I specially thank **Prof. N. Srinivasan** from IISc, for helping me in doing the homology modeling of the proteins. I am thankful to **Dr. Yogendra Sharma** for his suggestions and co-operation for measurement of CD spectra. I also thank **Drs. Ch. Mohan Rao** and **Prof. Ghanshyam Swaroop** for their valuable advices and suggestions.

I thank my seniors **Dr. Geetha Thiagarajan** and **Dr. Bindu Madhava Reddy** who taught me so many things in the lab and helped in establishing myself in the lab.

Thanks to my friend **Rajeshwari** who has always been with me to share the happiest and sorrowful moments through out my PhD. Special thanks to my Friends from LVPEI and University of Hyderabad and all LVPEI members who made my stay at LVPEI successfull.

The financial assistance from the Council for Scientific and Industrial Research (CSIR, India) is gratefully acknowledged.

My parents and my Uncle have always been my source of strength. I thank them for showing me the way and hope to reach the heights that make them proud parents.

-Venu

ABBREVIATIONS

λ:	Wavelength of light , in nm
µM:	Micromolar
µm:	Micrometer
εM:	Molar extinction coefficient
µs:	Microsecond
$^1O_2$:	Singlet oxygen
ABTS:	Azinobis-(3-ethylbenzothiazoline)-6-sulfonic acid
AGE:	Advanced glycation end products
AHBG:	4-(2-amino 3-hydroxyphenly)-4- oxobutanoic acid o-β-D-glucoside
ANS:	8-anilinonapthalene 1-sulfonic acid
AREDS:	Age-related Eye Disease study
BPTI:	Bovine pancreatic trypsin inhibitor
CA:	Catechin
CCRG:	Co-operative Cataract Research Group
CD:	Circular Dichroism
cDNA:	Complementary DNA
cM:	centimorgan
DAPI:	4’-6-Diamino modified eagle’s medium
DEAE:	Diethylaminoethyl
DMEM:	Dulbecco’s modified eagle’s medium
DNase I:	Deoxyribonuclease I
DTT:	Dithiothreitol
EDTA:	Ethylene diamine tetra acetic acid
EGCG:	Epigallocatechin gallate

EGFP:	Enhanced green fluorescence protein
FCS:	Fetal calf serum
GBE:	*Gingko biloba extract*
GPx:	Glutathione peroxidase
GR:	Glutathione Reductase
GSH:	Glutathione
HEPES:	N-(2-hydroxyethyl)piperazine-N'-(2-ethanesulfonic acid)
HGQ:	4-(hydroxyl 3-glycine)-quinoline
HLE:	Human lens epithelial cell line, SRA 01/04
HSF:	Heat shock factor
Hsp:	Heat shock protein
IPTG:	Isoprpyl -β-D-thiogalactopropyranoside
Kcal/m:	Kilocalories per mole
kDa:	Kilodalton
LB:	Luria-Bertani broth
LOCS:	lens Opacities Case-control Study
MTT:	3-(4, 5-dimethylthiazol-2-yl)-2, 5-diphenyl tetrazolium bromide
mW:	Milliwatt
NMR:	Nuclear Magnetic Resonance
ns:	Nanosecond
$O_2^{-\cdot}$:	Superoxide anion radical
OD:	Optical density
PAGE:	Polyacrylamide gel electrophoresis
PBS:	Phosphate buffered saline
PMSF:	Phenylmethylsulfonylfluoride
PON:	Peroxynirite

ps:	Picosecond
RF:	Riboflavin
RNase A:	Bovine pancreatic ribonuclease A
RNO:	N, N-dimethyl-4-nitrososaniline
RP-HPLC:	Reverse-phase high performance liquid chromatography
SDS:	Sodium dedecylsulhate
SIRC:	Rabbit corneal keratocyte cell line
SOD:	Superoxide dismutase
Tc:	Phase transition temperature
TFA:	Trifluoroacetic acid
Tris:	Tris(hydrocymethyl)aminomethane
WSE:	Withania somnifera extract

CONTENTS

AN OVERVIEW OF TWO MAJOR DISEASES OF HUMAN EYE

1.0. INTRODUCTION

Blindness is the most tragic, yet often avoidable, disability of people in the developing world. The personal, social and economic consequence of blindness has become an important public health issue, especially in underdeveloped and developing countries. In response to the global need, the World Health Organization (WHO) and the International Agency for the Prevention of Blindness (IAPB), along with various national organizations have come together with the common aim of tackling avoidable forms of blindness worldwide and have created a global movement called Vision 2020: The Right to Sight. This initiative's mission is to eliminate the main causes of avoidable blindness by the year 2020. A recent estimate by the WHO, released in 2004, has claimed that nearly 37 million people around the world were blind that includes 1.4 million children under the age of 15 years (Resnikoff *et al.,* 2004). The WHO report also suggests that 75% of blindness is caused by four specific age-related conditions such as cataract, glaucoma, age-related macular degeneration and diabetic retinopathy. Cataract is a leading cause of blindness, which accounts for 47.8% of total blindness, followed by glaucoma (12.3%), age-related macular degeneration (8.7%) and diabetic retinopathy (4.8%).

Childhood blindness accounts for 3.9% of global blindness (Resnikoff *et al.,* 2004). Though it looks less in comparison to other adult blindness, it is the second largest cause of blind-person years, following cataract. Children who are born blind or who become blind are blind for lifetime, with all the

associated emotional, social, and economic costs to the child, the family, and society. Hence childhood blindness also seeks immediate attention.

In this context, we have focused our study on two leading causes of global blindness, namely, cataract including congenital cataract and glaucoma, which together contribute to ~60% of global blindness.

1.1. CATARACT

Cataract is a well-known disease in the world since ages, particularly frequent in elderly population. It is characterized by opacification of the eye lens, located in the visual axis of the eye between the anterior aqueous humor and the posterior vitreous humor (see Figure 1.1). It can be broadly divided into

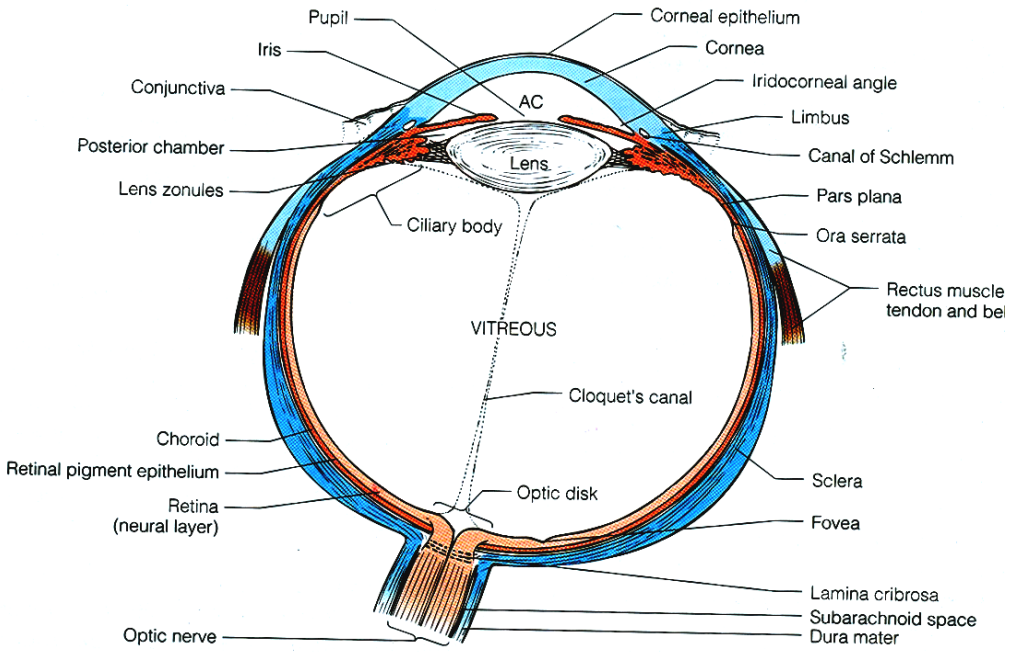

figure 1.1. schematic diagram of human eye cross-section. (Forrester *et al.*, the eye basic sciences in practice. 2nd ed. saunders: elsevier limited; 2002: p15).

early onset (congenital or juvenile) and age-related cataract. There are several ongoing epidemiological studies, which have helped to figure out the various risk factors associated with cataract. Some identified till date are ageing, metabolic disturbances, radiation (UV-A and UV-B), trauma, drugs, low antioxidant intake, cigarette smoking, alcohol, and genetic factors involving mutations in the various gene products which play a major role in eye lens transparency (Cumming *et al.,* 1997; Francis *et al.,* 1999; Hammond *et al.,* 2000; McCarty *et al.,* 2000, 2003; Harding *et al.,* 2002; Krishnaiah *et al.,* 2005). Restoration of lens transparency and vision is invariably through cataract surgery. This surgery is a simple procedure and takes less than 30 minutes to remove the cataractous lens and implant an artificial lens. Yet cataract remains the predominant cause of blindness, because the current level of surgery remains too low to tackle the backlog of cataract blind (16-20 million worldwide) and its rising world incidence due to the ageing population.

In contrast to age related cataract, congenital or infantile cataracts have an estimated prevalence of 1–6 cases per 10,000 live births and represent the most common treatable cause of childhood blindness (Lambert and Drack, 1996). Congenital cataract accounts for 10-15% of total childhood blindness. Genetic defects in various genes contribute to ~50% of congenital cataract. In this context, it is essential to understand the disease mechanism so as to develop alternative strategies to prevent/retard the progression of cataract. The personal, social and economic consequence of cataract blindness in the world has motivated extensive research, and enormous amount of knowledge has been accumulated on the genetic and biochemical aspects of lens opacification.

Congenital or hereditary cataract derives from mutations in a variety of genes, which affect the protein function in two distinct molecular routes: protein misfolding resulting in protein aggregation and/or altered interactions, and association between the structural proteins of the lens, called the crystallins, resulting in lower solubility and lens opacification. Here, we discuss the possible effects of mutations in the lens crystallins by focusing on available experimental data on the structure and functions of some crystallin mutants.

1.1.1. Hypothesis of lens opacification and cataract

Cataract is an opacification of eye lens, interfering with its normal function either due to the disturbances in the regular cytoplasm-membrane lattice repeats of the lens, or by disturbance in the local short-range order of the crystallins in lens fiber cells (Delaye and Tardieu, 1983). At the cellular level it can be due to osmotic pressure effects and at the molecular level it can be attributed to condensation of lens proteins into protein-rich and protein-poor phases, due to wrong protein interactions, intrinsic instability and protein mis-folding / denaturation, leading to protein aggregation. Protein aggregates that exceed 100 nm (Hejtmancik and Kantorow, 2004) or approximate molecular mass beyond 50 MDa will scatter light (Benedek *et al.,* 1971, 1997). Mechanistically, condensation of lens proteins can be due to (a) unfolding/mis-folding of lens proteins, in which case cataract could be considered as a protein-folding disease and (b) altered interactions of proteins cataract would then be the consequence of a loss of solubility (Bloemendal *et al.,* 2004). In both the cases cataract would be due to disturbances in the short range-order of crystallins.

1.1.1A. Cataract as a protein folding disease

Protein folding diseases are hypothesized to result from an insufficiency in the protein chaperoning system of the cell. Unfolded cytoplasmic proteins generally evoke heat shock response, while those in the endoplasmic reticulum evoke an unfolded protein response (Morimoto and Santoro, 1998; van den IJssel *et al.,* 1999; Patil and Walter, 2001; van Montfort *et al.,* 2001; Sonna *et al.,* 2002). In both the cases, there is an inhibition of general protein synthesis, and switching of the resources of cells to synthesize protein chaperones, thus giving cells time to switch on the machinery to deal with the unfolded protein stress.

The idea of cataract as a protein folding disease comes from the following arguments. The lens fiber cells lack the ability to mount a stress response since these cells lack the protein synthesis machinery and cannot increase protein chaperone content. The prominent lenticular structural protein (α-crystallin) is known to function as a chaperone. But as the lens ages, the endogenous available α-crystallin would have been used up by other lenticular proteins, which unfold or become modified upon ageing (Horwitz *et al*, 1992; Derham and Harding, 1999; Clark and Muchowski 2000). Though immature lens fiber cells can mount the heat shock response, if the misfolding protein is a mutant crystallin this system can be overwhelmed as the crystallin genes are expressed at very high levels. In this case an immature lens fiber cell may not be able to escape from unfolded protein stress, thus disturbing lens morphogenesis.

1.1.1B. Cataract resulting from altered protein interactions

Transparency and high refractive function of the lens arise due to the short-range order between highly concentrated crystallins. The high level of polydispersity among crystallin components will reduce the risk of protein crystallization and contribute to even and dense packing. In the lens cytoplasm, the mixture of crystallins displays overall repulsive interactions determined essentially by the dominating effect of α-crystallin (Veretout *et al.,* 1989) which plays a major role in the short-range ordering of crystallins. Changes in solubility or attractive properties can cause disturbances in the short-range order of crystallins, which can lead to cataract formation without any protein misfolding.

1.1.2. The eye lens structure and function

Understanding lens biology is essential in order to understand the pathogenesis of cataract. The lens is a principal component in the process of focusing incident light. In order to serve its function the lens has to fulfill certain requirements; it has to provide transparency, high refractive index and also the capacity to alter its shape, so as to focus near and distant objects. The cellular structure of the lens meets these biophysical requirements, thanks to its unique morphology and composition. Light, confocal and electron microscopic studies on vertebrate lenses reveal that these are composed of long ribbon-like fiber cells of uniform cross-sectional shape (hexagonal) and size (Cohen, 1965; Smelser, 1965; Kuszak and Rae 1982; Rae *et al.,* 1982; Rae *et al.,* 1983; Kuszak *et al.,* 1985; Kuszak *et al.,* 1996; Al-Ghoul and Costello, 1997; Bassnett and Winzenburger, 2003). These fiber cells are

formed throughout the life of the individual, in the form concentric growth shells, with the oldest cells in the centre and youngest on the outside (Figure 1.2). This highly ordered arrangement of lens fibers contributes to lens transparency by transforming the individual fibers into a series of coaxial refractive surfaces (Trokel, 1962). As a result, large particle scatter is minimized as light is transmitted through the membranes of hundreds of thousands of fibers. Small particle scatter is minimized through a gradient of refractive index established through and maintained by cytoplasmic crystallin proteins of the fibers.

The shape and size of the fiber cell is determined and maintained by a unique lens fiber cell-specific cytoskeletal structure, the beaded filament (cytoskeletal protein 49 (CP49) and filensin or beaded structural protein1 (Bfsp1)) (Maisel *et al.,* 1972, Alizadeh *et al.,* 2002). Homeostasis and nutrition to the lens fibers are taken care of by gap junction (membrane channel) proteins called connexins. Connexin 46 and Connexin 50 are two gap junction proteins predominantly seen in human eye lens.

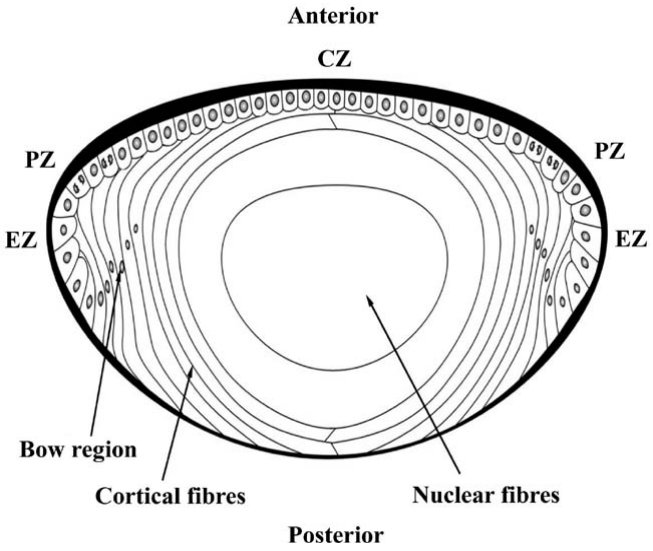

Figure 1.2. Schematic drawing of adult human lens. Based on the location the lens epithelium is divided into central (CZ), pre-equatorial (PZ) and equatorial zone (EZ) (Gupta *et al.*, 2004).

Proteins constitute about ~38% of the total mass of eye lens, with concentrations reaching upto 450 mg/ml and packed in very high densities in lens fibers. The abundant water-soluble crystallins account for ~90% of the lens fiber cell protein content and are responsible for the maintenance of transparency and refractive index (~1.40 in human) of the eye lens (Bloemendal *et al.,* 2004). The dense and highly ordered arrangement of the crystallin proteins is essential for the transparency and refraction of the eye lens. The lens transmits light efficiently over the entire visible range and beyond it till about 1200 nm but transmits very little below 300 nm. Protein turnover is absent in the lens because lens fibers lack nuclei and cellular organelles, and therefore proteins once synthesized in the lens fibers are remains life long. Indeed, it is this lack of turnover that can lead to cataract. With age, if chemical modifications (oxidation, glycation, degradation, cross-linking) occur to lens proteins, they can lead to scattering particles that are not cleared. This tends to compromised lens transparency and accommodation.

1.1.3. Molecular genetics of cataract

The first molecular genetic evidence of cataract dates back to 1878 when a Danish physician published a paper entitled, 'A cataractous peasant family' wherein he described the early onset cataract (Giersing, 1878). Later in 1949 the same family, with 8 generations and 542 members was followed up, and clinically and genetically analysed by Marner (Marner cataract) (Marner, 1949; Marner *et al*, 1989). Marner cataract was subsequently mapped to the haptoglobin locus on chromosome 16q22. In 1906, Nettleship and Ogilvie published a detailed description of an affected family of early onset cataract (Coppock family). In 1963, Renwick and Lawler showed the co-segregation of

Coppock cataract with the Duffy blood group locus (Online Mendelian Inheritance in Man, OMIM reference number 110700). This became the first autosomal disease to be genetically linked in man, when in 1968 the Duffy locus was assigned to chromosome 1. Further genetic studies on Duffy blood group locus refined it to 1q22-23 and identified mutations in Connexin 50 gene. Subsequent development of advanced molecular biological techniques facilitated the identification of 20 independent cataract loci.

The advent of Human Genome Project allowed the identification of several genes causing inherited cataract. The different gene families (structural proteins of the lens known collectively as the crystallins, cytoskeletal proteins, transcription factors, membrane transport proteins and proteins of unknown function) implicated in human cataract are shown in Figure 1.3. The hereditary cataracts that have been characterized so far show Mendelian inheritance and either result from single gene mutations or chromosomal translocations. Majority of inherited cataracts show the autosomal dominant mode of inheritance but X-linked and autosomal recessive forms are also seen. There are 16 genes which have

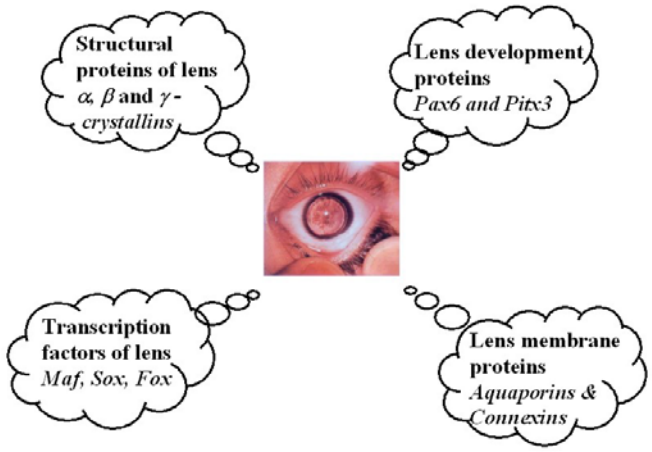

Figure 1.3. Categories of genes responsible for congenital cataract.

been shown to be linked with autosomal dominant congenital cataract (Table 1.1) and ~7 genes are associated with autosomal recessive congenital cataract (Table 1.2). The various gene mutations identified till date are listed in Table 1.3.

1.1.4. The Biochemistry of Cataract

1.1.5. The crystallins

The lens has proteins as the major component, among which the water-soluble proteins, the crystallins, form the major fraction, not only in quantity but also in the functioning of lens. Crystallins are broadly divided into two major families, α and $\beta\gamma$. These crystallins contribute to the transparency and refractive properties of the lens by forming a uniform concentration gradient. In order to fulfill their optical function, crystallins possess some characteristic features. They are highly water soluble and also highly stable as they last a lifetime. Since the structure of the crystallins must be highly preserved for decades, numerous studies have investigated the subunit structure, subunit-subunit interactions, quaternary structures using X-ray crystallography, single particle electron microscopy, spin labeling and nano-electrospray mass spectroscopy, mammalian two-hybrid analysis and so on. Here we review the various properties such as structure, stability, and function of the different families of crystallins and the effect of amino acid variations on their structure and function.

1.1.5A. The α-crystallins

The α-crystallins constitute nearly 40% of total crystallins and there are two α-crystallin genes, αA- and αB-, encoding proteins that share 60% sequence identity (Bloemendal and de Jong, 1991). The expression of α-crystallin is seen in lens epithelial cells but its levels are upregulated upon differentiation into the lens fiber cells. These crystallins are synthesized continuously during development and homogeneously distributed throughout the lens. In man, the ratio of αA- to αB- crystallin varies from 1:2 in the foetal lens to 1:3 in the adult lens. The α-crystallins are presumed to function both as structural components and as chaperones that help the folding and solubilization of other proteins in the lens.

i) Structure of α-crystallins

αA-Crystallin is a 19.09 kDa peptide made up of 173 amino acid residues and αB-crystallin is a 20.2 kDa protein with 175 amino acid residues. Both contain the "α-crystallin domain", a characteristic of small heat shock protein family (sHSPs). The eye lens α-crystallin exists as a polydisperse multimer with apparent molecular masses between 800-1200 kDa. Due to this polydisperse size distribution of α-crystallin, crystallographic studies have been unsuccessful so far. Thus, presently neither the detailed structure of the subunit nor the topology of the subunit assembly is known. Based on solution state spectroscopic data, the secondary structure is known to be predominantly made of β-pleated sheet, with less than 20% helix content.

Based on the available crystallographic data on the α-crystallin domain of archeal hyperthermophile (Kim *et al.,* 1998) and of wheat (van Montfort *et al.,* 2001) sHSPs, α-crystallin is thought to have the β-sandwich fold in which the C-side protection is provided by conserved I-X-I motif from the ordered extension of a partner subunit.

ii) Function of α-crystallins

a) Chaperone function:

α-Crystallin, being a member of sHSPs, acts as a molecular chaperone, and functions by storing aggregation-prone proteins as folding-competent intermediates and conferring enhanced stress resistance on cells by suppressing aggregation of denaturing proteins. This property of α-crystallin was discovered by Horwitz (1992), and demonstrated *in vitro* by using purified bovine α-crystallin and several model substrate proteins. The chaperone activity is most commonly assayed by measurement of the extent of light scattering by proteins exposed to heat or chemical denaturation. The mechanism of chaperone action of αA- and αB- has been thoroughly investigated and it is found that both have chaperone activity, and bind to misfolded proteins with high affinity.

In the lens, proteins do not turnover, and are prone to damage by several means i.e., ageing, oxidative stress, injury, UV exposure, and metabolic insults. To maintain transparency, the crystallins must remain stable without undergoing damage or denaturation. Horwitz *et al.* (1992) have

proposed that with ageing, α-crystallin would bind partially unfolded lens β- and γ-crystallins, thereby preventing their further aggregation and precipitation, and delaying lens opacification.

b) Role in maintaining cellular architecture:

The cytoskeletal elements undergo extensive remodeling during lens development and under stress conditions, thus making them a prime target for protection and repair. Several studies have showed that α-crystallin interacts with actin microfilament, the intermediate filaments and microtubules. Carter *et al.* (1995) demonstrated the role of α-crystallin in reconstituting lens specific beaded filament from intermediate filament protein in the lens. It has been shown that α-crystallin suppresses the *in vitro* denaturation and insolubilization of denatured tubulin (Arai and Atomi 1997; Fujita *et al.,* 2004). α-Crystallin appears to regulate the cytoskeleton by maintaining and controlling the availability of assembly-competent subunits and regulating the dynamic assembly of cytoskeletal polymers by sequestration of subunits. Overall, these studies suggest that the cytoskeleton may be an important physiological target of α-crystallin function *in vivo*. Future studies in this direction might give a better understanding of the disease pathogenesis.

c) Anti-apoptotic functions:

The anti-apoptotic functions of α-crystallin have been studied by several different groups. Andley *et al*. (1998, 2000) have shown that the cells induced to over-expressed αA- and αB-crystallin have enhanced resistance to thermal,

photochemical and other stress conditions. They also showed that αA- has higher protective ability against apoptosis than αB-crystallin in cultured cells. Xi *et al.* (2003) showed that lens epithelial cells where in α-crystallin has been knocked out had a higher level of cell death than wild type cells. While these effects are important in the lens, it can be suggested that the ability of αA- and αB-crystallins to interfere with apoptosis would offer a novel way to prevent cell death even in the retina and in other diseases like encephalomyelitis, and neurological disorders.

d) Proteasomal interactions and protein degradation:

Recent work by Boelens *et al.* (2001), and den Engelsman *et al.* (2003) has suggested a novel and specific function of αB-crystallin associated with the degradation of denatured proteins. αB-Crystallin specifically binds to components of the 20S proteasome both *in vivo* and *in vitro*. The interaction with C8/alpha7, subunits of the proteasome are thought to affect the assembly of proteasomal complex or facilitate the degradation of αB-crystallin-bound unfolded substrate proteins.

iii) Posttranslational modifications and gene mutations in α-crystallin – Cataract:

As a natural ageing process it is observed that most of the lens proteins undergo posttranslational modifications such as truncation, deamidation, oxidation, non-enzymatic glycosylation or glycation, phosphorylation and racemization/ isomerization. These kinds of changes in α-crystallin have been

reported in ageing organisms, apparently affecting its chaperone activity and solubility. The causal relationships between its glycation and chaperone activity in the case of diabetes has been established (Thampi *et al.,* 2002). α-Crystallin deamidation involves the nonenzymatic conversion of asparagine to aspartate or isoaspartate and glutamine to glutamic acid, and these have been found to be prevalent during cataract formation and ageing (Srivastava *et al.,* 2003). *In vitro* studies by site-directed mutagenesis of the residues Asn146Asp and Asn78Asp/Asn146Asp demonstrates that deamidation significantly impacts the chaperone function of αB-crystallin (Gupta *et al.,* 2004). In comparison to the wild type, oligomer size increases and chaperone activity decreases in these mutants, suggesting that deamidation disrupts lens αB-crystallin structure and chaperoning function, thereby compounding the role of this post-translational change as a causative agent of cataract.

Several α-crystallin gene mutations have been associated with autosomal dominant and recessive forms of congenital cataract (Table 1.3). The structural and functional consequences of these mutations have been studied by various groups and attributed to the loss of chaperone function and formation of high molecular weight aggregates (Table 1.4). For example the mutation responsible for autosomal dominant congenital cataract Arg116Cys (α-crystallin domain) in αA-crystallin results in a defective in chaperone function. Another dominant mutation Arg49Cys, (outside the α-crystallin domain) in αA-crystallin is associated with cataract.

The data obtained by mammalian two hybrid systems show that there is a definite change in self-interactions within the wild type and mutant α-crystallins, and interaction with different lens crystallins (β- and γ- crystallins) and which indicates that the mutant proteins are less effective in maintaining the proteins in the soluble state and promote cataract development (Fu and Liang, 2003).

1.1.5B. The β- and γ-crystallins

The β- and γ-crystallins both share common secondary structural element called the Greek key motif and are regarded as members of the same super-family. Yet they differ in three primary ways: (1) β-crystallins have N- and sometimes C-terminal extensions, while γ-crystallins do not. These arms have been implicated in molecular interactions between β-crystallins and with membrane or structural components of the cell (Wistow *et al.,* 1981); (2) the distribution of surface charges on the β- and γ-crystallin core domains differ (Lapatto *et al.,* 1991); (3) the connecting peptide linking the two domains is distinctly different in β- and γ-crystallins. The implications of these differences between the β- and γ-crystallins are yet to be fully understood.

Lens β-crystallins are a family of seven polypeptides and exist as dimers to octamers with molecular masses ranging from 50 to 200 kDa. They are categorized based on their surface charge and pI values into acidic (βA1, βA2, βA3 and βA4) and basic (βB1, βB2 and βB3) (Herbrink *et al.,* 1975; Berbers *et al.,* 1984; Lampi *et al.,* 1997). There is 45 to 60% sequence homology among the different β-crystallins and 30% homology with that of γ-

crystallins. The βA3 and βA1 are encoded by a single gene in humans and the difference between the two proteins is only in the N-terminal extension. These β-crystallin expressions are developmentally regulated in the mammalian lens. The βB1 and βB3-crystallins are early genes and found primarily in the lens nucleus, while βB2 is a late gene, expressed in the postnatal lens. The acidic β-crystallins have wide expression patterns and are found both in the center and cortex of lens.

Turning now to γ-crystallins, mammals are known to contain seven γ-crystallin genes. Six of these genes, γA-F, are closely linked and show high similarity in their sequence. The seventh gene, γS-crystallin, is located on a different chromosome and is divergent from the others. All γ-crystallins exist as monomers, with a molecular mass of 20 kDa. They are fiber cell specific and are not seen in immature fiber cells and the cortical region. Furthermore, γA-F-crystallin genes are early genes, expressed in early lens development and hence found mainly in lens core region. In the human lens only γC and γD-crystallins are expressed abundantly, and γE and γF-crystallins found to be pseudogenes. Table 1.3 lists some cataracts associated with mutations in the β- and γ-crystallins, while Table 1.4 summarizes the effect of some specific mutations on the structure and properties of these proteins.

i) Structure of βγ-crystallins

The crystal structures of a few (Table 1.5) β- and γ-crystallins have been delineated using x-ray crystallography. The main structural unit found in these crystallins is called the βγ-crystallin domain. This domain is made of two

consecutive Greek key motifs (Figure 1.4A) comprising eight β-strands, which intercalate to form two β-sheets that pack together to form a β-sandwich domain. These β-sandwich domains (Figure 1.4B) are characterized by their high internal conformational symmetry and a conserved folded hairpin structure for each motif. The double Greek key domain has a complex topology in that each linear 4-stranded motif exchanges its third β-strand to a β-sheet belonging to its partner motif. Each of the β-, γ-crystallin protein carries two such domains (Figure 1.4C).

The native β-crystallins in the lens form heterodimers of acidic and basic subunits as well as homodimers, whereas the γ-crystallins exist as monomers. As mentioned earlier, this distinction between β- and γ-crystallins derives mainly from the linker peptide conformation. The linker conformation in the γ-crystallin is 'V' shaped and allows only intramolecular domain interactions, whereas in β-crystallin the linker is straight and allows intermolecular quaternary interactions between two β-crystallins. But subsequent

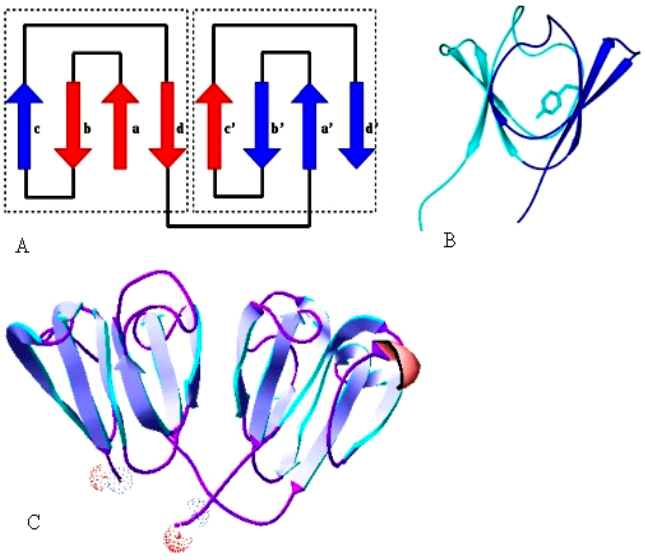

Figure 1.4. A). Schematic diagram of Greek key motif. B). γ-crystallin domain (Bloemendal *et al.*, 2004). C). Crystal structure of γD-crystallin retrieved from protein databank and produced three-dimensional structure Swiss-Pdb Viewer 3.7 software.

experiments involving domain swapping and linker peptide exchange between β- and γ-crystallins has ruled out the role of the linker peptide in the dimerization of β-crystallins (Hope *et al.,* 1994).

ii) Function of β- and γ-crystallins

Very little information is available on the function of βγ-crystallins. Crystallins of the βγ family were originally thought to be lens-specific and their expression thought to be a marker of lens differentiation. Recent work shows that most of these crystallin proteins are expressed in lens epithelial cells, retinal cells and other parts of the eye as well (Wang *et al.,* 2004). γS-crystallin is expressed outside the lens and its expression pattern suggests a stress related role (Sinha *et al.,* 2001). The expression of these crystallins in the retina suggests that they also may function as stress proteins. Work by Yogendra Sharma has suggested the possibility of the βγ-crystallins acting as a depot that sequesters free calcium ions in the lens (Rajini *et al.,* 2001; Jobby *et al.,* 2007). This is expected to be protective against Ca^{2+}-triggered proteolysis and degradation of the lens proteins.

The non-structural functions for the crystallins gain support from the observation that similar gene mutations lead to various phenotypes. If crystallins have only a structural role in the lens, then mutations in crystallin genes would be expected to give more or less the same phenotype, which itself is indicative of the non-structural function for βγ-crystallins. A number of γ-crystallin mutations have been shown to affect the developmental programs

rather than the short-range order of proteins (Graw, 1999; Graw and Loster, 2003; Loster *et al.,* 1994).

iii) Cataract and mutations in βγ-crystallins

Several β- and γ-crystallin gene mutations, associated with congenital cataract, are listed in Table 1.3. Understanding the effect of these mutations on the structure and functions of crystallins will help in predicting the disease pathogenesis and help to think about therapeutic strategies. There are quite a few studies undertaken to study the effect of various β- and γ-crystallin mutations, which have been associated with several forms of congenital cataract in infants (Table 1.4). In this thesis we report our studies on the structural analysis of two congenital cataract associated γ-crystallin mutants.

1.2. GLAUCOMA

Glaucoma is a leading cause of irreversible blindness and affects nearly 70 million people across the globe. It comprises a heterogeneous group of disorders characterized by widely diverse clinical and histopathological manifestations. Glaucoma encompasses many clinical entities with certain common denominators such as optic neuropathy and progressive visual field loss, which are attributed to the death of retinal ganglion cells (RGCs) (Shields, 2005). The usual cause is the rise of hydrostatic pressure or intraocular pressure (IOP), arising due to the blockage of aqueous humor flow. This in turn causes progressive degeneration of optic nerve axons.

Diagnosis of glaucoma is a challenging task, because the disease manifests with no obvious symptoms and is pain free. Half of the people with

glaucoma do not know it until significant visual damage occurs; hence the name "silent thief of sight". In other instances, symptoms include cloudy cornea, pain, visual field loss, optic disc changes and enlargement of eye (Khaw *et al.,* 2004).

1.2.1. Classification of Glaucoma

Based on mechanisms, glaucomas are classified into three types (Sheilds, 2005)

i) Primary open angle glaucoma (POAG)

It is classified based on the visibility of anterior chamber angle structures such as trabecular meshwork, scleral spur, and ciliary body band upon gonioscopy (Shields, 2005). Based on IOP these glaucomas are further divided into high-tension (HTG) (IOP greater than 21 mm Hg), and normal tension (NTG) glaucoma where the IOP is consistently less than 21 mm Hg. Though they differ with respect to IOP, both the forms ultimately lead to optic nerve atrophy, visual field defects and retinal ganglion cell death.

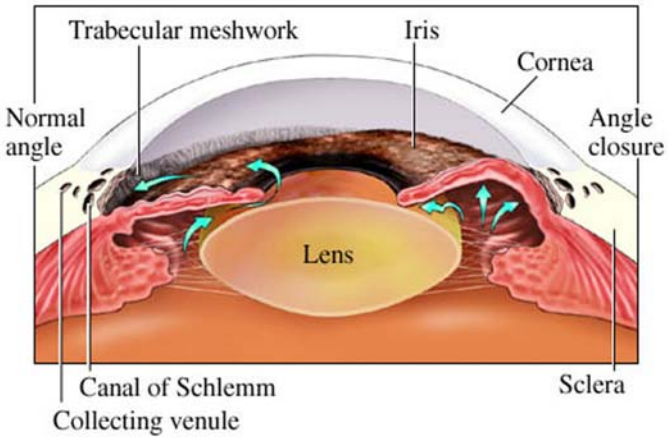

Figure 1.5. Schematic diagram of anterior chamber structures of the human eye, showing normal angle and angle closure (image adopted from. http://catalog.nucleusinc.com /displaymonograph.php?MID=42).

ii) Primary angle closure glaucoma (PACG)

It is mainly classified based on the narrow anterior chamber angle on gonioscopy. The peripheral iris occludes the anterior chamber angle (Figure 1.5), thereby blocking the aqueous outflow leading to elevated IOP and glaucoma.

iii) Developmental glaucoma

This is mainly classified based on the developmental abnormalities in the structures of conventional aqueous outflow pathway such as trabecular meshwork and Schlemm's canal.

Although individual clinical manifestations exist for different glaucomas mentioned, the ultimate pathology in all kinds of glaucomas involves the degeneration of retinal ganglion cell axons and soma, which is manifested as progressive visual field defects.

The major risk factor associated with glaucoma is high intraocular pressure (IOP). Understanding IOP and aqueous humor dynamics, which regulate the pressure, is critical mainly because they are the most common and best-understood causative risk factors and are presently the only factors that can be controlled to prevent progressive optic neuropathy.

1.2.2. Intraocular pressure (IOP)

This is the pressure created on the globe due to the continual renewal of fluids within the eye. IOP plays a major role in giving a shape to the eyeball and its maintenance. Most of the glaucoma patients show elevated IOP.

Patients with chronic high IOP will develop changes in the nerve fiber layer, optic nerve head, and progressive death of retinal ganglion cell death, which translates clinically as visual field loss. The IOP is mainly regulated by the production and flow of the aqueous humor, so it is important to know the aqueous humor dynamics in the eye.

1.2.3. Aqueous humor (AH) dynamics

Aqueous humor (AH) plays an important role in maintaining constant IOP; it nourishes the cornea, iris, and lens, removes metabolic waste products from the anterior segment. AH is continually produced from ciliary processes and flows through different parts of the posterior and anterior chamber and exits the eye. The production of AH must be balanced by an equal rate of AH drainage. Small variations in the changes in production or outflow of AH will have a large influence on IOP.

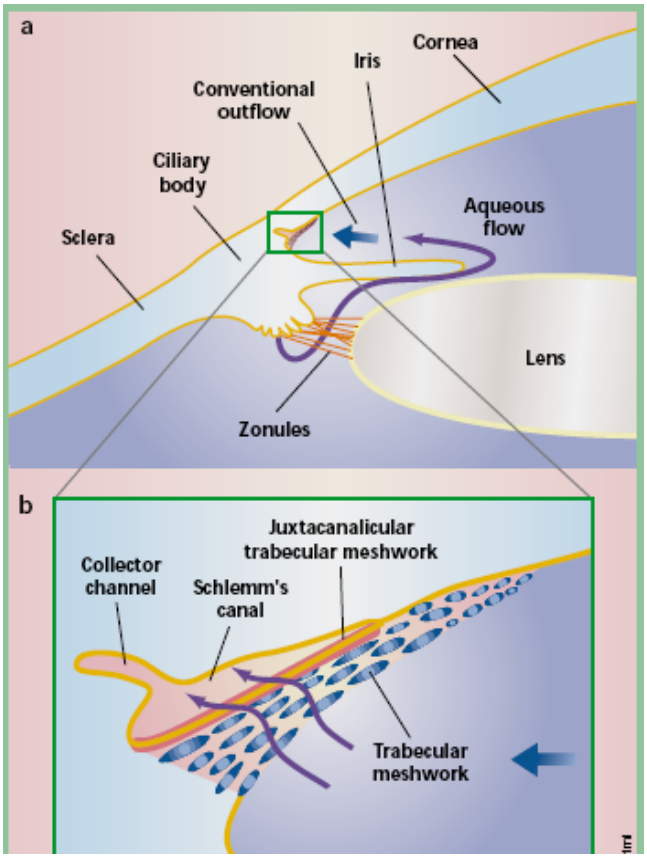

Figure 1.6. Schematic diagram of aqueous humor out flow pathway (Tomarev *et al.*, 2001)

There are two pathways by which AH outflow can occur. The conventional trabecular pathway, in which primary

route for AH outflow starts with the posterior chamber, then enters the narrow space between the posterior iris and the anterior lens and passes through the pupil to reach the anterior chamber. From there, it exits the eye through the trabecular meshwork (TM) into the Schlemm's canal (SC) as shown in Figure 1.6. It flows through 25 - 30 collector canals into the episcleral veins. This pathway is responsible for more than 75% of AH outflow. The TM provides the greatest resistance (~75%) to aqueous out flow due to blockage, but the exact mechanism involved in the AH resistance / blockage is unknown (Tomarev *et al.,* 2001). The second pathway is the non-conventional or uveoscleral pathway, Drainage of AH occurs here through the bundles of ciliary muscles. Uveoscleral pathway is responsible for 5 to 25% of AH drainage (Rudzinski *et al.,* 2005). Mechanistically, IOP elevation is mainly due to a decrease in the outflow of AH and not due to overproduction.

Some of the risk factors shown to be associated with elevated IOP and glaucoma include family history (genetics), increasing age, race (Blacks appears to be more susceptible to glaucoma than others), gender (females seem more susceptible than men), refractive error (myopic people) and systemic disorders (diabetes).

1.2.4. Molecular genetics of glaucoma

Several epidemiological studies on glaucoma have revealed the role of family history and the involvement of genetic component in glaucoma progression. This has led to the constant search for genes which contribute to glaucoma progression. The molecular genetic understanding of the disease is difficult due to the complex and multifactoral nature of the disease. Molecular

geneticists have identified 17 chromosomal loci till date, which have been shown to be linked with various forms of glaucoma (Table 1.6). Out of these loci, only 4 genes have been identified to be associated with glaucoma. The genes identified include myocilin (*MYOC*), cytochrome P450 1B1 (*Cyp1B1*), Optineurin (optic neuropathy inducing protein (*OPTN*)) and WD repeat-containing protein 36 (*WDR36*).

Several studies have reported a large number of mutations in these genes, yet the molecular understanding of the disease is poor, since the normal functions of these genes are not completely known.

1.2.5. Molecular mechanisms - Pathology of glaucoma

As elevated IOP is considered a primary risk factor for the progression of glaucomatous optic neuropathy, the current pharmacological therapy for glaucoma relies almost exclusively on the lowering of IOP. Even after adequate level of IOP control, glaucomatic progression of visual loss continues. There are situations where optic nerve damage takes place without the elevation of IOP, as it does in normal tension glaucoma (NTG). This has led to several studies which are aimed at understanding the disease pathogenesis using several means, looking for the cellular and molecular changes in the patients TM, ONH, RGCs etc., and also in several experimental glaucoma models.

These studies have resulted in the proposal of three theories, which could explain the IOP-dependent as well as IOP-independent mechanisms for

the progressive death of retinal ganglion cells. The three theories proposed are discussed here.

i) Mechanical theory:

According to this theory, the persistent elevation of IOP causes compression of the optic nerve fibers, deformation and backward bowing of the lamina cribosa, leading to an effective physiological axotomy which blocks anterograde and retrograde axonal transport. This theory mainly focuses on the susceptibility of optic nerve to mechanical stress; hence, there is little room for primary retinal injury. But, RGC soma would be expected to suffer retrograde injury, due to reduction in retrograde supply of brain derived trophic factors from lateral geniculate body (Quigley *et al.,* 2000).

ii) Vascular/Ischemic theory:

According to this theory, the elevation of IOP leads to compression of optic nerve fibers and the optic arteries at the lamina cribosa, which results in alterations in the blood supply to the optic nerve head, which leads to ischemic damage of optic nerve head and progressive death of retinal ganglion cells. The main evidence for this theory comes from I) blood flow incompetence at ONH in glaucoma patients (Chung *et al.,* 1999), and ii) presence of retinal blood flow abnormalities in glaucoma patients (Arend *et al.,* 2004).

iii) Excitotoxicity theory:

This theory is compatible with both the theories discussed above. Excitotoxicity is a pathological process, which describes the neuronal cell death induced by excitatory neurotransmitters. This occurs when the receptors for neurotransmitter are over-activated. An abnormally high concentration of the neurotransmitter induces excessive stimulation of neurons, which leads to Ca^{2+} influx. Excessive Ca^{2+} in the cell activates several enzymes such as phospholipases, proteases and endonucleases, which in turn damage the other cellular components. Glutamate is the major excitatory neurotransmitter in the retina and it is involved in the vertical pathway of phototransduction, i.e., at the photoreceptor/bipolar cell synapse and the bipolar cell/ganglion cell layer synapse. Excitotoxic amino acids such as glutamate have been found to be increased in glaucomatous eyes. Recent studies have shown that a persistent increase in glutamate levels may cause retinal ganglion cell death, which is independent of elevated IOP (Casson *et al.,* 2006).

1.2.6. Factors associated with retinal ganglion cell (RGC) degeneration

Studies based on such theories have resulted in the identification of several risk factors, other than IOP, that possibly contribute to retinal ganglion cell death. Some of these includes ischemia, excitotoxicity, autoimmunity, axonal injury and glial cell activation. Combination of any of these factors may be active in a given patients. The relative significance of each specific factor varies between patients depending on the magnitude of IOP elevation, oxidative stress and individual life style (John, 2005).

I. **Ischemia:** elevated IOP induces ischemia in the optic nerve, which results in a blockage of axoplasmic flow, and prevents normal transport of agents such as growth factors, leading to RGC death. Optic nerve blood flow is compromised in glaucoma patients. (Flammer, 1994) Ischemia enhances oxygen free radical, glutamate release, and nitric oxide production, which increase the levels of Ca^{2+} that show detrimental effect on RGC cells (Cioffi, 2005).

II. **Excitotoxicity:** Glutamate is an essential excitatory amino acid in the central nervous system and also in the retina. It has been shown in several neurological diseases that excessive glutamate induces over-excitation of neurons, which ultimately leads to the death of neuronal cells. It has recently been shown that glutamate excitotoxicity plays an important role in the pathogenesis of glaucoma (Vorwerk *et al.,* 1999). The evidence comes from the fact that i) vitreal glutamate levels are elevated in experimental and clinical glaucoma (Dreyer *et al.,* 1996), ii) ischaemia plays a role in glaucoma (Lam *et al.,* 1997), iii) neuroprotection based animal studies and iv) secondary degeneration of RGCs after optic nerve injury.

III. **Autoimmunity:** Franz *et al.,* (2004) showed circulating autoantibodies against several ocular antigens in glaucoma patients, and suggested the role of auto-immunity in glaucoma. The auto-antibodies observed include heat shock proteins (HSPs), rhodopsin, γ-enolase, glutathione-S-transferase (GST), tumor necrosis factor-α, and γ-synuclein. These antibodies may play role in the formation of inflammation that can induce apoptosis of RGCs.

IV. **Axonal Injury:** Excavation of the optic disc is a clinical feature of glaucoma. In animal models it has been shown that axonal injury will initiate the limited supply of trophic factors, and excitotoxicity that will induce RGC death (Osborne, 1999).

V. **Glial cell activation:** Glial cells are important structural and functional components of the ONH. The glial cells present in ONH and retina include astrocytes, oligodendrocytes and microglia. These glial cells support neuronal tissue by supplying metabolites, growth factors and by scavenging toxic metabolites. Therefore, glial activation in glaucomatous eyes may initially represent a cellular attempt to limit the extent of neuronal injury and to promote tissue repair. Consequently, activated

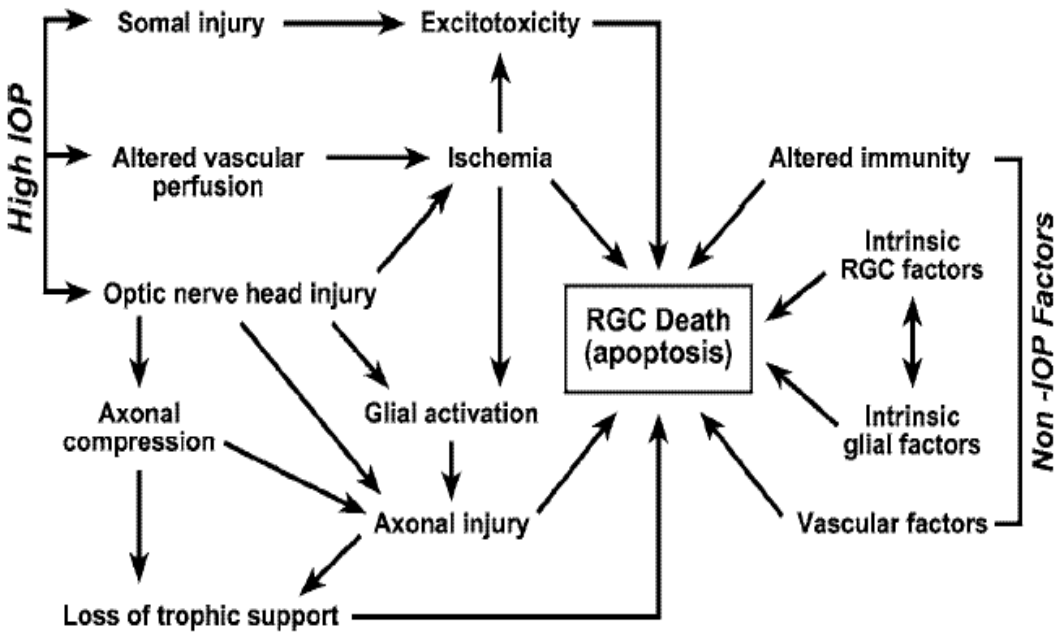

Figure 7. Proposed model for RGC death in glaucoma (Libby *et al.*, 2005)

glial cells may also have toxic effects on neuronal tissue by creating mechanical injury and/or changing the microenvironment of neurons. The

activated glial cells in glaucomatous eyes produce neurotoxic substances such as nitric oxide synthase and TNF-α. In addition, in vitro experiments have provided direct evidence that glial cells are activated in response to glaucomatous stressors such as elevated pressure and ischemia, and directly involved in facilitating the apoptosis of retinal ganglion cells due to increased production of apoptosis-promoting substances, including nitric oxide and TNF-α (Tezel *et al.,* 200**3**).

1.2.7. Experimental animal models for glaucoma

An experimental model for glaucoma is very much useful in order to study the effects of various risk factors on ocular tissues and for developing new therapeutic approaches to the disease. Good animal models are key for undertaking the pharmacological studies. A good animal model should have the following characteristics. It should reproduce human disease as closely as possible, the disease condition should be easily inducible, but should have minimum side effects and should be cost effective. The glaucoma model should also possess following characteristics: increased IOP should be sustained, it should allow for frequent IOP measurements to follow kinetics, and easy assessment of retinal neuronal damage. The following are a few animal models of glaucoma currently used for research purposes, each one with its own advantages and disadvantages.

1.2.7A. Elevated IOP models:

Based on mechanisms used in increasing IOP the glaucoma animal models are further classified as i) Pre-trabecular mechanisms, ii) Trabecular

mechanisms, and iii) Post-trabecular mechanisms. The various animal models and their advantages an disadvantages are listed in Table 1.7 (Rudzinski *et al.,* 2005).

1.2.7B. Acute Models of RGC death:

In addition to elevated IOP models for glaucoma, a few other rat models of RGC damage are used for research purpose. These models damage RGCs acutely, in contrast to glaucoma where it is a chronic.

i) Optic nerve axotomy/crush model:

This is the most extensively studied and used model. This model is generated by Schwartz *et al.,* (1999) by mechanically inflicting a partial lesion at the optic nerve, and is calibrated and reproducible (Yoles and Schwartz, 1998a). Due to the lack of retrograde transport, massive neuronal degeneration at RGC soma occurs within 2 weeks, which is attributed to lack of trophic factors from CNS. This model shows analogy with glaucoma because of two reasons; (I) retrograde pattern of axonal damage, and (ii) blocked of growth factor transport described during high IOP.

The aim of the generation of this model was (i) to demonstrate continuing optic nerve degeneration even after elimination of the primary cause of damage (IOP) and (ii) to determine the secondary degeneration initiation in glaucoma. Using this model it has been shown that elevated levels of intraocular glutamate (Yoles and Schwartz, 1998c), apoptosis effectors such as Caspase 3 and 9 (Kermer *et al.,* 2000), and T-cell mediated autoimmunity are relevent in glaucoma (Fisher *et al.,* 2001). This model also

provided a much-needed opportunity to study and screen for the anti-excitotoxic, anti-apoptotic compounds, which can be neuro protective and useful in treating the glaucoma and other neurological diseases.

The deficiency of this model is that recent data challenge the hypothesis of retrograde centripetal damage in glaucoma. Evidence of RGCs death earlier than 24 hrs of moderate increase in IOP (Lam *et al.,* 2003). This fact of RGC degeneration seems incompatible with the time that retrograde axonal degenerative mechanism would require to reach soma (Naskar *et al.,* 2002). Possible explanations include extreme sensitivity of subset of RGCs to axonal transport block, mechanisms other than retrograde axonal degeneration and direct damage to RGC soma due to high IOP(Rudzinski *et al.,* 2005).

ii) Ischemia/reperfusion model:

This model was generated by complete irreversible central retinal artery occlusion, which resulted in an inevitable course of necrosis of the retina. An extension of this model was the development of simple non-vascular method to cause ischemia-cannulation of the anterior chamber (AC) with subsequent elevation of IOP above systolic blood pressure for various periods of time.

The aim of this model was to mimic the possible chronic hypoxic stress that RGC might undergo in glaucoma. This hypoxic stress leads to the shutdown of all energy dependent functions in RGCs with swelling and disruption of the mitochondria and degeneration of microtubules on the axons.

This model has been used mostly to study damage in RGC. However because this damage is not specific to RGCs but is a general injury to whole retina, it is used to study damage in the outer retina as well. This model has given further evidence to the role of excitotoxicity; caspase mediated apoptosis in the disease pathogenesis.

iii) Excitotoxicity model:

Elevated levels of glutamate in the optic nerve crush model and ischemia/reperfusion model have led to the development of the excitotoxicity model. This model uses excitatory amino acids or their analogues (glutamate, NMDA, kainite), which are agonists of NMDA receptors, as initiators of damage. Glutamate induces selective death of RGCs and severe inflammation in the inner retinal layers, after 48 hrs of injection (Lam *et al.,* 1999).

Excitotoxic damage is suggested to be one of the mechanisms of RGC damage during glaucoma, and hyperactivity of NMDA receptors has been described in glaucoma. A partial NMDA receptor antagonist is being tested as a potential therapeutic agent in glaucoma (Lipton, 2003).

1.2.8. Neuro-protective drugs for glaucoma treatment:

The creation of several experimental models for glaucoma has resulted in a better understanding of the disease pathogenesis. This has resulted in the evolution of a new concept in glaucoma therapy, namely the use of neuro-protective drugs In addition to lowering IOP. These neuro-protective drugs

generally target indirect mechanisms of neuronal damage, such as glutamate release, NO_x production and immune system mediated damage.

Drugs which protect RGC degeneration belong to different groups, which include NMDA antagonists such as memantine and dexanabinol, inhibitors of inducible nitric oxide synthase (NOS-2), neurotrophic factors such as nerve growth factors (NGF), brain derived neurotrophic factor (BDNF), neurotropin 3 etc. Some of the neuro-protective drugs tested in more than two models are listed in Table 1.8 (Rudzinski *et al.,* 2005).

Though the above-mentioned strategies are useful in protecting RGC degeneration in various models, they have certain limitations when it comes to actual clinical use and success. For example, use of high-affinity NMDA blockers blocks virtually complete NDMA receptor activity, but normal activity of these receptors are essential for neuronal signaling. Excessive blockage of the NMDA receptors end up with unacceptable clinical side effects, including hallucination, drowsiness, and coma. This has prompted researchers to look for partial NMDA blockers such as memantine. But then, the use of this kind of drugs might not show complete neurological protection.

Similarly, trophic factors are used to protect degenerating RGC neurons. Trophic factors such as BDNF or NGF act on the tyrosine kinase (Trk) receptor signaling, but this kind of cell signaling is not specific to only RGCs. They will affect cells other than RGCs as well, which might lead to unwanted side effects.

Thus, there is a need to search for compounds which show maximum advantage, with minimum or no side effects. One such possibility is the search for natural anti-oxidants, which can also work through different and multiple mechanisms, such as oxidative stress induced or excitotoxicity induced mechanisms of RGC degeneration in glaucoma.

1.3. SCOPE OF THE STUDY

Congenital hereditary cataract arises due to mutations in various genes, which includes crystallins. Molecular genetic studies on congenital hereditary cataract have resulted in the identification of several mutations in various crystallins, more importantly in γ-crystallins. Understanding the molecular pathogenesis of these mutant proteins might help in looking for strategies which are helpful in preventing the cause. This can be brought about by cloning, expression, structural and functional characterization of the mutant crystallins and comparing them with wild type crystallins.

Since the lens is predominantly made of fiber cells, devoid of metabolism and turnover, molecular damage due to oxidative reactions and posttranslational changes accumulate. The use of compounds that would retard such progression, e.g., antioxidants and cytoprotective agents will be of value as cataractostatic agents. This is an aspect that we have attempted to study.

Glaucoma is the second leading cause of blindness. There is no proper therapy for glaucoma till date, except IOP lowering medications and surgery, which are not much effective in preventing neurodegeneration in glaucoma.

Screening of anti-oxidant compounds, which protect RGC from glaucomatous degeneration induced by various mechanisms, might be of value.

1.3.1. The focus of the thesis

1. Cloning, expression, and solution state, *in silico* and *in situ* (in cell cultures) structural characterization of various mutant γ-crystallins, associated with autosomal dominant congenital cataract.
2. Evaluation of the anti-oxidant and cytoprotective activity of active constituents of various plant extracts such as catechin, epigallocatechin gallate, quercetin, and withaferin A, and their ability to retard damage and death of human lens epithelial cells induced by oxidative stress.
3. Evaluation of the neuroprotective actions of catechin, epigallocatechin gallate, quercetin, and withaferin A, by inducing glaucomatous RGC degeneration in rat retinal ganglion cell lines by excitotoxicity, oxidative stress.

We have studied the solution state, *in silico* and *in situ* structural properties of four cataract-causing mutant γ-crystallins. The mutant proteins include R168W γC-crystallin, 5 bp (dup) γC-crystallin, W157X γC-crystallin and W157X γD-crystallin. We were able to show protein folding defects in 5 bp (dup) γC-crystallin mutant. R168W γC-crystallin showed no major changes in the secondary structure but had an altered quaternary structure. We have studied the importance of C-terminus residues in the stability and solubility of the W157X γC and D- mutant crystallins.

We have also studied the potential anti-oxidant and cytoprotective properties of catechin, epigallocatechin gallate, quercetin and withaferin A. The former three showed very good anti-oxidant properties, but only catechin and quercetin showed protection of lens epithelial cells against stress induced cell death. Epigallocatechin is shown to be toxic to the cells and to induce lens epithelial cell death. Withaferin A neither showed protection nor cellular toxicity.

Turning to the RGC degeneration experiments, catechin showed dose dependent protection against both oxidative stress induced as well as glutamate induced cell death. Quercetin showed protection against this, but did not show any protection against oxidative stress induced cell death in RGCs. Similarly, epigallocatechin gallate was found to be toxic to RGCs, whereas withaferin A did not show any effect.

Table 1.1. Genes associated with AD cataract

S.No.	Gene Symbol	Locus	Protein function
1	CRYAA	21q22-q22.3	Structural/chaperonic
2	CRYAB	11q22.3-q22.1	Structural/chaperonic
3	CRYBB1	22q12.1	Structural
4	CRYBB2	22q11.23	Structural
5	CRYBA1/A3	17q11.2	Structural
6	CRYGC	2q33-q35	Structural
7	CRYGD	2q33-q35	Structural
8	CRYGS	3q25-qter	Structural
9	MIP	12q13	Cytoskeletal
10	BFSP2	3q21-25	Cytoskeletal
11	GJA3	13q11-q12	Gap Junction
12	GJA8	1q21.1	Gap Junction
13	MAF	16q22-q23	Transcription Factor
14	PITX3	10q25	Transcription Factor
15	HSF4	16q21	Transcription Factor
16	GCNT2	6p24	Miscellaneous

Table 1.2. Genes associated with AR cataract

S.No.	Gene Symbol	Locus	Protein function
1	CRYAA	21q22.3	Structural/chaperonic
2	CRYBB3	21q11.23	Structural
3	LIM2	19q13.4	Membrane Protein
4	HSF4	16q21-q22.1	Transcription Factor
5	GCNT2	6p24	Miscellaneous
6	BFSP1	20p11.23-p12.1	Cytoskeletal
7	GJA8	1q21.1	Gap Junction

Table 1.3. Various gene mutations associated with cataract.

Gene Name	**Gene Symbol**	**Chromosomal Location**	**Amino Acid Change**	**Phenotype**	**References**
Crystallin, Alpha A	CRYAA	21q22.3	Trp 9 Term	Congenital Cataract	Pras *et al.,* (2000*) Invest Ophthalmol Vis Sci.* 41, 3511.
			Arg 49 Cys	Congenital Cataract	Mackay *et al.,* (2003) *Eur J Hum Genet*. 11, 784.
			Arg 116 Cys	Congenital Cataract	Litt. *et al.,* (1998) *Hum Mol Genet.* 7, 471.
			Gly 98 Arg	Pre-senile Autosomal Dominant Cataract	Santhiya *et al*. (2006*) Mol.Vis.* 12:768-73.
			Arg 12 Cys	Microcornea, Cataract	Hansen *et al.,* (2007) *Invest Ophthalmol Vis Sci.* 48, 3937-3944.
			Arg 21 Trp	Microcornea, Cataract	Hansen *et al.,* (2007) *Invest Ophthalmol Vis Sci*. 48, 3937-3944.
			Arg 116 His	Microcornea, Cataract	Hansen *et al.,* (2007) *Invest Ophthalmol Vis Sci.* 48, 3937-3944.
Crystallin, Alpha B	CRYAB	11q22.3-q23.1	149 fs	Posterior Polar Cataract	Berry *et al*. (2001) *Am J Hum Genet*. 69: 1141-1145.
			Arg 120 Gly	Alpha-B Crystallinopathy With Cataract	Vicart *et al.,* (1998*) Nature Genet*. 20: 92-95

			Pro 20 Ser	Autosomal Dominant Posterior Polar Cataract	Mugen Liu (2006) *Invest Ophthalmol Vis Sci.* 47:3461-3466
Crystallin, Beta B1	CRYBB1	22q11.2-q12.1	Gly 220 Term	Cataract, Autosomal Dominant	Mackay *et al.,* (2002) *Am J Hum Genet.* 71, 1216
			Ser 228 Phe	Autosomal Dominant Congenital Cataract	Wang *et al*. (2007) *Chin Med J.* (Engl). 120(9): 820-4.
			57 fs	Autosomal Recessive Cataract	Cohen *et al*. (2007) *Invest Ophthalmol Vis Sci.* 48(5): 2208-13.
			Stop 253 Arg	Cataract and Microcornea	Willoughby *et al.,* (2005) *Invest Ophthalmol Vis Sci.* 11:587-593
Crystallin, Beta B2	CRYBB2	22q11.2-q12.2	Gln 155 Term	Cerulean Cataract	Litt *et al.,* (1997) *Hum Mol Genet.* 6, 665.
			Trp 151 Cys	Central Nuclear Cataract	Santhiya *et al.,* (2004). *Invest Ophthalmol Vis Sci.* 45(10): 3599-6.
			Asp 128 Val	Nuclear Cataract	Silke Pauli *et al* (2007) *Mol Vis.* 13:962-7.
			Gene conv. causing C475T (Q155X) and C483T	Cataract, Autosomal Dominant	Vanita *et al.,* (2001) *J Med Genet.* 38:392.

Crystallin, Beta B3	CRYBB3	22q11.2-q12.2	Gly 165 Arg	Autosomal Recessive Cataract	Riazuddin *et al.,* (2005) *Invest Ophthalmol Vis Sci.* 46: 2100-2106.
Crystallin, Beta A1	CRYBA1	17q11.1-q12	IVS 3 G-A Splice+1site	Cataract, Zonular With Sutural Opacities	Kannabiran *et al.,* (1998) *Mol Vis.* 4, 21
			IVS 3 G-C Splice+1site	Cataract, Autosomal Dominant	Bateman *et al.,* (2000*) Invest Ophthalmol Vis Sci.* 41, 3278.
			∆ 279 Gly	Autosomal Dominant Congenital Nuclear Cataract	Qi Y *et al.,* (2004) *Hum Genet*. 114(2):192-7.
Crystallin, Beta A4	CRYBA4	22q11.2-q13.1	Phe 94 Ser	Microphthalmia	Billingsley *et al.,* (2006) *Am J Hum Genet.* 79(4): 702-9.
			Leu 69 Pro	Microphthalmia, Cataract	Billingsley *et al.,* (2006) *Am J Hum Genet.* 79(4): 702-9.
Crystallin, Gamma C	CRYGC	2q33-q35	Thr 5 Pro	Cataract, Coppock-Like	Heon *et al.,* (1999) *Am J Hum Genet.* 65, 1261.
			Arg 168 Trp	Cataract	Santhiya *et al.,* (2002) *J Med Genet*. 39, 352.
			41 fs	Cataract, Zonular Pulverulent	Ren *et al*. (2000) *Hum Genet.* 106(5): 531-7.
			Trp 157 Stop	Autosomal Dominant Congenital Nuclear Cataract	Zhang L. *et al*. (2007) *Inves. Ophthalmo. Vis Sci.* 48: E-Abstract 2443.
Crystallin, Gamma D	CRYGD	2q33-q35	Arg 14 Cys	Punctate Cataract, Juvenile Progressive	Stephan *et al.,* (1999) *Proc Natl Acad Sci.* U S A.96 (3): 1008-12.

			Pro 23 Thr	Cataract	Santhiya *et al.,* (2002) *J Med Genet*. 39, 352
			Pro 23 Ser	Cataract	Plotnikova OV (2007) *Am J Hum Genet*. 81(1): 32-43.
			Arg 36 Ser	Cataract, With Protein Crystallization	Kmoch *et al.,* (2000) *Hum Mol Genet.* 9, 1779
			Tyr 134 Stop	Microcornea, cataract	Hansen *et al.,* (2007) *Invest Ophthalmol Vis Sci.* 48, 3937-3944.
			Arg 58 His	Cataract, Aculeiform	Heon *et al.,* (1999) *Am J Hum Genet*. 65, 1261
			Trp 157 Term	Cataract	Santhiya *et al.,* (2002) *J Med Genet*. 39, 352
			Glu 107 Ala	Nuclear Cataract	Messina-Baas *et al* (2006) *Mol Vis.* 12:995-1000.
Crystallin, Gamma S	CRYGS	3q27.3	Gly 18 Val	Autosomal Dominant Cataract	Sun *et al.,* (2005) *J Med Genet*. 42(9): 706-10.
Major Intrinsic Protein Of Lens	MIP	12q14	Glu 134 Gly	Cataract, Polymorphic and Lamellar	Berry *et al.,* (2000) *Nat Genet*. 25(1): 15-7
			Thr 138 Arg	Cataract, Polymorphic and Lamellar	Berry *et al.,* (2000) *Nat Genet*. 25(1): 15-7.
			Arg 33 Cys	Autosomal Dominant Cataract	Gu *et al.,* (2007) *Mol Vis*. 13:1651-1656

			235 fs	Autosomal Dominant Cataract	David *et al.,* (2006) *Am J Ophthalmol*. 141(4): 761–763.
Beaded Filament Structural Protein-2	BFSP2	3q21.2-q22.3	Arg 287 Trp	Autosomal Dominant Juvenile-Onset Cataracts	Conley *et al.,* (2000) *Am J Hum Genet*. 66(4): 1426-31.
			Δ 233 Glu	Autosomal-Dominant Congenital Cataract	Jakobs *et al.,* (2000) *Am J Hum Genet.* 66(4): 1432–1436.
Beaded Filament Structural Protein-1	BFSP1	20p11.23	Δ 3343 bp	Autosomal Recessive Juvenile Onset Cataract	Ramachandran *et al.,* (2007) *Hum Genet*. 121(3-4): 475-82.
Connexin 50	CX50 (GJA8)	1q21.1	Arg 23 Thr	Progressive Congenital Nuclear	Willoughby *et al.,* (2003) *J Med Genet*. 40: e124.
			Val 44 Glu	Congenital or Developmental Cataract With Microcornea	Devi *et al.,* (2006) *Mol Vis.*12: 190–5.
			Glu 48 Lys	Zonular Nuclear Pulverulent	Berry *et al.,* (1999). *Hum Genet.* 105:168–70.
			Pro 88 Ser	Zonular Pulverulent	Shiels *et al.,* (1998) *Am J Hum Genet*. 62:526–32.
			Pro 88 Gln	Lamellar Pulverulent	Arora *et al.,* (2006). *J Med Genet*. 43: e2
			Val 79 Leu	‘‘Full Moon’’ With Y-Sutural Opacity	Vanita *et al.,* (2006) *Mol Vis*. 12:1217–22.
			Arg 198 Glu	Congenital or Developmental Cataract with Microcornea	Devi *et al.,* (2006) *Mol Vis*.12: 190–5.

			Ile 247 Met	Zonular Pulverulent	Polyakov et. al., (2001) *Clin Genet*. 60:476–78.
			203 fs	Autosomal Recessive Cataract	Surya Prakash *et al.,* (2007) *J Med Genet.* 44:e85.
			Pro 189 Leu	Microcornea, Cataract	Hansen *et al.,* (2007) *Invest Ophthalmol Vis Sci.* 48, 3937-3944.
			Val 64 Gly	Autosomal Dominant Congenital Nuclear Cataract	Ma *et al.,* (.2005) *Br J Ophthalmol.* 89: 1535-1537
Connexin 46	CX46 (GJA3)	13q11-13q12	Phe 32 Leu	Congenital Cataract	Jiang. *et al.,* (2003) *Mol Vis*. 9, 579
			Asn 63 Ser	Congenital Cataract	Mackay *et al.,* (1999) *Am J Hum Genet*. 64, 1357.
			Arg 76 His	Congenital Cataract	Burdon *et al.,* (2004) *J Med Genet*. 41, e106
			Pro 187 Leu	Congenital Cataract	Rees *et al.,* (2000) *Hum Genet*. 106, 206
			380 fs	Congenital Cataract	Mackay *et al.,* (1999) *Am J Hum Genet*. 64(5): 1357-64.
			Thr 87 Met	Congenital Cataract	Guleria *et al.,* (2007) *Mol Vis*. 13:797-803.
			Leu 11 Ser	Congenital "Ant-Egg" Cataract	Hansen *et al.,* (2006) *Mol Vis*. 12:1033-9.
			Asp 3 Tyr	Autosomal Dominant (AD) Zonular Pulverulent Cataract	Addison *et al.,* (2006) *Mol Vis* 12:791-5.

			Arg 76 Gly	Autosomal Dominant Congenital Cataract	Devi *et al.,* (2005) *Mol Vis*. 11:846-52.
			Val 28 Met	Autosomal Dominant Congenital Cataract	Devi *et al.,* (2005) *Mol Vis.* 11:846-52.
			Asn 188 Thr	Autosomal Dominant Congenital Nuclear Pulverulent Cataract	Li *et al.,* (2004) *Mol Vis*. 10:668-71.
			Pro 59 Leu	Autosomal Dominant "Nuclear Punctate" Cataracts	Bennett *et al.,* (2004) *Mol Vis*. 10:376-82.
			Arg 33 Leu	Autosomal Dominant Congenital Cataract	Guleria *et al.,* (2007) *Mol Vis*. 3:1657-1665
			Trp 45 Ser	Autosomal Dominant Congenital Nuclear Cataract	Ma *et al.,* (.2005) *Br J Ophthalmol*. 89: 1535-1537
V-Maf Avian Musculoaponeurotic Fibrosarcoma Oncogene Homolog; Maf	MAF	16q22-q23	Arg 288 Pro	Cataract, Ocular Anterior Dysgenesis and Coloboma	Jamieson *et al.,* (2002) *Hum Mol Genet*. 11, 33
			Lys 297 Arg	Autosomal Dominant "Cerulean Cataract"	Vanita *et al.,* (2006) *Am J Med Genet*. 140(6): 558-66
Paired-Like Homeodomain Transcription Factor 3	PITX3	10q25	Ser 13 Asn	Congenital Cataract	Semina *et al.,* (1998) *Nat Genet*. 19, 167
			216 fs	Congenital Cataract	Berry *et al.,* (2004) *J Med Genet*. 41, e109.
			220 fs	Posterior Polar Cataract	Berry *et al.,* (2004) *J Med Genet*. 41, e109.

Heat-Shock Transcription Factor 4	HSF4	16q21-q22.1	Ala 20 Asp	Cataract, Lamellar	Bu *et al.,* (2002) *Nat Genet*. 31, 276
			Ile 87 Val	Cataract, Lamellar	Bu *et al.,* (2002) *Nat Genet*. 31, 276
			Leu 115 Pro	Cataract, Lamellar	Bu *et al.,* (2002) *Nat Genet*. 31, 276
			Arg 120 Cys	Cataract, Lamellar	Bu *et al.,* (2002) *Nat Genet*. 31, 276
			XII intron Splice site	Cataract, Autosomal Recessive	Smaoui *et al.,* (2004) *Invest Ophthalmol Vis Sci.* 45, 2716
			Arg 74 His	Congenital Total White Cataract	Ke *et al.,* (2006) *Am J Ophthalmol*. 142(2): 298-303.
			Arg 175 Pro	Autosomal Recessive Congenital Cataracts	Forshew *et al.,* (2005) *Hum Genet*.117 (5): 452-9.
			c.595_599delGGGCC	Autosomal Recessive Congenital Cataracts	Forshew *et al.,* (2005) *Hum Genet*.117 (5): 452-9.
Glucosaminyl (N-Acetyl) Transferase 2, I-Branching Enzyme	GCNT2	6p24-p23	Trp 328 Term	Autosomal Recessive Congenital Cataracts	Pras *et al.,* (2004) *Invest Ophthalmol Vis Sci.* 45(6): 1940-5
			Trp 326 Term	Autosomal Recessive Congenital Cataracts	Pras *et al.,* (2004) *Invest Ophthalmol Vis Sci.* 45(6): 1940-5.
Lens Intrinsic Membrane Protein 2 (19kd)	LIM2	19q13.4	Phe 105 Val	Cataract	Pras *et al.,* (2002) *Am J Hum Genet* 70, 1363

Table 1.4. Effect of various mutations on the structure and function of crystallins

Crystallin	Mutation	Effect on Structure	Effect on Function	Solubility	Stability	Protein-Protein Interactions	Reference
αA-crystallin	Arg 49 Cys	-	Abnormally localizes in the nucleus. Loss of protection against apoptosis	-	-		Mackay *et al.,* (2003) *Eur J Hum Genet*. 11(10): 784-93
	Arg 116 Cys	Highly polydisperse homocomplexes. 4 fold decrease in ability to exchange subunits with wild type protein	4 fold decrease in chaperone activity. 10 fold increase in membrane binding affinity	-	-	Interaction with βB2- and γC-crystallins decreased and with αB- and HSP27 increased	Cobb BA and Petrash JM (2000) *Biochemistry* 39 (51): 15791-8. Fu L and Liang JJ. (2003) *Invest Ophthalmol Vis Sci*. 44(3): 1155-9

	Gly 98 Arg	Altered 2^o, 3^o and quaternary structure	Loss of chaperone function	Form Inclusion bodies in heterologous expression systems	Susceptible to heat inducible protein aggregation	-	Singh *et al.,* (2006) *Mol Vis.* 15; 12:1372-9
αB-crystallin	Arg 128 Gly	Probably misfolding	Loss of chaperone function	Forms inclusion bodies and aggresomes	-	Interaction with wild type αA and αB-crystallin decreased and with wild type βB2 and γC decreased	Fu L and Liang JJ. (2003) *Invest Ophthalmol Vis Sci*. 44(3): 1155-9. ChÃ¡vez Zobel *et al.,* (2003) *Hum Mol Genet.* 12(13): 1609-20
βB1-crystallin	Gly 220 Stop	-	-	Reduced solubility	-	-	Mackay *et al.,* (2002) *Am J Hum Genet.* 71(5): 1216-21
βB2-crystallin	Gln 155 Stop	Change in 2^o and 3^o structures	-		Reduced stability to Gdn. HCl	Weak interactions with αA-, αB and γC-crystallin	Liu BF, Liang JJ. (2005) *Mol Vis.* 11:321-7

βA1-crystallin	Δ91 Gly	Defect in folding	-	Reduced solubility			Reddy *et al.,* (2005) *Hum Mol Genet.*13(9): 945-53
γC-crystallin	Thr 5 Pro	Change in 2^o and 3^o structures	-	Reduced solubility	Reduced stability	Decreases interactions with αA-, αB-, βB2 and γC-crystallin	Fu L, Liang JJ. (2002) *FEBS Lett.* 513 (2-3): 213-6
	Arg 168 Trp	No major structural change	-	-	Susceptible to heat inducible protein aggregation	-	Talla *et al.,* (2006) *Invest Ophthalmol Vis Sci.* 47(12): 5212-7
	Trp 157 Stop	Not a major change in 2^o structure	-	Reduced solubility	Susceptible to heat inducible protein aggregation, Reduced stability. Forms scattering particles in-situ	-	Talla *et al.,* (unpublished)

γD-crystallin	Arg 14 Cys	No change in the structure	-	Undergoes thiol mediated aggregation	Forms disulfide linked oligomers	-	Pande *et al.,* (2000) *Proc Natl Acad Sci.* U S A. 97(5): 1993-8
	Pro 23 Thr	No change in the structure	-	Reduced solubility		-	Pande *et al.,* (2005) *Biochemistry* 44(7): 2491-500.
	Pro 23 Ser	No change in the structure	-	Reduced solubility		-	Pande *et al.,* (2005) *Biochemistry* 44(7): 2491-500
	Arg 36 Ser	No change in the structure	-	Reduced solubility	No effect on thermal stability	-	Kmoch *et al.,* (2003) *Hum Mol Genet*. 9(12): 1779-86
	Arg 58 His	No change in the structure	-	Reduced solubility	No effect on thermal stability	-	Pande *et al.,* (2001) *Proc Natl Acad Sci.* U S A. 98(11): 6116-20

	Trp 156 Stop	No change in 2^{o} structure	-	Reduced solubility	Susceptible to heat inducible protein aggregation, Reduced stability. Forms scattering particles in-situ	-	Talla *et al.,* (unpublished)

Table 1.5. Crystal structures and conformational features of different βγ-crystallin

Crystallin	Species	PDB	Resolution	Beta sheet	Helix	Residues	Size	Reference
γD-crystallin	Human	1HK0	1.25 °A	50%	8%	173	20635.1 Da	Basak *et al.,* (2003) *J Mol Biol.* v328 pp. 1137-1147.
γD-crystallin R58H mutant	Human	1H4A	1.15 °A	49%	9%	173	20616.1 Da	Basak *et al.,* (2003) *J Mol Biol.* v328 pp. 1137-1147.
γS-crystallin C-terminal domain	Human	1HA4	2.40 °A	48%	10%	87	10427.9 Da	Purkiss *et al.,* (2002) *J Biol Chem*. v277 pp. 4199-4205.
Truncated βB1-crystallin	Human	10KI	1.40 °A	41%	8%	210 (42-251)	24252.3 Da	Van Montfort *et al.,* (2003) *Protein Sci*. v12 pp. 2606-2612.
Affilin based on Human γB-crystallin	Human/ E.coli	2JDG	2.0 °A	43%	7%	183	21819.9 Da	Ebersbach *et al.,*
γB-crystallin	Bovine	1AMM	1.20 °A	48%	9%	174	20992.7 Da	Kumaraswamy *et al.,* (1996) Acta *Crystallogr Sect*.D v52 pp. 611-622.
C18S mutant γB-crystallin	Bovine	1I5I	2.4 °A	46%	7%	174	20976.6 Da	Asherie *et al.,* (2001) *J Mol Biol*. v314 pp. 663-669.
γD-crystallin	Bovine	1ELP	1.95 °A	45%	8%	173	20778.4 Da	Chirgadze *et al.,* (1996) *Acta Crystallogr Sect.*D v52 pp. 712-721.
γB- crystallin truncated c-terminal domain	Bovine	1GAM	2.60 °A	44%	10%	86	10352.8 Da	Norledge *et al.,* (1996) *Nat Struct Biol*. v3 pp. 267-274.
γF-crystallin	Bovine	1A45	2.30 °A	39%	5%	173	20985.4 Da	Norledge *et al.,* (1997) *Exp Eye Res*. v65 pp. 609-630.
γS-crystallin C-terminal domain	Bovine	1A7H	2.56 °A	40%	13%	80	10319.9 Da	Basak *et al.,* (1998) *Protein Eng*. v11 pp. 337-344.
βB2-crystallin	Bovine	1BLB	3.30 °A	26%	3%	204	23197.8 Da	Nalini *et al.,* (1994) *J Mol Biol*. v236 pp. 1250-1258.
γC-crystallin	Mouse	2V2U	1.90 °A	49%	8%	173	20814.6 Da	Purkiss *et al.,*
N-terminal domain of βB2-crystallin	Mouse/ E.coli	1E7N	2.35 °A			1-106	11911.2 Da	Clout *et al.,* (2000) *J Mol Biol*. v304 pp. 253-257
γE- crystallin	Rat	1A5D	2.30 °A	25%	10%	173	21163.7 Da	Norledge *et al.,* (1997) *Exp Eye Res.* v65 pp. 609-630
Circularly permuted βB2-crystallin	Rat	1BD7	2.78 °A	42%	9%	176	20153.6 Da	Wright *et al.,* (1998) *Protein Sci*. v7 pp. 1280-1285

Table 1.6. Loci and genes associated with glaucoma

Candidate Loci	Gene	Phenotype	Reference
GLC1A (1q24.3-q25.2)	Myocilin (MYOC)	JOAG	Stone *et al.,* 1997
GLC1B (2cen-q13)	-	POAG	Stoilova *et al.,* 1996
GLC1C (3q21-q24)	-	POAG	Wirtz *et al.,* 1997
GLC1D (8q23)	-	POAG	Tritanoc *et al.,* 1998
GLC1E (10p15-p14)	Optic neuropathy inducing protein (*OPTN*)	NTG	Rezaie *et al.,* 2002
GLC 1F (7q35-q36)	-	POAG	Wirtz *et al.,* 1999
GLC 1G (5q22.1)	WD repeat-containing protein 36 (*WDR 36*)	POAG	Monemi *et al.,* 2005
GLC 1H (2p16.3-p15)	-	POAG	Suriyapperuma *et al.,* 2007
GLC 1I (15q11-q13)	-	POAG	Allingham *et al.,* 2005
GLC 1J (9q22)	-	JOAG	Wiggs *et al.,* 2004
GLC 1K (20p12)	-	JOAG	Wiggs *et al.,* 2004
GLC 1L (3p21-22)	-	POAG	Baird *et al.,* 2005
GLC 1M (5q22.1-q32)	-	JOAG	Fan *et al.,* 2007
GLC 1N (15q22-q24)	-	POAG	Wang *et al.,* 2006
GLC3A (2p21)	Cytochrome P450 1B1 (*CYP1B1*)	PCG	Stoilov *et al.,* 1997
GLC3B (1p36.2-p36.1)	-	PCG	Akarsu *et al.,* 1996
GLC3C (14q24.3-q31.1)	-	PCG	Stoilov, 2002

Table 1.7. Glaucoma Models Classified by Mechanisms Used to Increase IOP (Rudzinski *et al.,* 2005).

Mechanism	Procedure	Species	Advantages	Disadvantages
Pre-trabecular	AC injection of viscoelastics substances	Primates, rats	High IOP is easily induced	Short lasting effect IOP spikes
Trabecular	Steroid induced glaucoma	Cat, dogs	High IOP is easily induced	Induction of cataract. Refractory in some rodents
	TM laser photocoagulation	Primates, rats	Resistance to AH outflow occurs in the TM as in humans	Repeat laser treatments to maintain high IOP, Hyphema, Corneal opacities
Post-trabecular	TM sclerosis induced by saline injections	Rats	No inflammation	Repeated injections to maintain high IOP. High variability between rats
	Episcleral venous cauterization	Rats	Easy to perform, Reproducible, Long term reliable high IOP	Choroid vein stasis?

Table 1.8. Neuro-protective drugs tested for glaucoma in animal models (Rudzinski *et al.,* 2005).

Drug	Tested models	Hypothesized mechanism
Dexanabinol	ON crush	Antagonist of NMDA receptors, Anti-TNF a properties
Memantine	Optic nerve crush, glaucoma	NMDA receptor channel blocker
Inhibitors of Inducible NO2	ON axotomy, glaucoma, retinal ischemia	Inhibition of retinal NO2 production
BDNF	ON axotomy, glaucoma	Activation of MAPK/Akt pathway in RGC
Brimonidine	ON crush, glaucoma, retinal ischemia	Upregulation of b-FGF, BDNF and bcl2/bclx, Activation of ERK and Akt survival pathways
Betaxolol	Retinal ischemia, glaucoma	Upregulation of BDNF, Suppression of RGC ionic channels, Downregulation of NO2 synthase
Copaxone	Excitotoxicity, glaucoma	Protective T- cell phenotype induction
Gabapentin-lactam	Retinal ischemia	Open ATP sensitive potassium channels
geranylacetone	Glaucoma	Induction of heat shock proteins by RGCs

MOLECULAR PHENOTYPING OF γ-CRYSTALLINS ASSOCIATED WITH AUTOSOMAL DOMINANT CONGENITAL CATARACT

2.1. INTRODUCTION

γ-Crystallins are the major eye lens crystallins. A large number of mutations in these crystallins are known to be associated with congenital cataract. There are 7 genes in humans, which code for various γ-crystallins, namely γA-F, and γS-crystallins; more than 75% sequence homology is seen among them. The genes γA-F are located on chromosome 2q33-q35 as a gene cluster, whereas γS-crystallin is located on chromosome 3q27.3.

At the gene level these crystallins are coded by 3 exons, and the number of amino acids found to be 173 residues, with the molecular mass of 20-21kDa. γ-Crystallins exist as monomers in the lens. These are the only crystallins which tend to reversibly aggregate at low temperatures, namely 4 °C and below, and are responsible for cold cataract. Any mutation in these crystallins is expected to alter their interaction with the rest of the molecules in the lens and result in opacification.

γC- and γD-crystallins are expressed abundantly in human eye lens, whereas γA and γB-crystallins are expressed in much lower concentration. γE and γF are known to be pseudogenes. γS-crystallin expression has been seen in lens as well as non-ocular tissues. Expression of γ-crystallins are known to be

lens fiber specific, but recent findings suggest that the γ-crystallin expression is seen in the retina and cornea as well.

Due to their abundant expression levels in the lens, and number of mutations identified, the focus of cataract research has shifted towards γC and γD-crystallins. Several studies have been undertaken on structural and functional aspects of these crystallins and the effect of mutation on them, and their relation with cataract phenotype.

The large number of mutations identified in γC and γD-crystallins are listed in Table 1.3. Studies on the structural aspects of γC and γD-crystallins have identified several critical residues which play a crucial role in the formation of stable and highly soluble structure.

Some of the studies focused on the solution state structural properties of the various mutants, and their possible effects on the structure and function of the protein, as listed in the Table 1.4. Structural biologists have elucidated the crystal structure of γD and γS-crystallins (Table 1.5), while those of γC and other γ-crystallins are awaited.

It has been possible for us to clone, express and study the solution state structural properties of crystallins, because of their high solubility and absence of any post-transnational processing. In this chapter we concentrate on four recently reported mutations in γ-crystallins.

2.1.1. A 5-base insertion in the γC-crystallin gene is associated with autosomal dominant variable zonular pulverulent cataract

This mutation was reported (Ren *et al*., 2000) in a seven-generation family consisting of 47 individuals including 30 affected individuals. A 5-base duplication (GCGGC) in exon 2 of γC-crystallin gene was found in all affected individuals. This mutation results in the coding of 38 amino acid residues of the first Greek key motif followed by a frame-shift, which results in 52 random amino acids. These random amino acids do not show any homology with known proteins in the protein databank. We have analysed the secondary structural properties of the mutant mRNA *in silico* using the Gene Bee software, and found that it forms a stable structure at the mRNA level, so that it is able to generate a protein. We further proceeded with the cloning, expression and solution state structural characterization of this mutant protein.

2.1.2. R168W, a point mutation (502 C→T) in exon 3 of γC-crystallin, which is associated with congenital lamellar cataract

Santhiya *et al*., 2002, report this mutation from a family of Indian origin. The Arg at position 168 is highly conserved in γ-crystallins among different species, and falls in the 4th Greek key motif of the structure. This mutation co-segregated in the family and was absent in unaffected family members and controls. We have analysed the effect of this mutation on the structure of γC-crystallin by three ways (i) cloning, expression in heterologous system (*E.coli*), purification and solution

state structural analysis, (ii). *in silico* analysis (homology modeling of proteins), and (iii) properties *in situ*, (cloning, transfection and expression in various cell lines).

2.1.3. A novel nonsense mutation (W157X) in CRYGC associated with autosomal dominant congenital nuclear cataract and microcornea

The mutation W157X in γC-crystallin was reported by Zhang *et al*., (2007) from a four-generation Chinese family affected with nuclear cataract and microcornea. This mutation results in the deletion of 18 residues from the C-terminus. Secondary structural analysis of the mRNA, as mentioned earlier, revealed it to form a stable structure and expected to code for a truncated protein. We have studied the structural properties of this protein by homology modeling and *in situ* by cloning and expressing the mutant protein in various cell lines, e.g., Human Lens Epithelial Cells (HLE3B), rat Retinal Ganglion Cell lines (RGC5) and African green monkey kidney (COS1) cell lines.

2.1.4. A point mutation in the third exon of CRYGD (470G→A) results in the W157X change in the protein associated with congenital central nuclear cataract

Santhiya *et al*., 2002, report this mutation from Indian family. This mutation results in premature termination, and leads to the loss of 18 residues from the C-terminus. Due to this mutation the 4^{th} β-sheet of the fourth Greek key motif in the protein might not be formed, thus leading to major changes in the structure. *In*

silico secondary structural analysis of the mutant mRNA found it to be stable, and expected to form a protein. We have thus gone ahead to study the structural properties of this protein in three ways: by cloning and expressing the protein and analyzing its solution state structural properties, homology modeling, and by transfecting into the cell lines HLE 3B, RGC5 and COS1.

2.2. MATERIAL AND METHODS

2.2.1. Material used

A). The vectors used for cloning and expression

PBSSK+ (Stratagene) and pJET1.2 (Fermentas) vectors were used for cloning and maintenance of various cDNAs. pET21a(+) (Novagen) and pGEX-5X-3 (Amersham Biosciences) were used for expression of recombinant proteins in *E.coli*. pEGFP-C1 vector (Clonetech) was used for the transfection (eukaryotic expression) experiments.

The cDNAs cloned into pET21a(+) vector were cloned in *Nde* I and *Hind* III sites which results in the expression of recombinant protein without any extra sequences. cDNAs cloned into pGEX-5X-3 were cloned in *Bam*HI and *Xho* I sites which resulted in the expression of recombinant protein as fusion at C-terminus of the GST protein. cDNAs cloned into pEGFP-C1 were cloned in *Xho* I and *Bam* HI sites which expresses recombinant proteins as fusions to the C-terminus of a fluorescent reporter EGFP.

B). Characteristics of the vectors used

pGEX-5X-3 vector: This uses the tac promoter for chemically inducible, high-level expression. Very mild elution conditions are sufficient for the release of fusion proteins from the affinity matrix, thus minimizing effects on antigenicity and functional activity. This has a Factor Xa protease recognition site for cleaving the desired protein from the fusion product. See Figure 2.1 for further details.

pET21a(+) vector: This uses the T7 promoter for recombinant protein expression; high levels of recombinant protein expression can be achieved in *E.coli*. The T7 polymerase expression is under the control of *lac* promoter, so that expression can be regulated by chemical induction. It uses the ampicillin selection marker for the selection of transforments. See Figure 2.2 for further details.

pEGFP-C1 vector: This vector codes for a red-shifted variant of wild-type green fluorescent protein which is optimized for brighter fluorescence and maximal expression in mammalian cultures. This uses the human cytomegalovirus (CMV) immediate early promoter for recombinant protein expression. The excitation and emission maxima for GFP are 488 nm and 507 nm, respectively. It uses kanamycin and neomycin resistance markers for selection in prokaryotes and eukaryotes, respectively (Figure 2.3).

C). Bacterial strains used for cloning and expression

DH5 α strain of *E.coli* (Novagen) was used for screening the recombinant clones and for maintenance of recombinant plasmids. BL21(DE3) pLys(S) strain of *E.coli* (Novagen) was used for the recombinant protein expression.

D). Cell lines used

Human Lens Epithelial Cell lines (HLE3B), rat Retinal Ganglion Cell (RGC5) lines, and African green monkey kidney cell (COS1) lines were used for the transfection experiments.

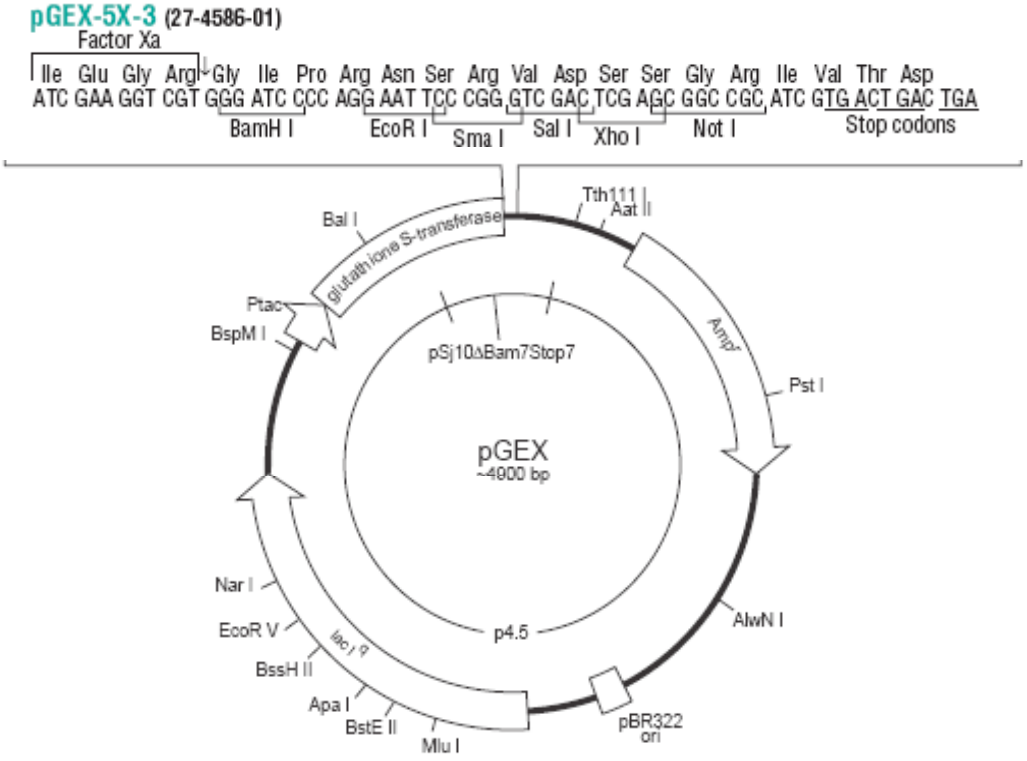

Figure 2. 1. Multiple cloning sites for pGEX-5X-3 vector showing, GST reading frame and Factor Xa recognition site. The reading frames of the recombinant proteins are reconstituted by adding G at 5' of the cDNA.

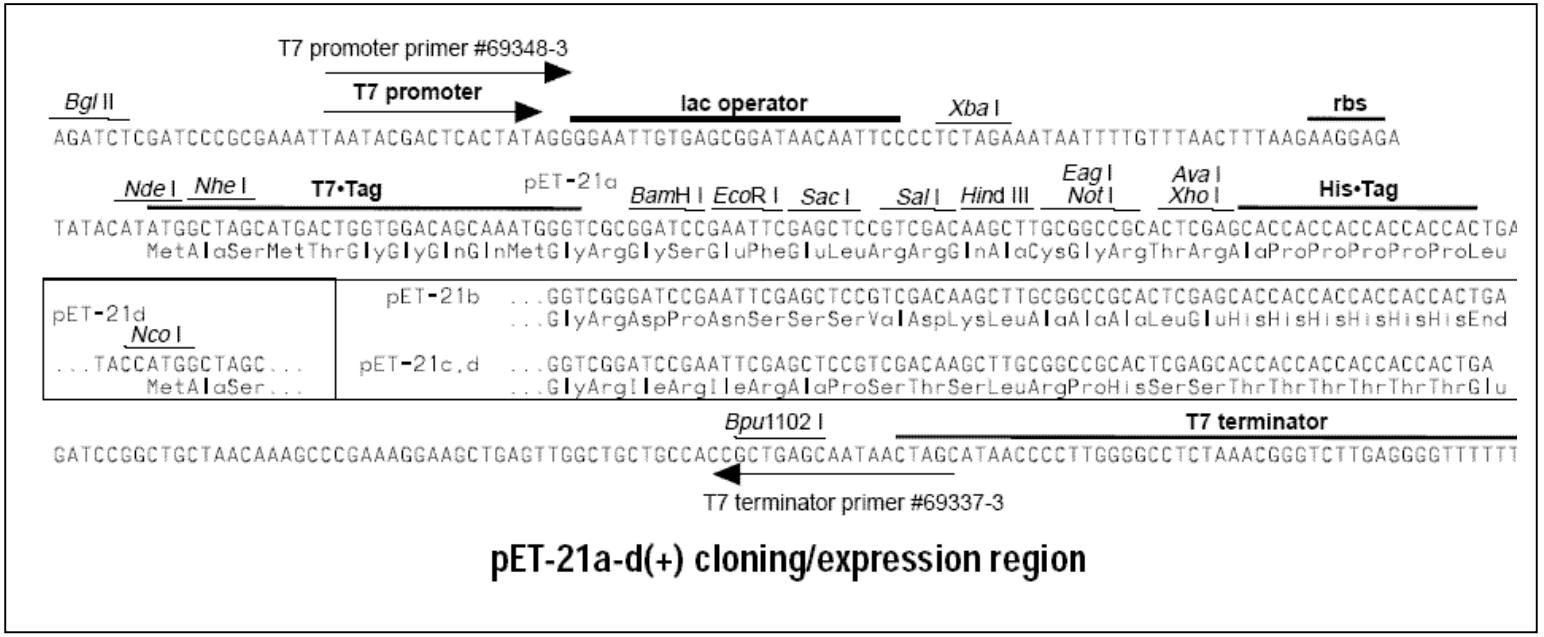

Figure2.1. Multiple cloning site region of pET21a (+) vector along with T7 promoter, ribosomal binding site and start codon.

Cloning of cDNA into *Nde* I site of pET21a (+) vector expressed a pure protein without any tag, which is important to carry out biophysical studies.

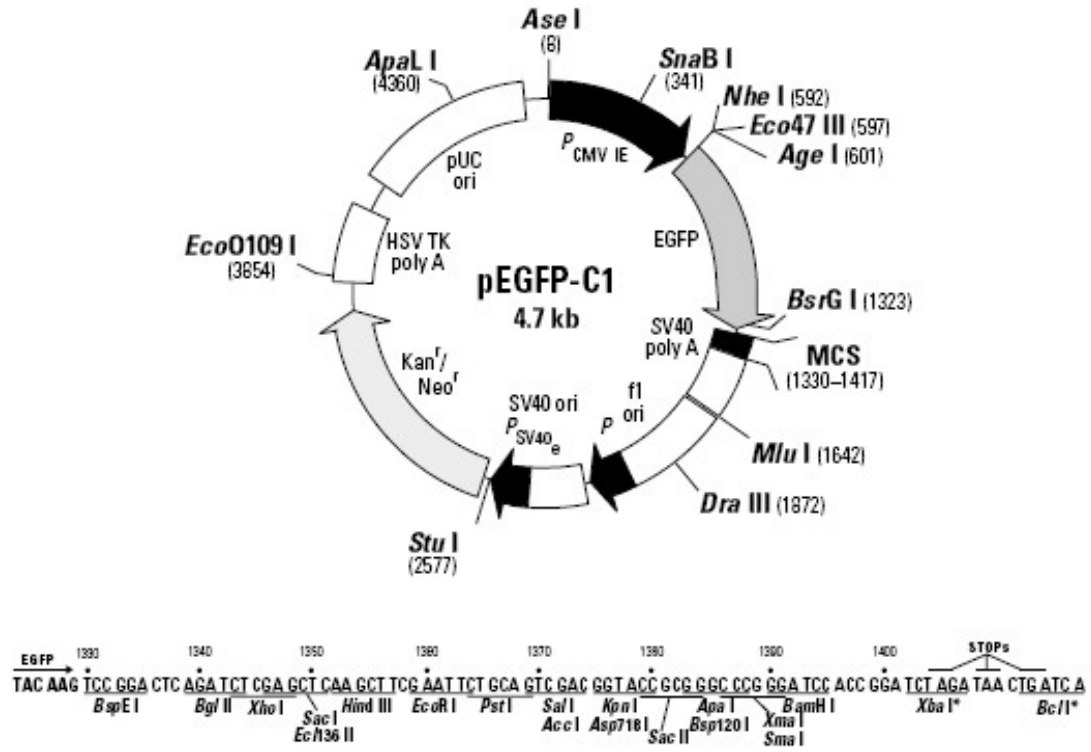

Figure 2.3. pEGFP-C1 vector map showing the reading frame of EGFP protein and the multiple cloning site. All cDNAs were cloned into Xho I and BamHI sites, and the reading frame was reconstituted in all cDNAs by removing the ATGG sequence from the 5' end of cDNAs.

2.2.2. Molecular and biochemical methods

2.2.2A. Total RNA isolation and cDNA synthesis

Human cadaveric eye lens (age 56 years) was collected from the Ramayamma International Eye Bank of the Institute, and total RNA was isolated using Trizol (Invitrogen). The first strand was synthesized by RT-PCR using an oligo-dT

primer and Mu-MLV reverse transcriptase. Human γC and γD-crystallin cDNAs were amplified from the first strand using gene-specific primers as listed in Table 2.1. The primers for the premature termination mutants i.e., W157X γC and W157X γD-crystallins, were designed from the site of mutation. R168W change was introduced in the reverse primer as underlined in the sequence.

2.2.2B. Cloning of wild type and mutant γ-crystallins

All the cDNAs synthesized above were cloned into *Sma* I site of pBSSK(+) vector. Briefly, the PBSSK (+) vector was digested with *Sma* I enzyme and dephosphorylated using Antarctic alkaline phosphatase. All PCR products were phosphorylated using T4 polynucleotide kinase. The phosphorylated PCR products were ligated with dephosphorylated pBSSK vector using T4 ligase. These ligated products were transformed into DH5α strain of *E.coli*, and plated on the LB agar plate containing ampicillin (50 μg/ml), X-Gal (20 μg/ml) and IPTG (1 mM), and incubated overnight at 37 °C. The recombinant colonies were selected using blue white screening and were further confirmed by polymerase chain reaction (PCR) and restriction digestion. The recombinant constructs were sequenced with a ABI prism automated sequencer using T3 and T7 primer, in order to ensure the sequence of normal and mutant cDNAs.

The cDNAs which had to be cloned into pEGFP-C1 vector, were first cloned into pre-digested pJET2.1 vector and the recombinants were further

confirmed by restriction digestion and the sequences were confirmed by sequencing.

i) Sub-cloning of wild type and 5 bp insertion mutant γC-crystallins into pGEX-5X-3 vector:

The pGEX-5X-3 vector was double digested with *Bam* HI, *Xho* I enzymes and the digestion was confirmed by agarose gel electrophoresis and ligating the double digested vector using T4 DNA ligase, followed by transformation. The cDNAs of wild type and 5bp insertion mutant γC-crystallins were released from pBSSK vector by digesting with *Bam* HI and *Xho* I enzymes. Both double digested pGEX-5X-3 vector and insert released from recombinant pBSSK vector were purified from the agarose gel using Qiagen gel extraction kit and the products were quantified spectrophotometrically (absorbance at 260 nm). Ligation reaction was performed at 16 °C overnight, with 1:3 molar ratio of vector and insert. The ligation mix was heat inactivated at 65 °C for 15 min, and transformed into DH5α. After transformation the cells were plated on LB agar containing 50 μg/ml ampicillin and incubated overnight at 37°C. The recombinants were screened using PCR, followed by restriction digestion. The recombinant constructs generated include pGEX-5X-3-γC and pGEX-5X-3-5 bp (ins) γC.

ii) Sub-cloning of wild type γC, γD, R168W mutant γC and W157X mutant γD-crystallin into pET21a (+) vector:

The pET21a (+) vector was double digested with *Nde* I and *Hind* III enzymes, and was purified from agarose gel using Qiagen gel elution columns. The cDNAs of the wild type and mutant γ-crystallins were released from recombinant pBSSK vector using the same enzymes, and were purified from agarose gel using Qiagen gel elution columns. The purified cDNAs were ligated with pET21a (+) vector using T4 DNA ligase. The vector to inset molar ratio used was 1:3, and the ligation reaction was performed at 16 °C overnight. These recombinant constructs generated were transformed into *E.coli* as mentioned above and recombinants were confirmed by PCR and restriction digestion. The recombinant constructs generated as follows, pET21a(+)-γC, pET21a(+)-γD, pET21a(+)-R168W γC, pET21a(+)-W157X γD.

iii) Sub-cloning of wild type γC, γD, R168W, W157X mutant γC and W157X mutant γD-crystallin into pEGFP-C1 vector:

The cDNAs cloned into pJET2.1 vector were released using *Xho* I and *Bam* HI enzymes and were gel purified. The pEGFP-C1 vector was digested with the same enzymes and was ligated with respective cDNAs. The ligated products were transformed into *E.coli*, and recombinants were confirmed by PCR and restriction digestion. The recombinant constructs generated includes pEGFP-γC. pEGFP-γD, pEGFP-R168W γC, pEGFP-W157X γC, and pEGFP- W157X γD.

Similar way the w157X γD and wildtype γD-crystallins were subcloned into Xho I and Bam HI sites of pcDNA3.1(-) vector.

2.2.2C. Induction and over-expression of recombinant γ-crystallins in *E.coli*

The recombinant constructs generated above were transformed into *E.coli* BL21(DE3) plys(S) and were plated on an LB agar plate containing 50 μg/ml ampicillin and 17 μg/ml chloramphenicol , incubated overnight at 37 °C. Single colony was inoculated in 10 ml of LB broth containing 50 μg/ml ampicillin and 17 μg/ml chloramphenicol , incubated at 37 °C, 150 rpm, overnight. A 1% inoculum of the overnight culture was added to fresh 10 ml LB broth with 100 μg/ml ampicillin, 34 μg/ml chloramphenicol and incubated at 37°C, 250rpm, till an OD of 0.6 was obtained at 600 nm. Overexpression was induced using 1 mM isopropyl-β-D-thiogalactopyranoside (IPTG) and the culture was grown at 37°C, 250 rpm. 1 ml of culture was collected after every hour from the time of induction. 1 ml of zero hour culture was collected just before induction as a control sample. Both pre-induction and post-induction samples (1ml each) were removed, centrifuged and cells resuspended in SDS sample buffer (100μl). Expression of the mutant and wild type γ-crystallins was monitored on a 15% SDS/PAGE, after normalizing the cell density, and time point of maximum induction was noted.

2.2.2D. Extraction of recombinant γ-crystallins from *E. coli*

The procedure followed for the extraction of recombinant proteins were adopted from Sun *et al*,. (1997).

1. Cells were harvested by centrifugation at 5000 rpm for 5 min at 4°C. The cell pellet was resuspended in 3 ml of lysis buffer (50 mM Tris.Cl, pH 8.0, 1 mM EDTA, 100 mM NaCl) per gram of *E.coli*.
2. PMSF (0.15 mM final conc.) and lysozyme (250 μg/ml final conc.) was added to above solution and incubated at room temperature for 20 min with occasional stirring.
3. Deoxycholic acid (4 mg per gram of *E.coli*) was added while stirring continuously and incubated at 37 °C. Once the lysate become viscous, DNase I (0.5 μg/ml final conc.) was added and incubated at room temperature until the solution become clear (~30 min).
4. The lysate was then centrifuged at 13,000 rpm for 15 min at 4 °C, the supernatant collected into separate tube and the pellet was dissolved in 100 μl water.
5. Both supernatant and dissolved pellet was loaded on SDS-PAGE to know the status of recombinant protein, i.e whether in soluble fraction or in inclusion bodies.

i) Purification of recombinant wild type and 5 bp (ins) mut γC -crystallins expressed with GST fusion tags

We started with induction of 1L culture, cells were harvested and proteins were extracted as mentioned above. Both the proteins were essentially found in soluble fraction and were purified using GST affinity columns (glutathione Sepharose 6B, from Amersham Biosciences). The recombinant proteins were eluted using glutathione Tris.Cl buffer pH 8.0, and the GST tag was cleaved off by incubating the purified fusion protein with factor Xa at 4 °C for 16 h. The cleaved GST was removed from the recombinant protein by using glutathione Sepharose 6B column, and the added factor Xa was removed by using Benzoyl Sepharose 6B column (Amersham Biosciences).

ii) Purification of recombinant γD, γC and R168W mut γC -crystallins

Induction was done using a 1 L culture, and protein extraction was done as mentioned in the previous session. The cell lysates were collected and ammonium sulphate fractionation was done at 20%, 30% and 60% concentrations. All the fractions were loaded on 12% SDS-PAGE gel and monitored for the recombinant protein. The fraction containing the recombinant protein was taken and excess salt was removed by dialysis using 50 mM Tris.Cl buffer pH 8.0 with 100 mM NaCl. The proteins were further purified by DEAE cellulose column at pH 8.0 and elution by salt gradient of 0-1M NaCl. The OD_{280} was noted for all the fractions, which were pooled checked by SDS-PAGE. The fraction containing the required protein was dialyzed against 50 mM Tris.Cl pH

7.4 with 100 mM NaCl. The recombinant proteins were further purified to homogeneity by gel filtration chromatography on Sephadex G-200. Purity of the protein was assessed by appearance of a single band on SDS-PAGE. The concentration of each protein was calculated based on their molar extinction coefficient.

2.2.2E. Extraction of recombinant W157X γD-crystallin

1. After induction of 1L culture for 3 h, cells were harvested by centrifugation at 5000 rpm for 10 min at 4 °C and the pellet was resuspended in 40 ml ice cold buffer A (20 mM Tris.Cl, pH 7.4, 20% (w/v) sucrose, 1 mM EDTA) and incubated on ice for 10 min.
2. The cell suspension was centrifuged at 11,000 rpm for 5 min at 4 °C (Sorvall RC5 plus) and the cell pellet was resuspended in 40 ml ice-cold water, incubated on ice for 10 min.
3. The cell suspension was centrifuged again at 11,000 rpm as mentioned above and the cell pellet was resuspended in 10 ml of ice cold buffer P (PBS 10 mM, pH 7.2, 5 mM EDTA, 20 μg/ml Aprotinin, 1 mM PMSF) and sonicated at 25 X 30 s (with 30 sec intervals) [Ultrasonics Sonicator].
4. DNase I (250 μg), RNase A (50 μg) and 0.5M $MgCl_2$ (200 μl) was added and incubated at room temperature for 10 min.
5. The inclusion bodies were harvested by centrifugation at 11,000 rpm for 30 min at 4 °C.

6. The pellet was resuspended in 1 ml buffer P and 40 ml buffer W (10 mM PBS, pH 7.2, 25% sucrose (w/v), 5 mM EDTA, 1% Triton X-100, 1 mM PMSF) and centrifuged at 20,000 rpm for 10 min at 4°C,
7. The washing was repeated two to three times, and the final pellet was resuspended in buffer D (50 mM Tris.Cl, pH 8.0, 5 mM EDTA, 8M Urea, 5 mM DTT) at room temperature and either stored at –20 °C or continued with folding immedietly.

i) Re-folding of recombinant W157X mutant γD-crystallin

The solubilized protein in buffer D was diluted 10 times in ice cold folding buffer (50 mM HEPES, pH 7.5, 0.2M NaCl, 1 mM DTT, 400 mM L-Arginine, 1 mM PMSF). The protein solution was dispensed into the folding buffer using a syringe, under vigorous stirring using a magnetic stirrer and the stirring was continued for 2 min even after addition and incubated at 4°C for 1 h. The protein solution was dialyzed against buffer containing 50 mM Tris.Cl, pH 8.0 at 4°C, with four changes of buffer.

ii) Purification of recombinant W157X γD-crystallin

The re-folded W157X γD-crystallin was concentrated using ultra-spin columns and further purified to homogeneity by gel filtration chromatography on Sephadex G-75. A single band on SDS-PAGE confirmed the purity of the mutant protein. The concentration of the mutant protein was estimated based on its theoretical molar extinction co-efficient.

2.2.2F. Spectroscopic analysis of recombinant proteins

i) Fluorescence spectra

a) Intrinsic fluorescence spectra

Intrinsic fluorescence spectra were recorded at 20°C using a Hitachi F-2500 fluorescence spectrophotometer equipped with circulating water bath to control temperature. The fluorescence emission spectra were recorded in the range of 300-400 nm by using an excitation wavelength of 295 nm, with 2.5 nm excitation and emission slits. The concentration of protein used was 0.1 mg/ml. Three scans for each spectrum were averaged and baselines (buffer alone) subtracted.

b) Extrinsic fluorescence spectra:

Extrinsic fluorescence spectra of proteins were recorded using 100 μM final concentration of 8-anilinonaphthalene-1-sulffonate (ANS) as an external probe. The spectra were recorded in the range of 400-600 nm by using an excitation wavelength of 390 nm. The protein concentrations used in these experiments were 0.1 mg/ml in Tris.Cl buffer pH 7.4. Three scans for each spectrum was averaged and baselines (buffer alone) were subtracted.

ii) Circular Dichroism spectra

Circular Dichroism (CD) spectra were recorded (at CCMB, Hyderabad) with a Jasco J-715 spectropolarimeter at room temperature. Protein concentrations of

0.6 mg/ml and 0.1 mg/ml were used for recording the near- and far- UV CD spectra, with 1 cm and 0.1 cm path length quartz cells, respectively. Three scans of each spectrum were averaged, smoothed, and baselines (of buffer) substracted. The ellipsity values obtained were converted into mean residue mass units and were plotted against the wavelength.

iii) Guanidinium chloride (Gdn.HCl) induced unfolding and refolding

Un-folding experiments were carried out by diluting the wild type and mutant γ-crystallins to 25 μg/ml into increasing concentrations of Gdn.HCl from 0 to 6 M. The unfolding samples were incubated at room temperature for 24 hours, by which time equilibrium had been reached.

Refolding experiments were carried out by initially preparing an unfolded stock solution of 100 μg/ml proteins by incubating for 24 hours in 6 M Gdn.HCl. Unfolded proteins were refolded by dilution into the folding buffer (50 mM HEPES pH 7.5 containing 0.2 M NaCl, 1 mM DTT, 400 mM L-arginine and 1mM PMSF) to a final concentration of 10 μg/ml γ-crystallins and 1 to 5 M Gdn.HCl. Fluorescence emission spectra were recorded in the range of 300-400 nm using an excitation wavelength of 295 nm, and baseline spectra of Gdn.HCl solutions from 0-6 M were subtracted. Data was analyzed by plotting the fluorescence intensity at 360/320 nm versus Gdn.HCl concentration.

iv) Thermal stability measurement

Thermal denaturation properties of the wild type and mutant crystallins were studied by monitoring the temperature dependent changes in the trp emission intensity and wavelength. Fluorescence spectra were recorded between 20-70°C at 5 °C intervals. A 15 min equilibrium time was allowed for each temperature and the temperature was controlled with a Julabo F-12 circulating water bath. The fluorescence emission spectra were collected in the range of 300-400 nm, using excitation wavelength of 295 nm, and base line spectra of buffer alone (Tris. Cl pH 7.2) were subtracted. Data was analyzed by plotting the % decrease in fluorescence emission at 320 nm versus temperature.

v) Time dependent light scattering experiments

For the time dependent light scattering measurements, a fluorescence spectrophotometer was used with both excitation and emission wavelengths set at 600 nm, and measurements were done at 65 °C. Solutions of the wild type and mutant proteins, each at 10 μg/ml in Tris. Cl buffer, were taken and scattering at 600 nm was measured as a function of time, up to 1200 sec. The base line for the buffer alone was subtracted. Average values from three scans were plotted in the graphs.

2.2.3. Homology modeling of γ -crystallins

2.2.3A. Sequence-based search

The sequence of γC-crystallin was queried against the Non-Redundant Database (NRDB) using the position-specific search strategy called PSI-BLAST (Altschul *et al*., 1997), with an E-value cut-off of 0.001 to obtain all possible proteins based on sequence homology. The Hidden Markov Model (HMM) based search, HMMPfam (Eddy, 1998), was also done against the Pfam database (Bateman *et al*., 2000) to assign Pfam domains to this protein.

2.2.3B. Structure-based search

The sequence of γC-crystallin was submitted to the different fold recognition servers including Fugue (Mizuguchi *et al*., 1998; Shi *et al*., 2001) and position-specific scoring matrix or 3D-PSSM (Kelly *et al*., 1999) to obtain homologs based on sequence-structure comparison. A hit obtained with high reliability, determined by the score corresponding to each hit, was used as a template to generate the structure of this protein.

2.2.3C. Comparative modeling of γ- crystallins

The three-dimensional structure of γC-crystallin was modeled using the crystal structures of proteins obtained with high reliabilities in the structure-based search procedure. The crystal structure of bovine γB-crystallin (PDB ID 1gcs) (Lindley *et al*., 1993) was used as a template. The structure was generated using the

homology modeling software MODELLER (Sali and Blundell, 1993) version 7. The so generated structure was energy minimized using the computational toolkit SYBYL (Tripos, Inc., St. Louis, MO, USA) to remove short contacts and to optimize the stereochemistry of the molecule. Minimization was done with the consideration of the electrostatic term in presence of the force field termed as AMBER (Weiner *et al*., 1984). The surface potential of the protein was determined using GRASP, which does a graphical representation and analysis of structural properties, (Nicolls *et al*., 1991) to study the distribution of charge on the surface of this protein.

i) R168W mutant structure generation

The structure of the mutant was generated by replacing the arginine residue at position 168 with tryptophan (R168W), in the MODELLER generated structure of γC-crystallin. The mutant structure thus obtained was optimized by energy minimization in SYBYL using the AMBER force-field. The surface charge distribution of the mutant structure was determined using GRASP. The GRASP outputs of the wild type and the mutant structures were analyzed to study the possible structural and surface changes in the mutant structure that leads to the enhanced aggregation of the mutant protein.

ii) Analysis of W157X mutant γC and γD-structures using molecular modeling

The three-dimensional structure of the human γC-crystallin was modeled on the basis of the crystal structure of bovine γB-crystallin (PDB ID 1gcs) as discussed above. The human γD-crystallin model was retrieved from the crystal structure data provided by Basak *et al.,* (2003) in the Protein Data Bank (PDB, ID 1HK0). The effect of the deletion of C-terminus 18 residues on the structure of the two proteins was analyzed using the software SETOR. Surface charge distributions of the wild type and mutant molecules were estimated and visualized using the software GRASP. The three dimensional solid model representations were generated using the software SETOR (Evans, 1993). All the modeling studies were done in the laboratory of professor N. Srinivasan of the Molecular Biophysics Unit of the Indian Institute of Science, Bangalore.

2.2.4. Cell culture experiments

2.2.4A. Cell culture

The Human Lens Epithelial (HLE3B) cell lines, rat Retinal Ganglion Cell (RGC5) lines and African green monkey kidney (COS1) cell lines were cultured in the DMEM medium with 10% FCS at 37^0C and 5% CO_2 until it reaches to the 70% confluency in the T-25 culture flask. The cells were trypsinized with the 0.025% trypsin. Once the required confluency was obtained, the cells were washed with

PBS in order to remove trypsin and cell debris. Cell counting was done using heamocytometer, and was used for further transfection experiments.

2.2.4B. Transfection into various cell lines

One day before transfection the cells (~ 60,000) were seeded on 22 mm cover slip in a 6 well culture plate and incubated in humidified, 5% CO_2 incubator at 37 °C for 24 hours. The medium was removed and PBS wash was given in order to remove the cell debris and FCS. Serum free DMEM (100 μl) was added to the cells on the clover slip. The cells were then transfected with the recombinant constructs using the Lipofectamine 2000 reagent at the ratio 1:2 (~500 ng of vector: 1 μl of reagent). After incubation for 4-5 h, the serum-free medium was replaced with complete medium (DMEM + 10% FCS) and incubation continued 24 to 48 h for imaging analysis. The constructs used for the transfections were, pEGFP-WT γC, pEGFP-WT γD, pEGFP-R168W γC, pEGFP-W157X γC, pEGFP-W157X γD, pcDNA 3.1(-)-WT γD, pcDNA 3.1(-)-W157X γD, pEGFP-C1 and pcDNA3.1(-) vector.

2.2.4C. Confocal microscopic imaging

Following incubation, the transfected cells were washed with PBS and fixed using 4% para-formaldehyde for 30 min. The cells were washed with PBS thrice for 5 min each, and were stained with propidium iodide for one min. Excess amount of the stain was removed by a PBS wash. The cover slips with the cells were then mounted using 50% glycerol in PBS and observed using a LSM510

Zeiss laser scanning confocal microscope. The excitation lasers used were 488/543 nm and the emission of green fluorescence was collected using the 505-530 nm band-pass filter (channel 2) and red fluorescence was collected with the 585-615 nm band-pass filter (channel 3).

2.2.4D. Immunofluorescence for γ-crystallins

The cDNAs of wild type and mutant human γD-crystallin were cloned into pcDNA3.1(-) vector under the Xho 1 and Bam H1 sites and were transfected into RGC5 and HLE3 cell lines on 22 mm2 cover slips. The cells were fixed using 4 % formaldehyde and permeabilized using PBS containing 0.1% Triton X100 for 10 min. The cells were washed thrice with PBS and incubated with anti-human γ-crystallin antibody (raised in rabbit, and kindly gifted by Dr. J. Samuel Zigler) for 1 hr. They were then washed thrice and incubated with TRITC conjugated anti rabbit antibody. Excess and unbound antibody was removed by washing the coverslips with PBS, mounted on glass slides and observed using a confocal microscope. The excitation lasers used were 514/543 nm and fluorescence emission was collected using 585-615 nm band-pass filter.

2.2.4E. Western blotting

Cells were harvested from T-25 culture flask 48 hrs after transfection and suspended in 300 μl of Brij buffer (0.1 M Tris. Cl, pH 7.5, O.5 M NaCl, 1% Brij 96, 1% NP40, 2 mM EDTA, 1 mM PMSF, 3μg/ml aprotinin) and lysed by sonication 4X30 s (30 sec intervals) at 35% amplitude using a Sonics Vibra Cell (Sonics &

materials Inc. USA). The cell lysate was centrifuged at 13,000 rpm, 4°C for 15 min. Supernatant was separated and the pellet was dissolved in 50 μl of 1X SDS loading buffer. Both lysate and cell pellet dissolved in SDS loading buffer were separated on 12% SDS-PAGE, and blotted on to nitrocellulose membrane using a horizontal semi-dry blotting apparatus (Amersham Biosciences). The nonspecific binding sites were blocked with TBS (0.05% of Tween 20 and 5% non-fat milk in PBS) overnight at 4 °C. The membrane was incubated with rabbit monoclonal antibody raised against purified EGFP (Santa-Cruz Biotechnology, Inc), 1:1000 in blocking buffer for 2 hours at room temperature. Three TBST (0.05% of Tween 20 in PBS) washes (5 min each) were given to remove the unbound antibody and the membrane was incubated with horseradish peroxidase (HRP)-conjugated anti-rabbit immunoglobulin G (Sigma Aldrich, 1:6,000 in blocking buffer) for 1 hr at room temperature. Excessive amount of the secondary antibody was removed by washing the membrane three times (5 min. each) with TBST and the bands were visualized with enhanced chemiluminescence method. Briefly the membrane was incubated for 1 min with HRP substrate (1:1 ratio of solution I (100 mM Tris pH 8.5, 0.4 mM coumaric acid, 2.5 mM luminol) and solution II (100 mM Tris Cl pH 8.5, 5 mM H_2O_2). The substrate was drained off, the membrane was wraped in a saran wrap and exposed to hyperfilm X ray sheet for desired length of time (1 min, 2 min, 5min, 10 min). The hyperfilm exposed to membrane was then developed and fixed using a Kodak X-ray developer and fixative.

Table 2.1. Primeres used for amlification and cloning of various γ-crystallins

S. No	Recombinant γcrystallin constructs generated	Primers used for cDNA synthesis & cloning	Restriction enzymes
1	pGEX-5X-3-WT γC	F 5'-GCGGATCCGGGAAGATCACCTTCT-3'	*Bam HI*
		R 5'-GCCTCGAGTAATACAAATCCACCACTCT-3'	*Xho I*
2	pGEX-5X-3-5bp dup γC	F 5'-GCGGATCCGGGAAGATCACCTTCT-3'	*Bam HI*
		R 5'-GCCTCGAGTAATACAAATCCACCACTCT-3'	*Xho I*
3	pET21a(+)-WT γC	F 5'-GCCATATGGGGAAGATCACCTTCT-3'	*Nde I*
		R 5'-CCAAGCTTTTAATACAAATCCAC CACTCT-3'	*Hind III*
4	pET21a(+)-R168W γC	F 5'-GCCATATGGGGAAGATCACCTTCT-3'	*Nde I*
		R 5'-CAAGCTTTTAATACAAATCCACCACTCTCCAC-3'	*Hind III*
5	pEGFP-C1-WT γC	F 5'-GCCTCGAGGGAAGATCACCTTCTA TG-3'	*Xho I*
		R 5'-GCGGATCCTTAATACAAATCCACCACTCT-3'	*Bam HI*
6	pEGFP-C1-W157X γC	F 5'-GCCTCGAGGGAAGATCACCTTCTA TG-3'	*Xho I*
		R 5'-GCGGATCCCTAGTCCTGGTAGCGCCTATA-3'	*Bam HI*
7	pET21a(+)-WT γD	F 5'-GCCATATGGG GAAGATCACCCTCTA-3'	*Nde I*
		R 5'-GCAAGCTTTCAGGAGAAATCTATGA CTCT-3'	*Hind III*
8	PET21a(+)-W157X γD	F 5'-GCCATATGGG GAAGATCACCCTCTA-3'	*Nde I*
		R 5'-GCAAGCTTCTAGTCCTGGCA CCGCCTGTA-3'	*Hind III*
9	pEGFP-C1-WT γD	F 5'-GCCTCGAGG GAAGATCACCCTCTA-3'	*Xho I*
		R 5'-GCGGATCCTCAGGAGAAATCTATGA CTCT-3'	*Bam HI*
10	pEGFP-C1-W157X γD	F 5'-GCCTCGAGG GAAGATCACCCTCTA-3'	*Xho I*
		R 5'-GCGGATCCCTAGTCCTGGTAGCGCCTATA-3'	*Bam HI*

2.3. RESULTS

Molecular genetic analysis of cataract have revealed an association of various gene mutations with the congenital cataract phenotypes. But these studies cannot provide the mechanistic insights into the effects of the mutation on the cells. Studies on mutant proteins at the molecular structural level would be able to provide the necessary information on the pathophysiology.

In this chapter we describe the molecular structural features of some of the mutant crystallins studied, i e., 5 bp dup, R168W, W157X γC- and W157X γD-crystallins. Here we provide the evidence for the aggregation-prone status of mutant proteins by three different means. The first one is based on *in silico* analysis (protein homology modeling) of the mutant proteins in comparison to wild type proteins; the second is based on solution state structural properties of mutant proteins in comparison to wild type proteins; and the third one is the monitoring of mutant protein aggregation *in situ* in various cell lines, namely Human Lens Epithelial Cells (HLE3B), rat Retinal Ganglion Cell (RGC5) and African green monkey kidney cell (COS1) lines, upon transfection with the mutant cDNAs.

2.3.1. The 5-base insertion mutant γC-crystallin:

2.3.1A. *In Silico* analysis of 5 bp dup γC-crystallin

Duplication of the 5-base sequence GCGGC at position 230 that falls in exon 2 of the γC-crystallin gene disrupts the reading frame. Thus, the resultant protein shows homology only in the N-terminal 38 residue sequence of the

first “Greek key” motif with the wild type molecule. This homologous sequence is followed in the mutant by a 62-residue-long sequence of random amino acids. These 62 random amino acids did not show any homology with the proteins present in the available protein data bank. Homology modeling of this mutant protein sequence revealed that the N-terminal 38 residues represent the first half of the first domain of the canonical two-domain structure of the γ-crystallins. The other half of the first domain is a structural repeat of the first half. Considering all known structures of the crystallins and related systems, we infer that there is no evidence that the first half of the first domain (i. e., the N-terminal 38- residue sequence) has a stable structure on its own. Also, the amino acid sequence of the latter part of the mutant molecule suggests no ordered structure. We thus expect that this mutant γC-crystallin molecule to exist in a disordered chain conformation.

2.3.1B. Over-expression and solution state structural properties of wild type and 5 bp dup γC-crystallin

The cDNAs of wild type and 5 bp dup γC-crystallin were first cloned into *Nde* I / *Hin* dIII sites of pET21a(+). Restriction digestion and direct sequencing confirmed the sequences of the recombinants. These recombinant constructs were transformed into the BL-21(DE3) pLys(S) strain of *E. coli* and used for induction and over-expression of the recombinant proteins. Induction of recombinant constructs with various concentrations of IPTG and time points resulted in the over-expression of wild type protein but not the mutant protein. We then re-cloned the wild type and mutant cDNAs into *Bam* HI / *Xho* I sites of pGEX-5x-3 vector which contains the N-terminus GST tag. The presence of

GST tag is expected to stabilize and increase the solubility of recombinant proteins, and also helps in their purification. The pGEX-5X-3 vector also harbors the factor Xa recognition site immediately after the GST protein. The recombinant constructs were transformed into BL-21(DE3) pLys(S) and induction was done with 1 mM IPTG which resulted in the over-expression of both wild type and mutant proteins. The expression levels of recombinant proteins increased with time, reaching maximum at 3-4 hr post induction. Both the over-expressed recombinant proteins were seen in the soluble fraction.

The purified proteins were near homogeneity as shown on SDS PAGE gel (Figure 2.4). Upon removal of GST, the wild type protein was found essentially in soluble fraction, whereas major amount of the mutant protein was in the aggregated form. We further noted that this protein was soluble only at concentrations below 0.1 mg/ml. When the concentration is increased to 0.3 mg/ml and beyond, the protein coagulates and drops out of solution.

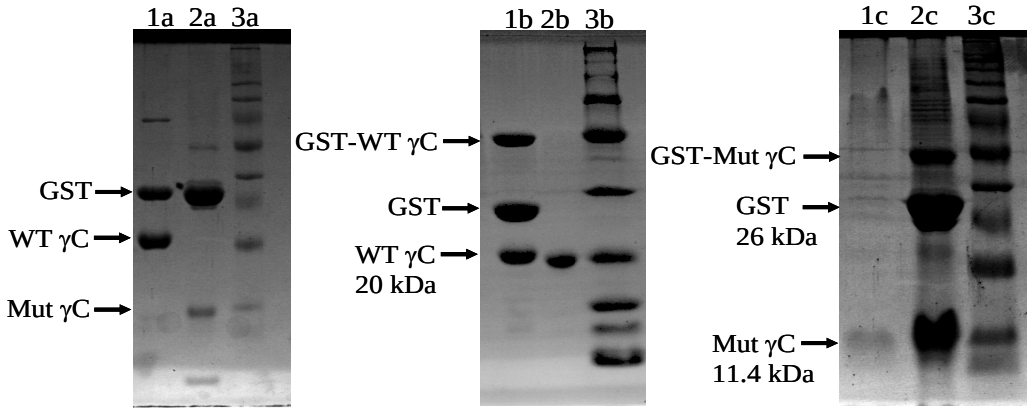

Figure 2.4. SDS-PAGE (12%) showing purified wild type and mutant γC-crystallins, along with the cleaved GST tag. GST-WT γC cleaved with Factor Xa (lane 1a, 1b), GST-mut γC cleaved with Factor Xa (lane 2a, 2c), purified wild type γC (lane 2b), purified mut γC-(lane 1c) and the broad range molecular weight marker from sigma (3a, 3b and 3c)

Spectroscopic study of the protein, shown in Figure 2.5 and Figure 2.6,

supports our in silico analysis results. The intrinsic fluorescence of the protein, largely due to its Trp residues, showed a band maximum at 340 nm, red-shifted by 14 nm from that of the wild type molecule (Figure 2.5A). The surface hydrophobicity of the mutant was evaluated using the fluorescence spectrum of the extrinsic probe ANS (Figure 2.5B). The 20 nm blue shift and three-fold enhanced intensity of the probe bound to the mutant, compared to the situation when it is bound to the wild type molecule, point out that the mutant molecule has a more pronounced hydrophobic surface (Cardamone, *et al*., 1992).

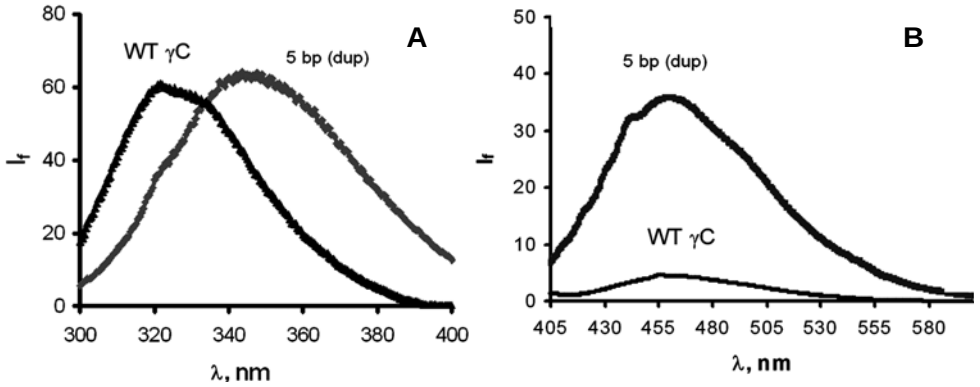

Figure 2.5 A) intrinsic fluorescence of wild-type and 5-bp dup mutant human γC-crystallin. Excitation at 295 nm. B). extrinsic fluorescence of the surface hydrophobicity probe ANS bound to WT and 5-bp dup human γC-crystallin. Excitation at 390 nm.

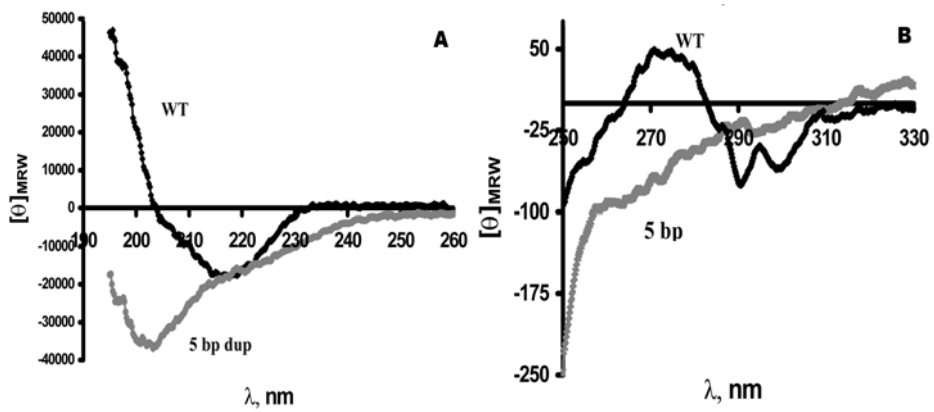

Figure 2.6. **Panel A**) Far UV CD spectra of the wild-type (WT) and 5-bp dup mutant human γC-crystallin. **Panel B**) Near UV CD spectra of the WT and 5-bp dup mutant human γC-crystallin. Ellipticity values are expressed in residue molar units.

The far-UV CD spectrum (Figure 2.6A) corresponds to that of a random coil, and the near-UV spectrum (Figure 2.6B) too shows no tertiary structural order.

2.3.2. R168W γC-crystallin:

2.3.2A. Homology modeling studies

The HMM based search of the γC-crystallin sequence against the Pfam database led to the identification of two domains, both corresponding to the βγ-crystallin family of proteins (E=8.8 X 10^{-47} and E=2.2 X 10^{-49} respectively). The query picked up homologous γ-crystallin proteins as hits with high reliabilities in the PSI-BLAST search against the Non-Redundant database. Several γ-crystallins, whose crystal structures have been determined, were picked up with high sequence identities of around 75%. The structure-based search using the different fold recognition servers led to the identification of several γ-crystallins with high reliability (Fugue Z score >6.0). The top hit with the highest score, a bovine γB-crystallin mutant (Asherie *et al*., 2001) (protein databank code: 1I5I), shared a

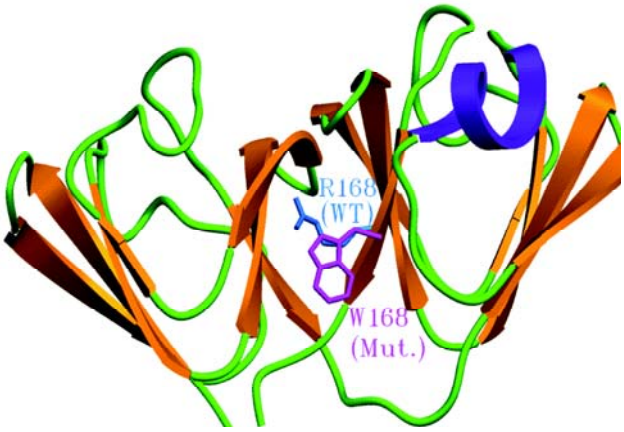

Figure 2.7. Structure of human γC-crystallin (wild type), generated using MODELLER. The structure also shows the superimposition of tryptophan on arginine at position 168 and the side chain orientation pattern in wild type and in R168W mutant.

75% identity with the human γC-crystallin. The structure of this protein was therefore used as a template to generate the model of the human γC-crystallin.

The structures of γ-crystallins are known to be (Figure 2.7) composed of two similar domains folded into a Greek key motif pattern, each of which, in turn, is composed of two similar motifs. A short loop region connects the two domains. The R168W mutant structure is expected to retain the overall fold as the wild type as the site of mutation is solvent exposed and the modeled structure confirms that Trp in the mutant is accommodated comfortably in the classical γ-crystalline fold. This Trp168 residue is observed to be solvent accessible with the nitrogen atom of the side chain towards the exterior suggesting a possible polar interaction of the Trp side chain.

In the model of the wild type, the Arg side chain is seen to form hydrogen bonds within the domain in which it is situated. No strong interaction is seen between the Arg side chain and the other domain across the domain-domain interface. In the mutant structure, Trp is exposed due to lack of sufficient space between the two domains of the crystallin fold (Figure 2.8).

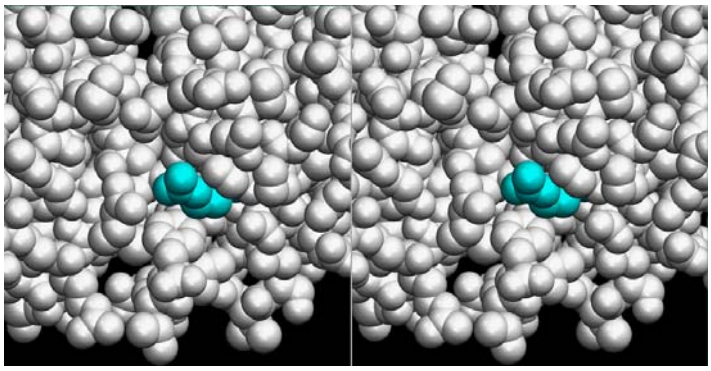

Figure 2.8. Stereo pair of the close-up of the inter-domain interface in the R168W mutant model, with the Trp at the site of mutation highlighted. This Trp residue is seen to be exposed, due to lack of sufficient space in the domain-domain interface; this feature might contribute towards aggregation. Figure produced using the 3-dimensional model representation 'SETOR'.

The three dimensional model of the molecule shows a good number of exposed aromatic side chains, positively charged side chains, and Cys and Met residues, which are capable of interacting with the exposed Trp in the site of mutation (Figure 2.9).

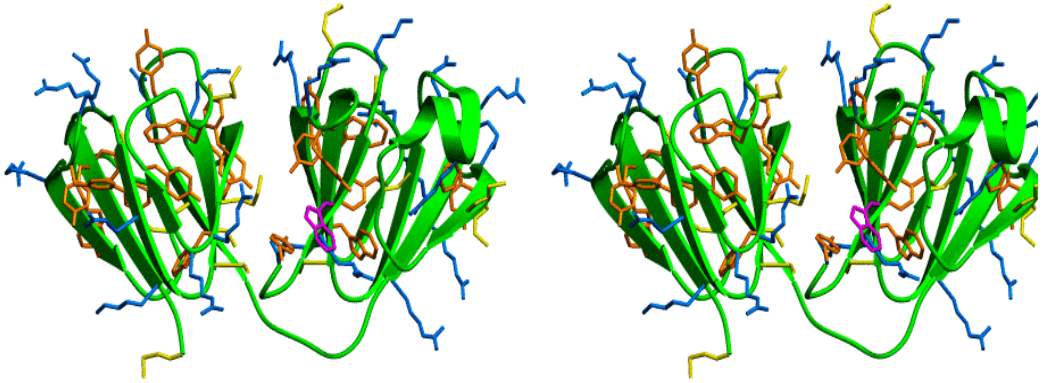

Figure 2.9. Stereo pair of the modeled structure of the R168W mutant, with all aromatic, basic (cationic) and sulfur-containing residues shown in different colors. Many of these residues are exposed. The Trp at the site of mutation is highlighted in pink color. Figure produced using SETOR

The mutant structure shows a long stretch of hydrophobic residues on the surface in addition to a small hydrophobic patch (Figure 2.10), with a gap in between that could possibly accommodate the Trp side chain. The overall

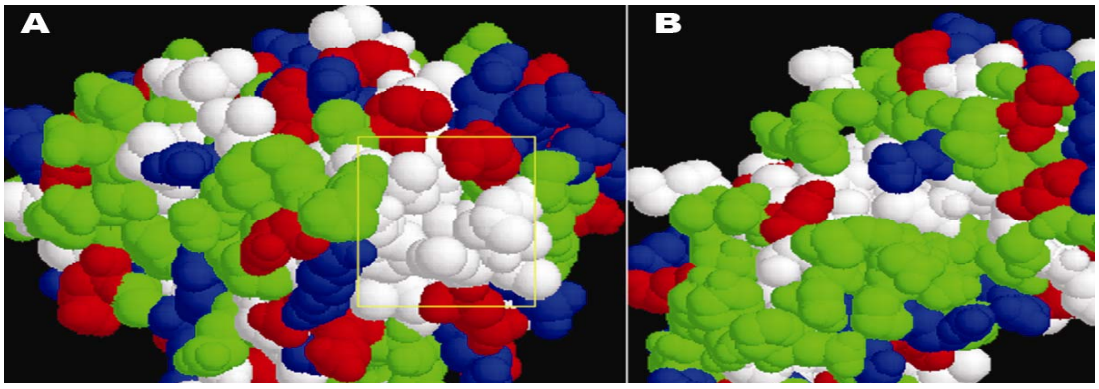

Figure 2.10. Hydrophobic residue distribution of the R168W mutant: The space-filled representation of the mutant structure was generated using the molecular visualization freeware RASMOL. The hydrophobic residues are shown in white, while the polar residues are green, the acidic residues red and the basic residues blue. The yellow box in the **Panel A)** highlights the hydrophobic patch while **Panel B)** shows the long stretch of hydrophobic residues.

solvent accessible surface areas of Arg (in the wild type) and Trp (in the mutant) in the modeled structures are 11.3Å2 and 12.5Å2 respectively. While this overall difference in accessible surface area is not prominent the accessible surface area contributed by hydrophobic surface of Arg and Trp are 2.7 Å2 and 9Å2 respectively. Thus in the tertiary structure of the mutant there is a substantial increase (6.3Å2) in the hydrophobic surface compared to the wild type. The above features provide a possible explanation of the faster aggregation rate of the mutant structure in comparison to the wild type human γC-crystallin.

The surface charge distribution data, obtained by using GRASP (Figure 2.11) does not show any significant changes in the charge distribution on the surface of the wild type and mutant γ-crystallins.

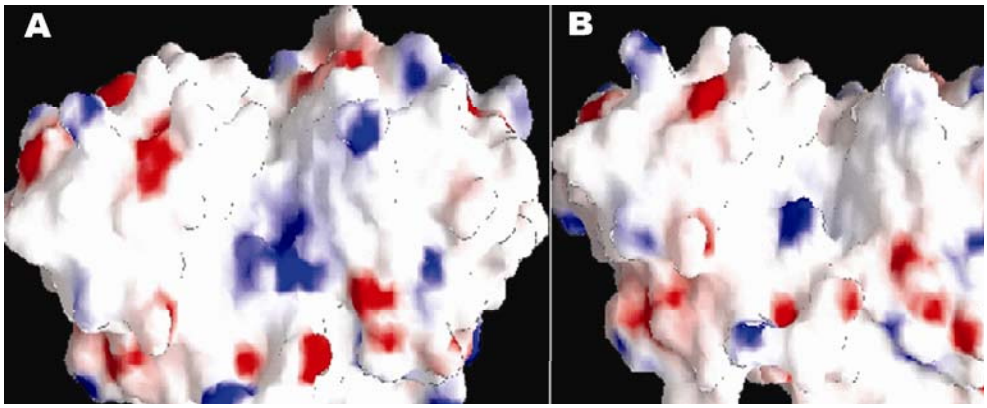

Figure 2.11 Surface charge distribution of the human gC-crystallin wild type (**panel A**) and mutant (**panel B**) structures generated using GRASP.

2.3.2B. Over-expression and solution state structural properties of wild type and R168W γC-crystallin

The recombinant constructs, pET21a(+)-WTγC, pET21a(+)-R168WγC generated were used for over-expression.

Upon over-expression both the proteins were essentially found in the soluble fraction. These proteins were purified to homogeneity as shown on SDS-PAGE (Figure 2.12A). The R168W mutant protein was found to be migrating slower on native PAGE comparative to wild type protein which indicates change in pI (Figure 2.12B) due to the replacement of Arg by Trp. We did not find any change in solubility between two proteins at least until the 10 mg/ml concentrations tested here.

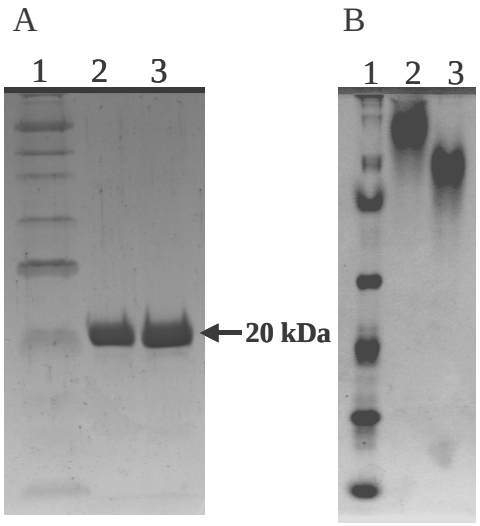

Figure 2.12. A).SDS-PAGE, B). Native-PAGE showing the purified WT (lane 2), R168W mutant (lane 3) γC-crystallin and broad range protein molecular weight marker from Sigma (lane 1).

Figure 2.13A compares the far-UV CD spectra, and reveals that the mutation has not affected the secondary structure or backbone conformation of the molecule. Figure 2.13B, which compares the tertiary structural features revealed by near-UV CD spectroscopy, shows some minor differences, which might have come about in the neighborhood of the aromatic side chains molecule upon replacement of R168 by W.

Fluorescence emission of the mutant is red-shifted by 14 nm compared to that of the wild type (340 nm, cf. 326 nm) and also enhanced in intensity as shown in Figure 2.14A. Though the increased fluorescence emission can

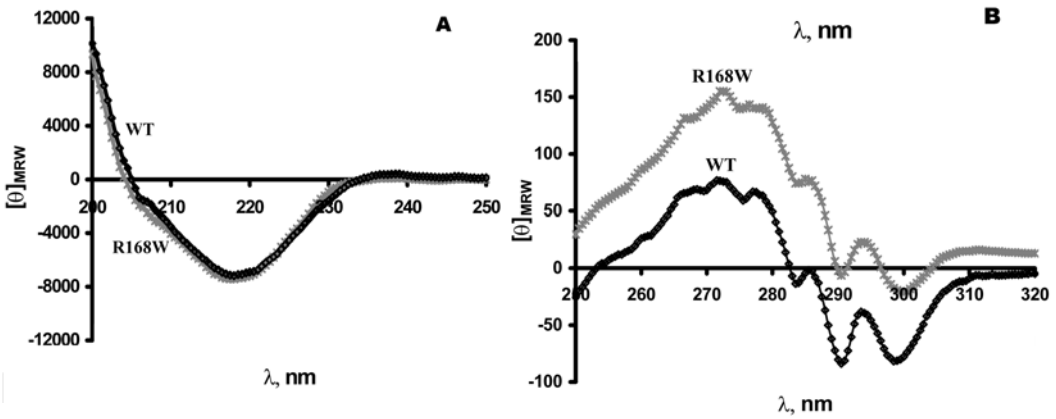

Figure 2.13. Far UV CD (panel A) and Near UV CD (panel B) spectra of wild type (WT) and R168W human γC-crystallin.

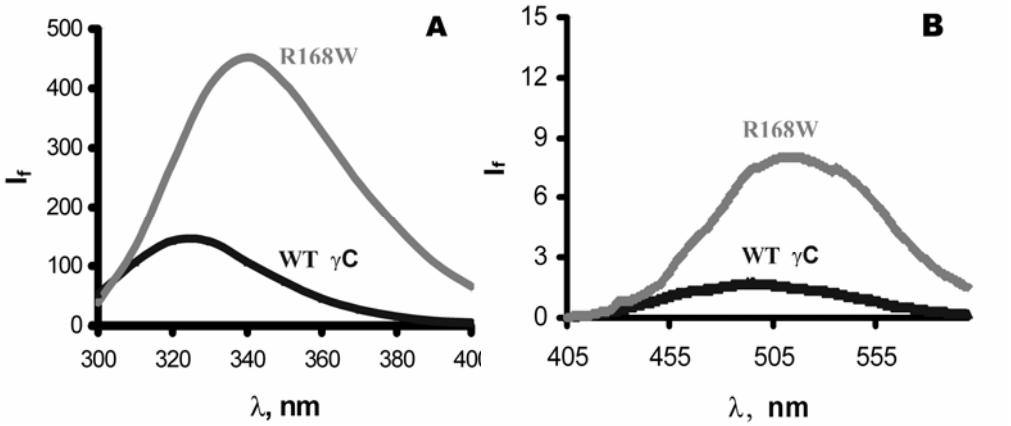

Figure 2.14. Panel A: Far- UV CD spectra of the wild type (WT) and R168W mutant human γC-crystallin. Ellipticity values are expressed in residue molar units. **Panel B:** Near- UV CD spectra of the wild type (WT) and R168W mutant human γC-crystallin.

partially be attributed to the extra Trp residue present in the R168W mutant, both of these features also indicate the Trp residues to experience a more polar environment.

Extrinsic fluorescence studies, using the apolar reporter ANS, showed a modest enhancement in the emission intensity of the probe bound to the R168W mutant, in comparison to when it is bound to the wild type protein (Figure 2.14B), which is consistent with the suggestion that the mutant has a larger surface hydrophobicity.

Figure 2.15 shows (A) the guanidinium chloride- induced denaturation, and (B) thermal denaturation curves of both the wild type and R168W γC-crystallins. As can be seen, there is very little difference between the two, indicating that the structural stability of the molecule is not altered much by the replacement of the Arg residue at this position by Trp.

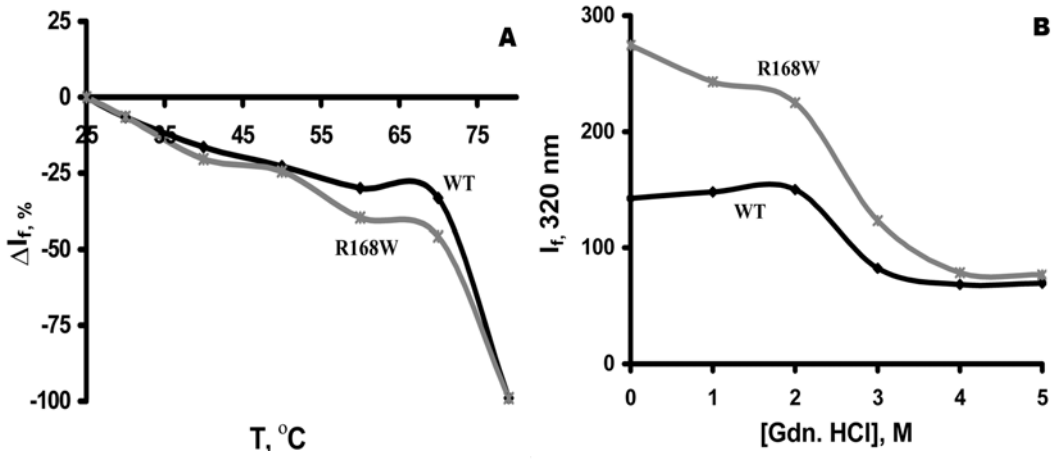

Figure 2.15. Comparison of the thermal (**panel A**) and Gdn.HCl induced (**panel B**) denaturation profiles of wild type (WT) and R168W human γC-crystallin. Denaturation was monitored using Trp fluorescence.

An interesting property of γ-crystallin solutions, thought to be relevant to the opacification of the eye lens, is their tendency upon heating to produce self-aggregates of sub-micrometer sizes which scatter light (Raman and Rao, 1994; Kundu *et al*., 2003; Mandal *et al*., 1988). This property has enabled γ-

crystallins to be used as target proteins to evaluate the solubilizing ability, or the chaperone-like action, of lens α-crystallin (Horwitz, 1992; Liang, 2004). We thus decided to compare the thermally induced light scattering of wild type and R168W γC-crystallins. Figure 2.16 reveals that at 65° C the light scattering intensity of the mutant rises eight-fold within 15 minutes, while that of the wild type protein increases only two-fold. It takes about 30 minutes for the wild type protein solution to increase its light scattering eight-fold, by which time the mutant protein precipitates out of solution.

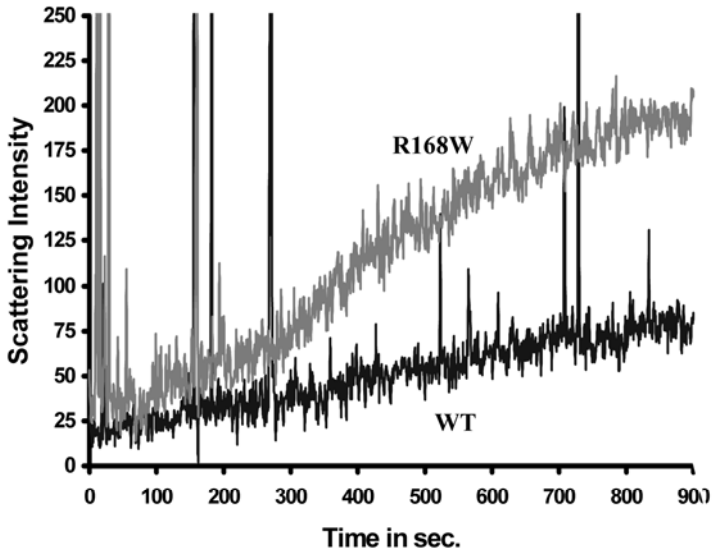

Figure 2.16. Thermal aggregation profiles of wild-type (WT) and R168W human γC-crystallin.

2.3.2C. R168W γC *in situ*

As high transfection efficiency can be achieved in COS1 cells, we have first studied the behavior of recombinant constructs (EGFP, wild type and R168W γC-crystallin) in COS1 cells. Figure 2.17 shows the confocal microscopic images of the EGFP (panel A) wild type and R168W mutant crystallin constructs (panel B, C respectively) transfected into COS1 cell lines. The nuclei of the cells were stained red and the transfected cells appear green on

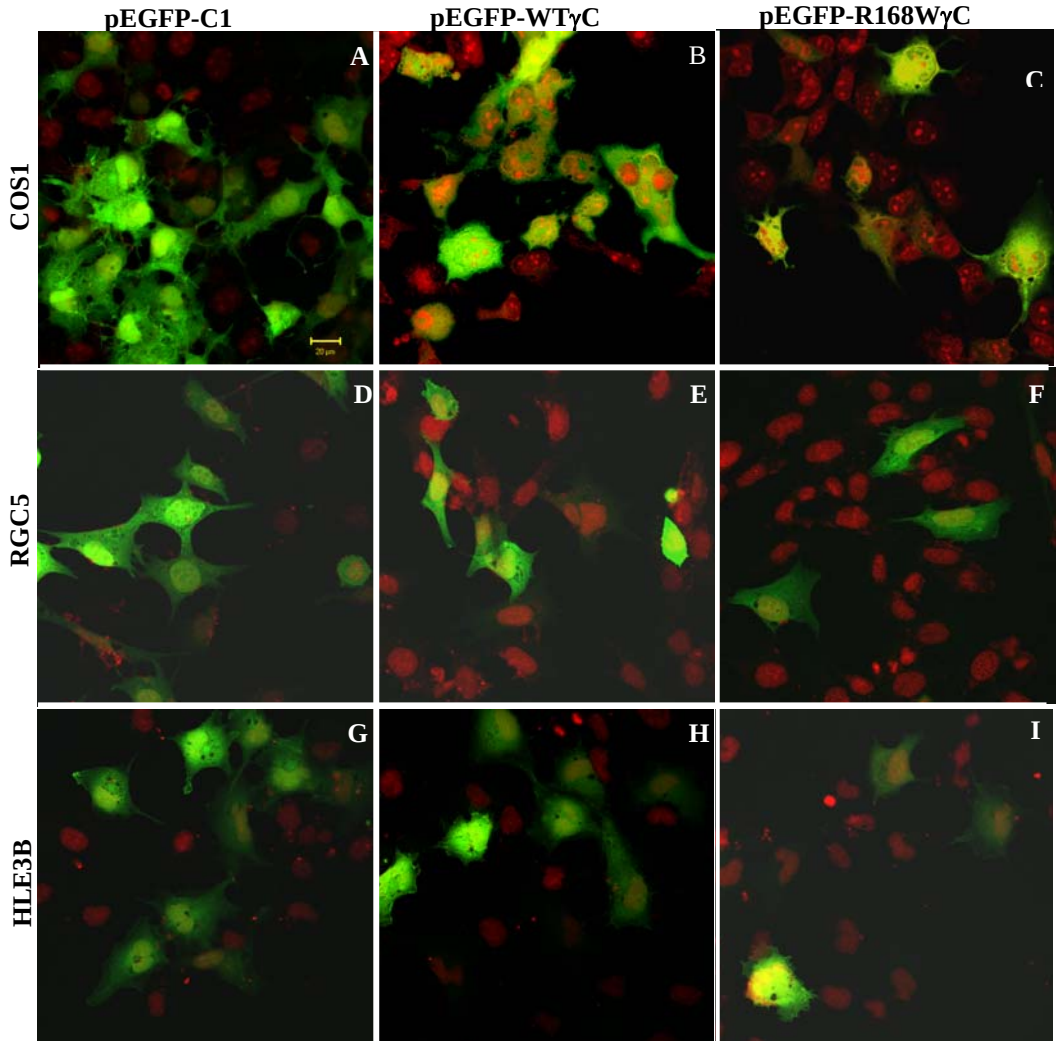

Figure 2.17. Confocal microscopic images of the COS1, RGC5 and HLE3B cells transfected with pEGFP, pEGFP-WT γC and pEGFP-R168W γC-crystallin constructs Images were shown were magnified by 400 times.

confocal microscopic images. The R168W mutant protein in COS1 cell lines behaved similar to that of wild type protein, in the sense that the mutant protein did not show any extra protein aggregation.

Crystallins are reported to be present in non-lens tissues and cells such as retina, hence we looked at the behavior of the recombinant proteins in the rat retinal ganglion cell line (RGC5) cell lines. Figure 2.17 shows the

transfection of these recombinant constructs into RGC5; the recombinant proteins were seen to behave similar to COS1 transfected cells.

Since the pathophysiology of cataract is due to opacification of the lens and crystallins are found in much higher amounts in the lens, it is more appropriate to study the behavior of the mutant crystallins in lens cells. Figure 2.17 compares the behavior of wild type (panel H) and mutant R168W γC-crystallins (panel I) when their cDNAs are transfected into the HLE3B human lens epithelial cell lines. The recombinant proteins found to be distributed evenly through out the cell cytoplasm and the cell nucleus, and there is no major difference between the wild type and R168W γC-crystallin behavior. As shown in Figure 2.18, there is an endogenous expression of αA- and αB-crystallins in HLE3Bcell lines. Thus, the in situ behavior of the R168W mutant is no different from that of the wild type molecule in all the cell lines tested.

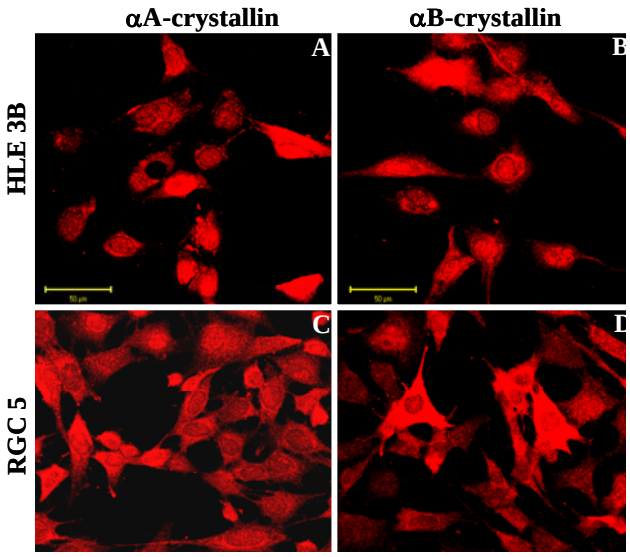

Figure 2.18. Immunofluorescence pictures of HLE3B, RGC5 cells showing positivity for αA- and αB-crystallins

2.3.3. W157X γC-crystallin

2.3.3A. *In silico* analysis of W157X γC-crystallin

The 3D structure of the wild type γC-crystallin, modeled on the basis of the crystal structure of bovine γB-crystallin, was used for the analysis of the effect of deletion of C-terminal 18 residues. Figure 2.19A shows the 3D structure of the γC-crystallin generated, and the portion shown in blue color is suggested to get deleted in the mutant. Figure 2.19B shows the exposed apolar residues in W157X mutant which are otherwise buried by the C-terminal region in the wild type. A list of apolar residues that are buried (recognized by less than 7% solvent accessibility) in the wild type, but exposed (greater that 7% solvent accessibility) in the mutant is provided in Table 2.2. Figures 2.19C and D highlight this differential exposure, where the mutant molecule is seen to present a continuous patch of hydrophobic sidechains exposed to the surface. The loss of the C-terminal 18 residues leads to notable effects in the tertiary structure and aggregational properties of the mutant.

S.No.	Amino acid & position	Solvent accessibility %	
		WT γC	W157X γC
1	Ile 82	0.9	11.1
2	Leu 90	1.8	8.1
3	Leu 92	2.7	10.1
4	Ile 112	3.7	31.9
5	Ile 121	3.8	22.2
6	Leu 124	0.1	8.1
7	Trp 131	0.6	19.8
8	Val 132	0.0	7.6
9	Leu 133	0.2	39.1
10	Tyr 134	3.3	16.3
11	Tyr 144	3.5	43.4
12	Leu 146	1.6	9.3
13	Tyr 151	4.7	11.8

Table 2.2. Change in solvent accessibility of the residues in wild type and mutant γC-crystallins

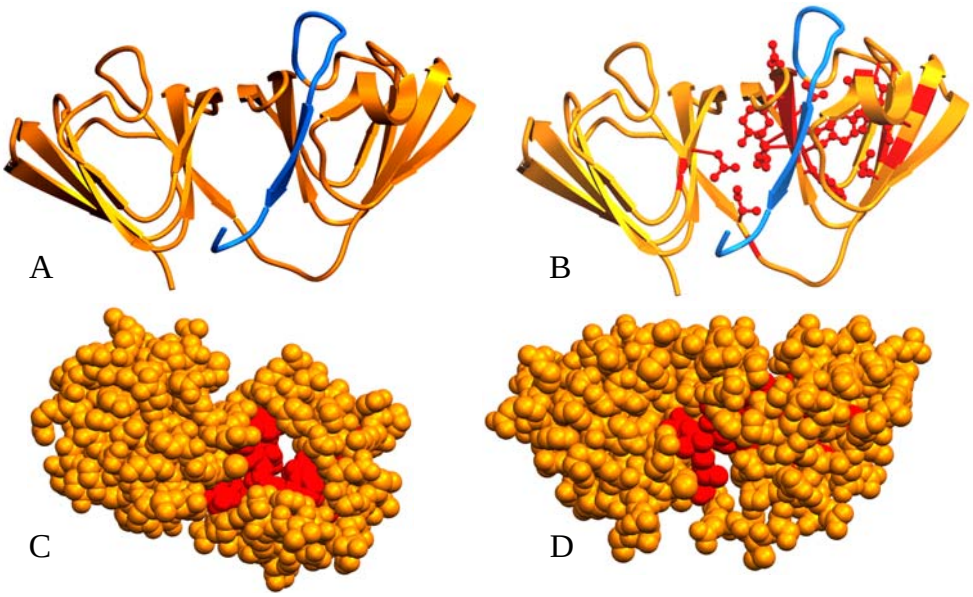

Figure 2.19. A. Structure of wild type human γC-crystallin. The part colored blue is deleted in the mutant. **B.** Shows the interacting residues in the C-terminal region in the wild type molecule that is lost in the mutant. **C & D.** Space filling model of the mutant, showing the continuous apolar patch (shown in red).

2.3.3B. W157X γC *in situ*

Figure 2.20 shows the confocal microscopic images of the COS1 cells transfected with various constructs. The red fluorescence in the confocal images indicates the cell nuclei and the green fluorescence indicates the transfected cells expressing the recombinant proteins. While EGFP and the wild type γC-crystallin proteins distribute evenly in the cell cytoplasm and cell nuclei (panel A, B respectively), the mutant appears to aggregate in the cytoplasm and does not enter into the nucleus, seen as a punctate green fluorescence in the cytoplasm (panel C).

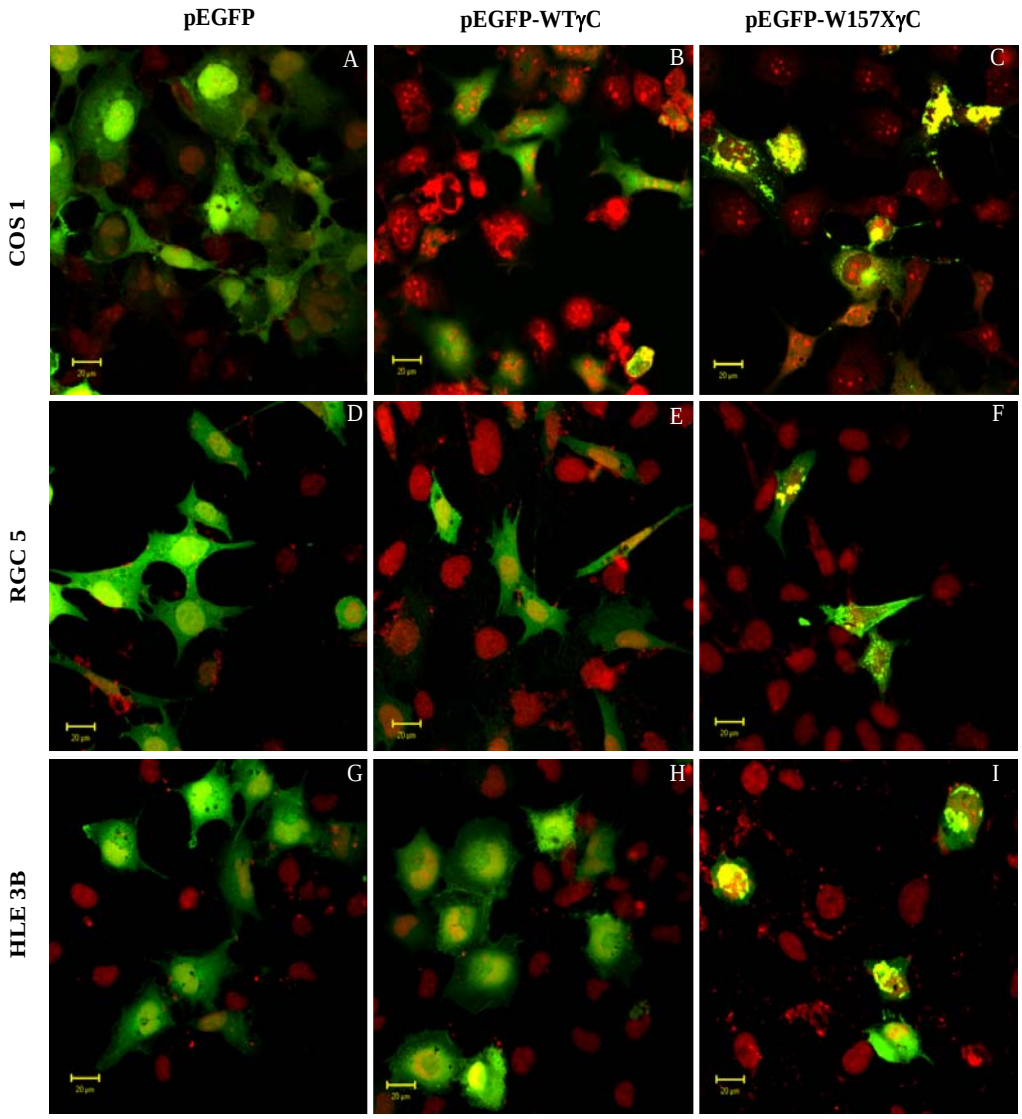

Figure 2.20. Confocal microscopic images of the COS1, RGC5 and HLE3B cells transfected with pEGFP, pEGFP-WT γC and pEGFP-W157X γC-crystallin constructs. Images shown were magnified by 400 times.

We further looked at the behavior of the recombinant proteins in the RGC5 cell lines. Figure 2.20 (panel D, E and F) shows that the mutant crystallin in RGC5 cells behaves very similar to in COS1 cells.

Figure 2.20 compares the behavior of wild type (panel H) and mutant γC-crystallins (panel I) when their cDNAs are transfected into the HLE3B human lens epithelial cell lines. Distinct cytoplasmic localization and protein aggregates are displayed by the mutant crystallins. Interestingly endogenously present α-crystallins are not able to prevent the mutant protein aggregation, presumably because the levels of α-crystallins are not sufficient.

These results are similar to the protein aggregates seen when the V76D mutant of murine γD-crystallin is transfected into mouse lens epithelial cells (Wang *et al*., 2007), and the T5P mutant of γC-crystallin was transfected into HEK293 cell lines (Pigaga and Quinlan, 2006).

The western blot analysis result shown (Figure 2.21) that the EGFP alone and wild type γC-crystallin seen in soluble fraction where as the mutant protein was seen essentially in insoluble fraction. Western blot analysis clearly shows that the mutant is in aggregated form which is in consistent with our *in situ* transfection and confocal microscopic analysis.

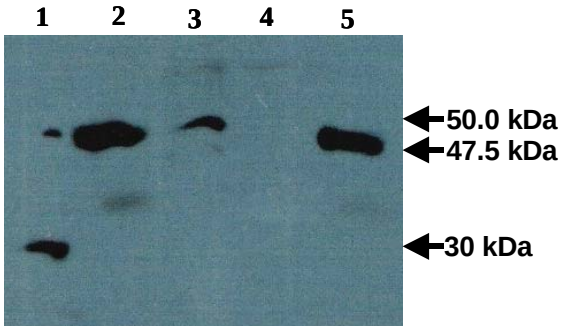

Figure 2.21. Western blot probed with anti-EGFP antibody. Lanes 1. EGFP from the soluble fraction, 2. EGFP-fused WT γC from the soluble fraction, 3. EGFP-fused WT γC from the insoluble fraction, 4. EGFP-fused W157X γC from the soluble fraction, 5. EGFP-fused W157X γC from the insoluble fraction.

2.3.4. W157X γD-crystallin

2.3.4A. *In silico* analysis of W157X γD-crystallin

The crystal structure of wild type human γD-crystallin, retrieved from the Protein Database (PDB) is shown in the Figure 2.22A. The part of the structure shown in red color is deleted in the Trp157Stop mutant. The region of deletion includes the β strand between the residue 166-170, this β strand is a part of a β sheet, which is an integral component of the C-terminal domain. The region of deletion also includes a few hydrophobic residues. Some of these, such as Val 164 and Leu 167, are completely buried in the wild type. Figures 2.22B and 2.22C show the interaction patterns in the hydrophobic pocket of the wild type molecule, e.g., involving Leu112, Ileu121, Tyr134, Glu135, Val164, Leu167, and Arg168. A list of hydrophobic residues that are buried (recognized by less than 7% solvent accessibility) in the wild type, but

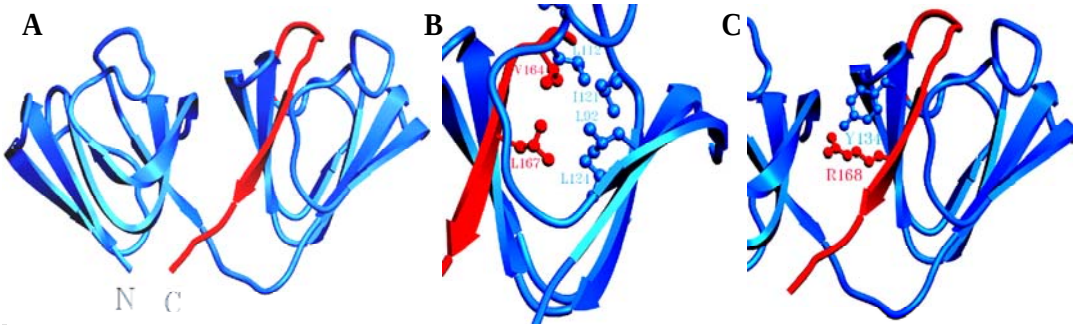

Figure 2.22: Panel A: The structure of human γD-crystallin retrieved from protein data bank. The part of image shown in red is deleted in the W156X mutant. **Panel B:** Model showing the hydrophobic pocket involving the amino acid residues from the deleted region as well as other parts of protein. **Panel C:** Model showing the aromatic-cation interaction between Tyr 134 and Arg 168 located in the region of deletion.

exposed (greater that 7% solvent accessibility) in the mutant is provided in Table 2.3. The residues that undergo major solvent accessibility changes lose their interaction with the surrounding as discussed below.

(a): Leu 112: The solvent accessibility of this residue in the wild type and mutant structures are estimated, using the software analysis, to be 0% and 15%. This residue gets exposed to water upon the deletion of C-terminal residues of 157-174. It interacts with Leu 167 and Val 164 (which are buried in the wild type and lost in the mutant), and also with Leu 92. Thus Leu 112 contributes significantly to the stability of the core or C-terminal domain.

(b): Ile 121: This residue is involved in forming a tight, hydrophobic core by interacting with residues Leu 124, Leu 92 and Val 164 (which is lost upon mutation). Its accessibility vis as to 51% in the mutant.

(c): Val 132: This residue has solvent accessibility of 0% and 58% in wild type and mutant γD-crystallin respectively. This is buried mainly by interacting with Ile 81, Phe 56 and Val 170 (which is lost in the mutant).

S.No.	Amino acid & position	Solvent accessibility %	
		WT γD	W157X γD
1	Leu 112	0.0	14.9
2	Ile 121	0.0	50.5
3	Val 132	0.0	58.4
4	Tyr 134	0.0	60.6
5	Glu 135	5.0	64.0
6	Leu 136	0.0	16.0

Table 2.3. Change in Solvent accessibility of the residues in wild type and mutant γD-crystallins

(d): Leu 136: This residue has solvent accessibility of 0% in wild type structure and 16% in mutant. It does not appear to be involved in the stability of the core, but is seen to have contacts with Arg 140, Glu 135 and Arg 163 (which is lost in the mutant).

(e): Glu 135: This residue is highly conserved among all γ-crystallins and its solvent accessibility is 5% in the wild type and 64% in the mutant. This residue being charged is unusually buried and is stabilized by the formation of a hydrogen bond with the main chain amide at position 142 and by an ion-pair with Arg163, which is lost in the mutant. Absence of this ion-pair interaction in mutant is expected to increase the negative charge at this part of the structure.

(f): Tyr 134: This residue is highly conserved among all γ-crystallins and its accessibility changes from 0% to 61% from wild type to the mutant. This residue forms an aromatic- cation interaction with Arg 168 located in the region of deletion, while the exposure of Tyr in the mutant is may not be unfavorable, loss of its interaction with Arg 168 could contribute towards the destabilization of structure.

2.3.4B. Properties of the recombinant W157X γD-crystallin in solution

In an effort to understand the molecular basis behind the formation of protein aggregates and cataract formation, we cloned and expressed the wild type and W157X γD-crystallin proteins, isolated and purified them, and compared their properties in the solution state. Over-expression of the wild type protein partitioned into the supernatant where as W157X γD-crystallin form an

inclusion bodies. The inclusion bodies were easily dissolved upon addition of 8 M urea and were refolded back upon removal of the urea by dialysis. Upon refolding only minor fraction of protein got refolded and partitioned into the soluble fraction where as the major fraction of protein got aggregated.

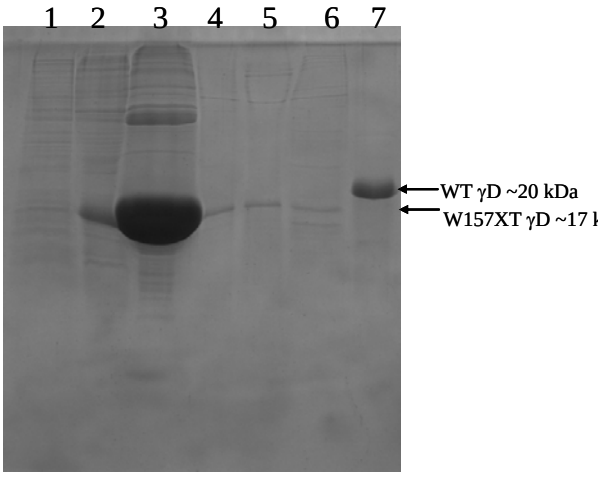

Figure 2.23. SDS-PAGE showing over-expressed and purified mutant and wild type γD-crystallins. Lane 1: Un induced W157X; lane 2: W157X γD 3 hrs after induction; lane 3 : W157X γD in inclusion bodies; lane 4&5 purified refolded W157X γD-crystallins; lane 6:refolded W157X efore purification and lane 7 purified WT γD-crvstallin.

Figure 2.23 shows the purified wild type and W157X γD-crystallins on 12% SDS PAGE. The concentration of protein came into the soluble fraction was found to be 0.2 mg/ml. Concentrating of the protein above this level led to the aggregation of protein and precipitation.

Figure 2.24 compares the circular dichroism spectra of the wild type and mutant protein, in the (far-UV) spectral region 250 – 200 nm, reflecting the secondary structural

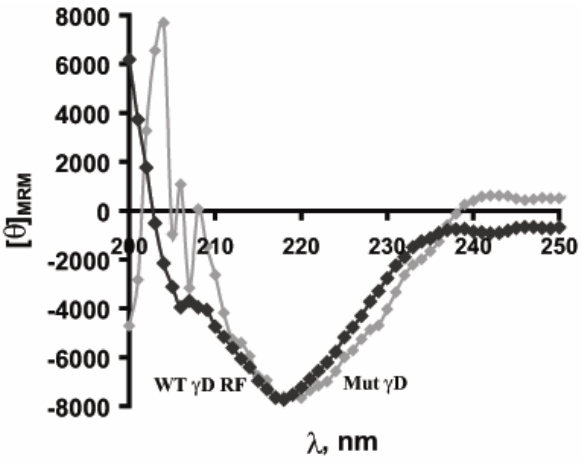

Figure 2.24. Far-UV CD spectra of the wild type (WT) and W156X mutant human γD-crystallin. Ellipticity values are expressed in residue molar units.

features of the molecules. As can be seen, there is no great difference between the spectra of the two proteins, suggesting that the loss of the C-terminal fragment does not seem to affect the backbone conformation of the molecules in a major manner. The mean residue molar ellipticity on both proteins shows a negative peak at 218 nm (with a value of -8000), in keeping with the earlier reports, suggesting that they are largely in the β-pleated sheet conformation.

Figure 2.25A shows the intrinsic fluorescence spectra of wild type and W157X human γD-crystallins. While the wild type molecule shows an emission maximum at 327 nm (in agreement with earlier reports) with an (arbitrary) intensity of about 120 units, the mutant emits at 336 nm, with almost half the intensity of the wild type molecule. The red-shift seen in the mutant suggests that the aromatic (predominantly trp) residues are relatively more exposed to the solvent than in the wild type molecule. Figure 2.25B shows the extrinsic fluorescence of the surface hydrophobic probe 8-anilinonaphthalene 1-sulfonate (ANS), bound to the two proteins. When bound to the wild type protein, ANS displays its broad

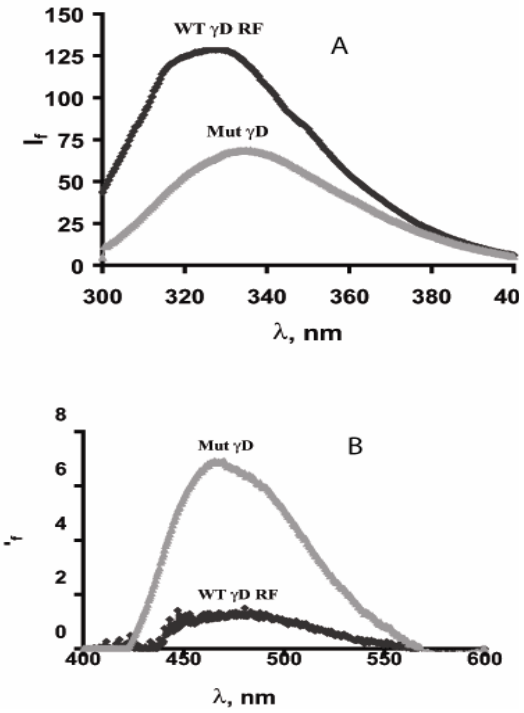

Figure 2.25. Panel A: Intrinsic fluorescence spectra of wild type (WT) and the mutant samples. $\lambda_{ex.}$ 295 nm. **Panel B:** Extrinsic fluorescence of the surface hydrophobicity probe ANS bound to γD-crystallins

emission maximum around 484 nm of relatively low intensity; while bound to the mutant, the probe shows a blue-shifted band around 466 nm with a three-fold higher intensity. These data suggest that the mutant molecule has a more pronounced hydrophobic surface (Cardamone *et al*., 1992).

The structural stability of the mutant is lower than that of the wild type protein (Figure 2.26), and chemical denaturation using Gdn.HCl as the denaturant too reveals the same. Interestingly, while the refolding curve of the wild type molecule traces the same path as the unfolding curve (Figure 2.26B), those of the mutant molecule are not superimposed; the molecule seems to show hysteresis (Figure 2.26C). Such non-coincidence of the unfolding and refolding pathways is thought to be indicative of intermediate states during the folding/refolding pathway of a protein chain. In other words, it would appear that the folding of the mutant does not

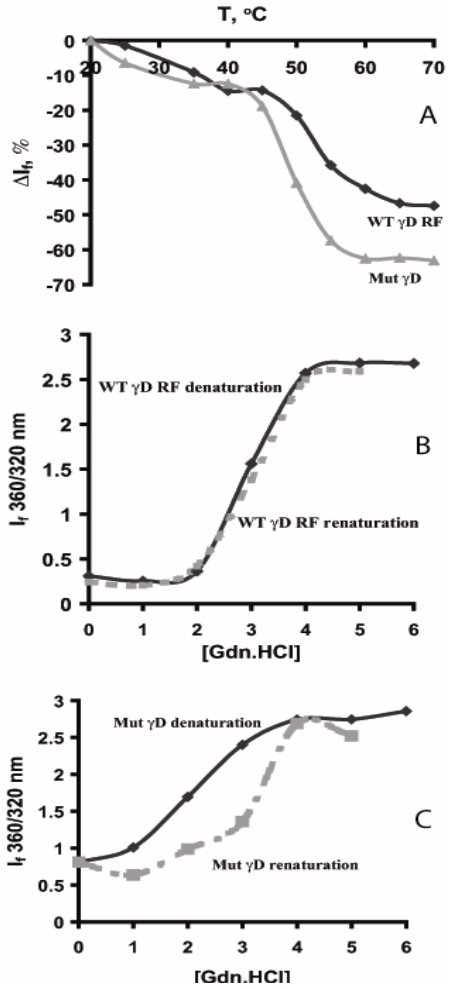

Figure 2.26. Panel A: Thermal denaturation profiles of the wild type and W157X mutant. Panel B & C: Gdn. HCl induced denaturation / renaturation curves of WT D-crystallin and W157X mutant respectively. The graphs were constructed by plotting the fluorescence intensity ratio at 360/320 versus Gdn. HCl concentration.

obey the classical two-state (native/denatured) pattern that the wild type displays. Interestingly, Kosinski-Collins and King (2003) have shown that when hydrophobic pockets of wild type human γD-crystallin are exposed (by adjusting the amount of Gdn.HCl in the solution), the protein displays hysteresis and self-aggregation. Unfortunately however, the solubility of the mutant γD-crystallin is remarkably low (less than 0.25 mg/ml, far lower than that of the wild type). Because of this, it has not been possible to explore the folding-refolding features of this molecule in greater detail using other experimental techniques at this low concentration. Likewise, the aqueous solubility of W157X γC-crystallin was also remarkably low (comparable to its γD-crystallin analog). We have thus resorted to in silico comparison of the mutant and wild type proteins using molecular modeling.

Figure 2.27 shows the difference in the thermal aggregation profiles of the wild type and the mutant. γ-Crystallins are known to aggregate (Mandal *et al*., 1998) upon heating to 65° C. The light scattering intensity of the W157X mutant is increased threefold within 15 min, while that of the wild type is negligible. In order to probe into the solution state structural differences between the two, we compared their conformational properties.

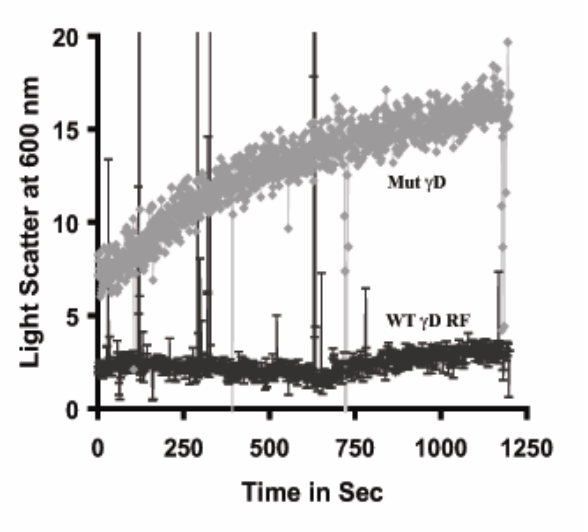

Figure 2.27. The thermal aggregation profiles of wild type (bottom) and W157X mutant human γD-crystallin (top line).

2.3.4C. W157X γD *in situ*

Figure 2.28 shows the confocal microscopic pictures of just EGFP, wild type, and W157X human γD-crystallin (panels A, B and C respectively) cDNAs tagged with EGFP, transfected in COS1 cell lines. While EGFP and the wild type molecules are seen to be uniformly present, with no special features, in

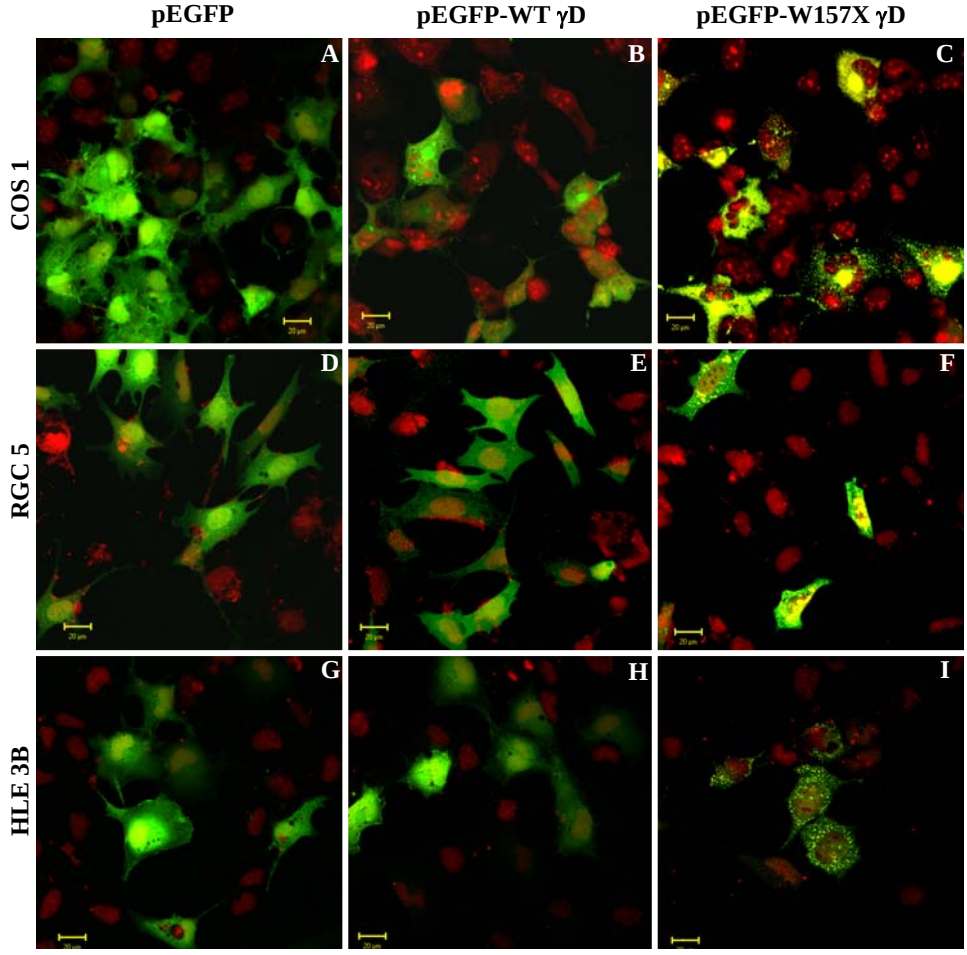

Figure 2.28. Confocal microscopic images of the COS1, RGC5 and HLE3B cells transfected with pEGFP, pEGFP-WT γD and pEGFP-W157X γD-crystallin constructs. Images shown were magnified by 400 times.

the cytoplasm and nuclei of the cells, the mutant molecule is seen to clump up into scattering particles, largely in the cytoplasm.

Figure 2.28 (panels D, E and F) shows the results of similar experiments, using the retinal ganglion cell line RGC5 for transfection. Here again, while the wild type molecule (panels E) display normal distribution across the cell, the mutant γD-crystallin (panel F) is seen to aggregate in cytoplasm.

Figure 2.28 (panels G, H and I) compares the behavior of wild type (panel H) and mutant γD-crystallins (panels I) when their cDNAs are transfected into the HLE3B human lens epithelial cell lines. Distinct cytoplasmic localization and protein aggregates are displayed by the mutant crystallins. Interestingly, endogenously present α-crystallins are not able to prevent the mutant protein aggregation, presumably because the levels of α-crystallins are not sufficient.

The western blot analysis of the proteins isolated from transfected COS1 cells showed the EGFP and EGFP tagged wild type γD crystallins to be in soluble fraction. The EGFP tagged W157X mutant protein was seen essentially in the insoluble fraction (Figure 2.29), which is consistent with the confocal microscopic and solution state structural studies.

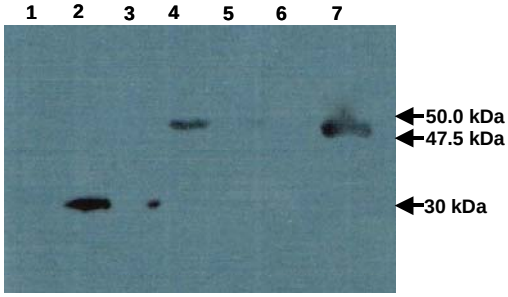

Figure 2.29. Western blot probed with anti-EGFP antibody. Lanes 1. Cell lysate without transfection, 2. EGFP from the soluble fraction, 3. EGFP from insoluble fraction, 4. EGFP-fused WT γD from the soluble fraction, 5. EGFP-fused WT γD from the insoluble 6. EGFP-fused W157X γD from the soluble, 7. EGFP-fused W157X γD from the insoluble fraction.

In order to rule out the possible effect of the GFP tag on the properties of the mutant proteins the wild type and W157X γD-crystallins were cloned into pcDNA3.1(-) vector and transfected into RGC5 and HLE3B cell lines and probed with anti-human γ-crystallin antibody. The confocal microscopic images shown in Figure 2.30 also conforms the cellular aggregation of the mutant protein in RGC5 and HLE3B cell lines where as the wild type protein is distributed uniformly in the cell.

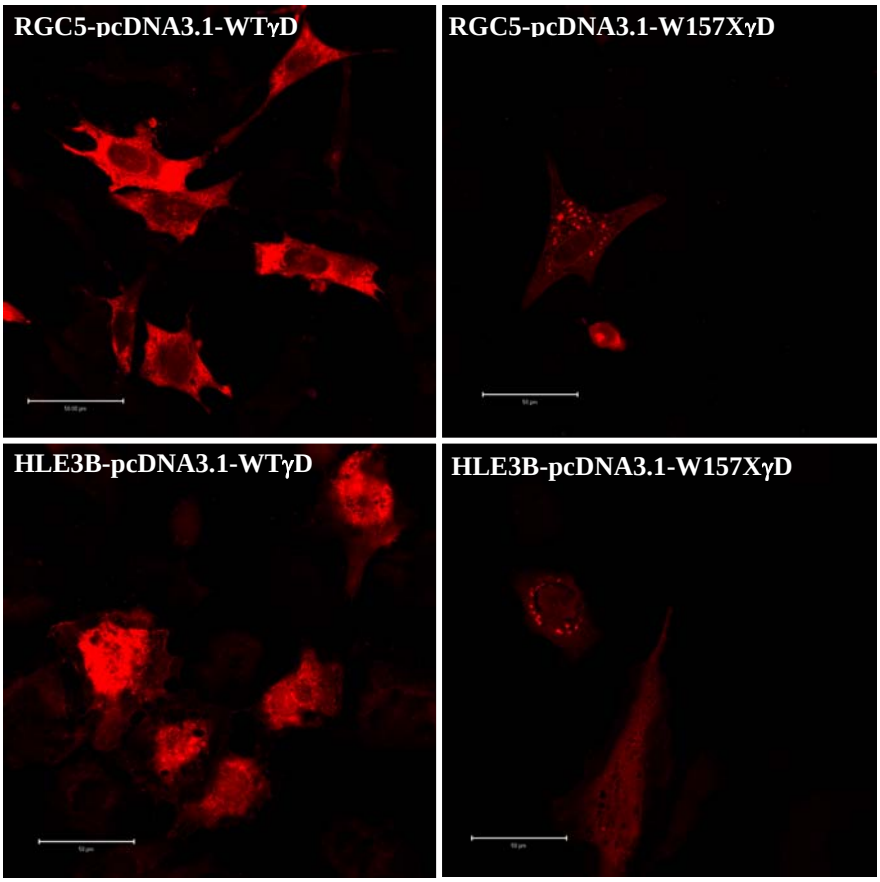

Figure 2.30. Top pictures show the images of RGC5 cells transfected with pcDNA3.1(-) recombinant constructs of untagged, neat wild type (top left) and W156X human γD-crystallin (right), probed with anti-human γ-crystallin antibody (raised in rabbit), and TRITC conjugated anti-rabbit secondary antibody. Bottom pictures show the same using HLE3B cell lines. Here too, bottom left refers to WT and bottom right to the mutant.

2.4. DISCUSSION

The 5bp mutant of γC-crystallin has, as shown above, lost much of the chain conformation and also exhibits reduced solubility. Surface probe studies reveal this molecule to have a noticeable hydrophobic surface, which might be related to its lower solubility and greater tendency to self-aggregate. These features of conformational loss and increased tendency to self-aggregate are in contrast to those of wild type γC-crystallin, and provide a molecular phenotypic explanation of its association with congenital cataract. The properties of this protein support the hypothesis that cataract is a protein folding disease.

It is, however, the case of the R168W that is unusual. Its chain conformation and tertiary structure, as revealed by spectroscopy, are not very different from the wild type molecule. Modeling studies show subtle variations in the side chain interactions, which are not reflected as major changes in tertiary structure or in structural stability. They seem reflected more in terms of aggregation and precipitation properties. In this regard, R168W is reminiscent of the behavior of two other cataract-associated crystallin mutants namely R14C and R58H human γD-crystallins, studied by Pande *et al*, (2000, 2001). These two mutants display essentially the same secondary and tertiary structures, and stability to thermal unfolding but aggregate and precipitate more readily than wild type γD-crystallin. Pande *et al*. had therefore suggested that it is the self-aggregation or quaternary structural difference that is responsible for the phenotypic association with lens opacification or cataractogenesis in these cases. Our results support this hypothesis.

Many of the genetic cataracts are associated with mutation of Arg residues of crystallins (Heon *et al*., 1999; Stephan *et al*., 1999; Kmoch *et al*., 2000). The Arg residue, as our results from modeling analysis shows, makes extensive contacts with other residues and with solvent water. Substitution with another residue appears to disturb this networking, and this alters the quaternary structure in turn. This has been clarified by the crystal structural comparison of wild type γD-crystallin with its R58H mutant (Basak *et al*., 2003). In the present study too, substitution of Arg by Trp results in a marked increase in the exposed hydrophobic surface in the tertiary structure, consistent with the observation of aggregation. That such behavior is not limited to Arg mutants alone has recently been shown by Evans *et al.,* (2004), and Pande *et al.,* (2005), in the case of the P23T mutant of γD-crystallin, which self-aggregates more readily than the wild type molecule. It would thus appear that unfolding or destabilization of the crystallins is not always necessary for them to generate lens opacification.

However, R168W mutant γC-crystallin in cell cultures did not show any protein aggregation. This could be because of two possible reasons; the first one is the endogenous expression of α-crystallins in the cell lines studied. Presence of αA- and αB-crystallins is expected to prevent proteins from aggregation by chaperone function. Pigaga *et al*., (2006) showed this possibility in case of T5P γC-crystallin, where they could show the prevention T5P γC-crystallin aggregation upon over-expression of α-crystallin in Hela cells. Our results in the COS1 cell (the expression status of α-crystallin is not known) lines also supports this possibility; while see protein aggregation in

both the cases, such aggregation is not seen in HLE3B and RGC5 cells, where we find the expression of αA- and αB-crystallins. This indicates that endogenously expressed α-crystallin is sufficient to prevent R168W γ-crystallin from aggregation. The second reason could be that the protein aggregation not only depends on self-assembly, but also on protein-protein interactions. It is known that in the normal human lens γ-crystallins show attractive interactions with α- and β-crystallins. It is also known that most of the native crystallins (except α-crystallins) do not express in the cell lines studied (HLE3B, RGC5 and COS1 cells). Absence of endogenous crystallins might contribute to the absence of protein aggregation in these cell lines.

Turning to the W157X mutant of human γC-crystallin, Table 2 lists some of the apolar residues that are buried by the C-terminal region in the wild type molecule but exposed in the mutant. Residues such as Leu 57, Ile 112, Ile 121, Trp 131 and Leu 133, which are buried in the wild type surface out in the mutant. There are also a few apolar residues such as Leu 105 that are already exposed in the wild type, which become even more so in the mutant. We also note that a few in the N-terminal domain, and in the domain-domain interface of the structure, have increased accessible surface area in the mutant, since part of the deleted C-terminal region is involved in the inter-domain interface. The overall increase in the solvent accessible surface area (ASA) in the mutant (compared to the wild type) is computed to be about 307 $Å^2$, of which 133 $Å^2$ is contributed by apolar side chains. Apart from this large increase in ASA, we also notice a continuous hydrophobic patch in the mutant (Figure 2.19C and D), which would lead to decreased aqueous solubility, self-aggregation and scattering particles. These are again visualized when the

cDNA of W157X human γC-crystallin is transfected into cells (Figure 2.20). As shown in Figure 2.18 the endogenous α-crystallins present in the cells are not sufficient to prevent the protein aggregation formed by W157X γC-crystallin.

W157X is yet another example of mutation in human γD-crystallin associated with cataract, the others being R14C, P23T, R36S and R58H. All these mutants display much lower solubility in water than the wild type molecule (<20 mg/ml for most of the mutants, < 100 mg/ml in the case of R14C, cf. >200 mg/ml of the wild type; all at 20°C). The solubility of W157X is even lower, below 0.25 mg/ml. The loss of the C-terminal 18 residues appears to have a more drastic effect on solubility. It would seem that the terminal residues play a greater role in hydration, intermolecular interactions and solubility. Crystal structural analysis of wild type human γD-crystallin indicates the involvement of Asp 156, Arg 163 and Arg 168 in charge interactions, and of Phe 173 in amine-aromatic interactions, as well as in hydrophobic contacts. Not only are these lost in the deletion mutant but, as Table 2.3 shows, several other residues in the rest of the sequence are now exposed to the solvent. Some of these are: (a) Leu 112 which is in contact in the wild type molecule with Val 164 and Leu 167, (b) Ile 121 which is in contact with Leu 92, Leu 124 and Val 164, (c) Val 132 which interacts with Val 170, (d) the highly conserved, and thus crucial, Tyr 134 which is well buried in the wild type and now exposed to a great degree in the mutant, and (e) another conserved residue, the acidic Glu 135 which had an ion pair interaction with Arg 163 in the wild type is now left exposed. It is worth noting that all these changes affect not the secondary structure, or chain conformation, of the molecule; much of the effect is in the tertiary structure and surface hydrophobicity of the

molecule. They however lead to a weakening of the stability of the mutant molecule, as seen by its easier denaturation.

It would thus seem that of all the mutants of human γD-crystallin, the consequence of the loss of the C-terminal 18 residues is more drastic, lading to significant loss of solubility and to self-aggregation and scattering particles. These are visualized in situ in cells.

The results presented here thus show that the loss of the C-terminal fragment in human γD- and in γC-crystallin leads to (a) greatly reduced solubility of the molecule and (b) formation of substantial intermolecular aggregates in a variety of cells, notably in human lens epithelial cells. Such aggregates would be expected to generate light scattering particles, compromising the transparency of the cells and their assemblies.

NATURAL COMPOUNDS FROM PLANTS OF POTENTIAL THERAPEUTIC VALUE IN AGE-RELATED CATARACT

3.0. INTRODUCTION

Age related cataract is one of the leading causes of blindness worldwide. According to the recent World Health Organization (WHO) report (Resnikoff *et al.,* 2004), cataract accounts for 47.8% of all causes of blindness. Cataract blindness is a needless form of blindness, which can be avoided with a relatively simple treatment called cataract surgery. Though great advances have been made in surgical procedure with respect to quality of vision, time taken for the surgery, and postoperative surgical care, the incidence of the cataract in developing countries is so high that it always overwhelms the surgeries performed.

Oxidative stress has long been found to be a major risk factor (either as a primary event or secondary to risk factors like ageing and smoking) that mediates the apoptosis of lens epithelial cells and plays an important role in cataractogenesis (Spector, 1995). The major mode of damage in the lens involves oxidation of the lens proteins and DNA. Oxidative damage to the lens proteins results in a variety of modifications such as recemization, carbonyl compound formation, protein aggregation, dityrosine cross-linking, and insolubilization of lens proteins (Stadtman, 1998; Balasubramanian and Kanwar, 2002) leading to cataract. For this reason considerable interest has focussed on the use of anti-oxidants in delaying the onset or progression of age-related cataract. The lens is continually exposed to sunlight, a rich source of reactive oxygen species (ROS). The lens is inherently rich in endogenous

defense mechanisms which can counter oxidative damage. The antioxidants present in human lens include compounds like glutathione, ascorbate and antioxidant enzymes like catalase, superoxidedesmutase, glutathione reductase (Zigman *et al.,* 1979; Varma *et al.,* 1984; McCay *et al.,* 1985). Although these strong defense mechanisms exist in the lens, these protective enzymes are known to decline in the human eye with increasing age. (Garland *et al.,* 1991). Mounting evidence suggests that chronic exposure to oxidative stress over long term may damage the lens and predispose it to cataract development (Hung *et al.,* 2006). Supplementations with antioxidants thus appear to be a possibility to delay the onset of age-related cataract. Kupfer *et al* (1984) have estimated that a delay of 10 years in cataract formation would probably reduce the surgical burden perhaps by 45%.

3.0.1. Vitamins and cataract: an Epidemiological evidence

In light of the above-mentioned reasons some aspects of cataract research have been directed towards the use of antioxidant vitamins (vitamins A, C and E). The Blue Mountain Eye Study (Cumming *et al.,* 2000), The Roche European American Cataract Trial (REACT) (Chylack *et al.,* 2002), AREDS (Age-Related eye Disease Study Group, 2006), are a few prominent studies which have done randomized clinical trials on the supplementation of various vitamins (Vitamins A, C and E) and their role in delaying cataract formation. These suggest that regular intake of vitamins may have potential value in reducing the risk of cataract. Supplementation of antioxidant vitamins on a regular basis is, however beyond the economic reach of people in the developing world who form the major fraction of cataract-afflicted across the globe. Several nutritional studies have shown that special dietary additives

may provide an alternative to multivitamin tablets and thus offer potential therapeutic value for a variety of oxidative-stress-related diseases. This has shifted the approach of research towards the search for natural plant products which can be beneficial to the health.

3.0.2. Natural compounds from plants as antioxidants

Several studies have focused on plant extracts and compounds which are rich in antioxidants and micro-nutrients and thus beneficial to health. In this connection, we have studied the role of certain plant extracts that are easily available, affordable, culturally acceptable, and which form a part of the daily diet of many people. Earlier work from our laboratory (Thiagarajan *et al.,* 2001, 2002, 2003) had shown that extracts of tea (*Camellia sinensis*), *Ginkgo biloba* and Ashwagandha (*Withania somnifera*) display very good antioxidant activities, and also exhibit cataractostatic ability in animals in which oxidative cataract was induced through selenite. Here we have concentrated on the two plant extracts which are widely used in ayurvedic medicines in India, Ashwagandha, and *Salacia oblonga.* We have also attempted to sort the phytochemical variability among the various formulations available in the Indian market on the name of *Ashwagandha*. While such kind of studies give the useful information, it is also important to know the active principles present in the plant extracts and their mode of action. We have thus selected some of the purified compounds from some of these plants and studied their effect on proteins, DNA as well as their cyto-protective ability, and potential use in delaying age-related cataract, using human lens epithelial cell lines as a model system.

a). *Withania somnifera* (Ashwagandha) extract

Ever since ancient times, drugs derived from plant sources have been used to alleviate or cure human diseases. One such traditional plant that finds importance in Indian Ayurveda is Ashwagandha (*Withania somnifera*, also called winter cherry, Indian ginseng). Ayurvedic medicine includes *Withania somnifera* in the class of herbs called 'adaptogens' or 'vitalizers', used for centuries. These relatively innocuous adaptogens cause adaptive reactions to disease and appear to produce a state of nonspecific increased resistance to adverse effects of biological agents (Mishra *et al.,* 2000). The medicinal properties of Ashwagandha have been attributed to its chemical constituents, mainly alkaloids and steroidal lactones (primarily of the withanolide class). A monograph on this plant describing the extensive characterization of its chemical and medicinal aspects has recently been published (Singh and Kumar 1998). Ashwagandha is a dicotyledonous plant belonging to the family Solanaceae. It can be found growing in Africa, the Mediterranean, and India. As a result of this wide growing range, there are considerable morphological and chemotypical variations in terms of local species. The extract of *Withania somnifera* (WSE), is being recommended in traditional medicine for a variety of illnesses such as asthma, as a uterine sedative, antispasmodic, sedative and hypnotic, rheumatic pain, inflammation of joints, nervous disorders, epilepsy and against eye diseases.

Withania somnifera has been reported to have a wide range of biological activities. It shows antimicrobial activity (Kurup 1958; Sethi *et al.,* 1974), anti-tumor and radiosensitizing effects (Devi *et al.,* 1995; 2003), anti-angiogenic (Mohan *et al.,* 2004) anti-inflammatory, immunomodulatory,

antistress adaptogenic activity, anti-convulsive, hemopoetic, and rejuvenating properties. Recent literature suggests its efficacy as a cardioprotective agent (Dhuley, 2000), inhibitor of drug-induced urotoxicity (Davis *et al.,*2000), enhancer of white blood cell and platelet counts (Agarwal *et al.,*1999), an agent that enhances immunoprotection, cytokine production and stem cell proliferation, and an antioxidant (Davis *et al.,* 1999; Bhattacharya *et al.,* 1997).

There are various formulations of Ashwagandha, which are available in the market and there exists a wide variation in the constituents found in these extracts as studied by Sangwan *et al.,* (2004). It is for this reason that we decided to compare the properties of several available samples.

b). *Salacia oblonga* extract

This is a woody plant found in the forests of Sri Lanka and Southern parts of India and locally is called as Saptrangi, Ponkoranti and Chundan. The roots and stems of Salacia Oblonga have been used extensively in Ayurveda and traditional Indian medicine for the treatment of type 1 and type 2 diabetes. The roots of the *Salacia oblonga* have also been extensively used as a remedy for gonorrhea, rheumatism, and asthma.

The biological activities of the extract have been attributed to two major endogenous compounds, salacinol and kotalanol 9. These are known to be potent inhibitors of α-glucosidase, which plays a major role in converting carbohydrates into glucose (Heacock *et al* 2005). The extract also inhibits aldose reductase, which is relevant to chronic diabetic complications as peripheral neuropathy, retinopathy, and cataracts (Matsuda *et al.,* 1999). Here we further extend our studies on its anti-oxidative and cyto-protective abilities.

While studies of the plant extracts give us useful information, looking at the active principles involved in these extracts and their biological effects will give us an idea of the molecular basis behind these. We have therefore focused on some isolated and purified individual compounds from the plant extracts. The compounds include (+) Catechin (EC), Epigallocatechin gallate (EGCG) (polyphenolic compounds present in tea extract), Quercetin (present in *Ginkgo biloba*, and in several vegetables and fruits) and Withaferin A, a major compound present in Ashwagandha.

c). (+) Catechin (EC) and Epigallocatechin gallate (EGCG)

EC and EGCG are a polyphenolic compounds belonging to the flan-3-ol class of flavonoids. They are abundantly present in green and black tea leaves, and known to show antioxidant, anti-inflammatory, antibacterial and antiviral activity. These compounds are widely used in traditional medicines to treat cancers, cardiovascular diseases (Goldbohm *et al.*, 1996; Dufresne *et al.*, 2001; Hamza *et al.*, 2006; Katiyar *et al.,* 2007).

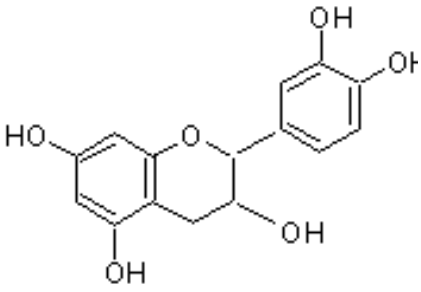

Catechin (+) (EC)
Molecular formulae- $C_{15}H_{14}O_6 \cdot xH2O$
Molecular weight: 290.3 Da

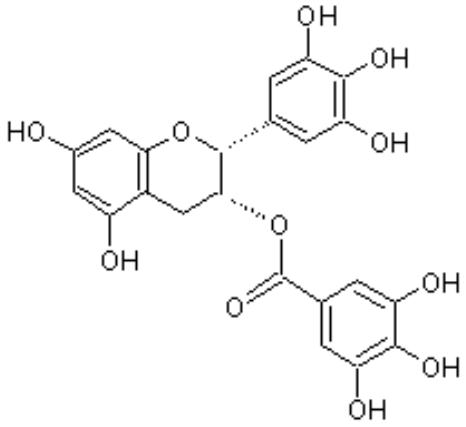

Epigallo catechin gallate (-) (EGCG)
Molecular formulae- $C_{22}H_{18}O_{11}$
Molecular weight: 458.4 Da

d). Quercetin

Quercetin also a flavonoid present abundantly in several fruits (apple, berries), onion, nuts, cauliflower, and cabbage. Its reported biological activities include antioxidant, anti-inflammatory and anti-histamine effect. Quercetin is widely used in traditional medicines to treat the cancers, arthritis and asthma. (Lamson *et al.,* 2000; Guardia *et al.,* 2001; Paliwal *et al.,* 2005).

Quercetin
Molecular formula- $C_{15}H_{10}O_7$
Molecular weight: 302.24 Da

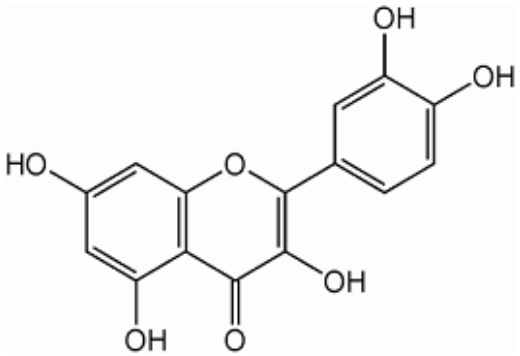

e). Withaferin A

Withaferin A belongs to the withanaloid family of compounds present abundantly in *Withania somnifera* (Ashwagandha). Some of its biological activities include; 1) antiangiogenic activity: It inhibits endothelial cell sprouting by altering the cytoskeletal architecture. It binds covalently to annexin II and stimulates the basal F-actin cross-linking activity which inhibits the migratory and invasive capability of the endothelial cells. It

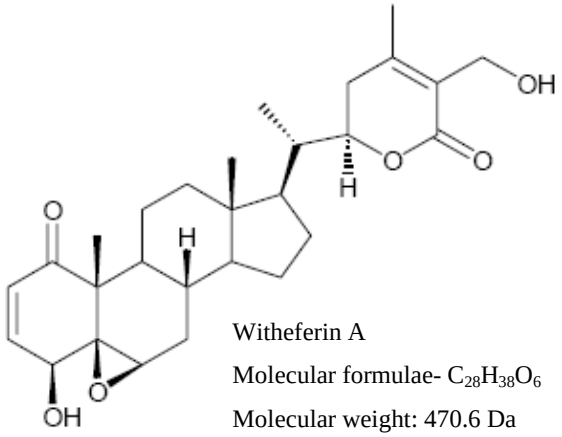

Witheferin A
Molecular formulae- $C_{28}H_{38}O_6$
Molecular weight: 470.6 Da

also acts as a neuronal regenerative agent. 2) neuro-regenerative ability: this was studied in amyloid β-induced axonal atrophy model, where it induced significant regeneration of both axons and dendrites. 3) inhibition of NFκB activation: It appears to prevent TNF-induced activation of IκB kinase ß (IKKß), and elicit IKKß hyperphosphorylation concomitant with inhibition of its kinase activity.

3.1. MATERIAL AND METHODS

3.1.1. Materials

Ashwagandha formulations were purchased from Kotakkal Arya Vaidya Sala, Kerala, Dabur India Ltd. New Delhi, Shree Baidyanath Ayurved Bhawan Pvt. Ltd. Nagpur, and Himalaya Drug company, Bangalore, India. Catechin (+) hydrate, Epigallocatechin gallate (EGCG), Quercetin and Withaferin A were purchased from Sigma-Aldrich.

3.1.2. Preparation of the standard stock solutions of the various compounds and extracts used in the study

A sample of the root powder of Ashwagandha obtained from Kotakkal Arya Vaidya Sala, Kerala, was used as the 'standard' (sample A). Three other formulations were purchased from the local market and are manufactured by Dabur, Baidyanath and Himalaya herbal companies and used for comparison (samples D, B and H, respectively). Stock solution of the root powder (100 mg/ml) was prepared in water and the soluble part was used to determine the antioxidant activity as well as for protein cross-linking studies. For experiments with cell lines, solutions were made in sterile phosphate buffered saline (PBS) and filtered using a 0.2 mm filter. 1 mM stock solutions were

prepared for Catechin (in 10% ethanol), Epigallocatechin gallate (in water) and Quercetin (in acetone). Hydrogen peroxide was used to induce the oxidative stress in HLE3B. The transformed cell lines of human lens epithelial cells, called HLE3B, was used to analyze the cyto-protective functions of the compounds mentioned above.

3.1.2. ABTS antioxidant assay

This assay was performed based on the protocol mentioned by Miller *et al.* (1993). Briefly, when 2,2'-azinobis-(3-ethylbenzothiazoline-6-sulfonic acid) or ABTS is incubated with a peroxidase (such as metmyoglobin) and H_2O_2, the relatively long-lived radical cation $ABTS^{\bullet+}$, is formed which has an absorption maximum at 734 nm. In the presence of an antioxidant, the absorption of this radical cation (at 734 nm) is quenched. In a typical experiment, ABTS (30 μl, 5 mM), 50 μl of metmyoglobin (50 μM), and 820 μl of phosphate buffer (50 mM, pH 7.4) (of which 10 μl is replaced with test compound (1 mM stock) when the samples are being investigated) are mixed, and the reaction is initiated by the addition of 100 μl of H_2O_2 (1 mM). The absorbance at 734 nm is measured as a function of time at 5- min. intervals for 30 min.

3.1.3. Assay for inhibition of photo-oxidation of proteins

The protein bovine pancreatic ribonuclease A, or RNase A, (1mg/ ml) was irradiated in the presence of the photosensitizer riboflavin, which upon irradiation at 445 nm, yields singlet oxygen in high quantum yield (Murali Krishna *et al.,* 1991). The damage to the protein, and protection offered by test compounds was monitored by SDS/PAGE.

3.1.4. Assay of cytoprotective ability

The cytoprotective ability of these compounds were studied using the MTT assay (Hansen *et al.,* 1989). This assay is based on the ability of living cells to reduce MTT to form formazon products, which can be quantified at 540 nm, by the intensity of blue color. HLE cells (1 x 10^5 cells per well in 0.5 ml medium) were seeded in a 24-well tissue culture plate and incubated at 37°C, 5% CO_2. After 22 h of incubation, when cells were about 75 % confluent, oxidative stress was induced using H_2O_2 (100 - 500 μM), in the presence or absence of the test compound 12-16 h at 37°C and 5% CO_2. The medium was removed and fresh DMEM with 5% FCS was added to each well, followed by 50 μl of 5 mg/ml MTT in PBS. The cells were further incubated for 4 hours at 37°C in a humidified 5% CO_2 incubator. The medium was removed and 500 μl of 40 mM HCl/ isopropanol added to stop MTT reduction. The blue color developed was read at 590 nm using an ELISA reader from Bio-Rad.

3.2. RESULTS & DISCUSION

3.2.1. Phytochemical variability of the Ashwagandha extracts

The free-radical scavenging activity of the root powder of *W*. *somnifera* has been reported earlier (Panda *et al.,* 1997). Bhattacharya *et al*. (1997) studied the antioxidant activity of the glycowithanilides of *W. somnifera*, where the effect of intraperitoneal injections of glycowithanolides on concentrations of antioxidant enzymes in brain frontal cortex and striatum of adult male Wistar rats was studied.

We have been working in our laboratory with a standardized monoherbal extract provided to us by Kottakkal Arya Vaidyasala, Kerala, to assess the antioxidant, cytoprotective and cataractostatic ability of Ashwagandha (Thiagarajan *et al.,* 2003). In light of the report by Sangwan *et al.* (2004), we undertook a comparison of the antioxidant properties of three other commercially available products with this kotakkal 'standardized' extract (called A). Equal concentrations of the four products were taken and their antioxidant abilities compared under identical conditions, using the ABTS assay. Figure 1 compares their abilities at a representative concentration (4 mg/ml). Product B displays the best antioxidant ability and would therefore seem to be the best of use; however, it is a polyherbal mixture. Of the others, which are all claimed to be monoherbal, product H displays the best antioxidant property. These differences appear consistent with the phytochemical variability referred to by Sangwan *et al*. (2004) and lend support to the suggestion that such variations might arise from locale-dependent physiological and ecological variations in plantations, harvest and post-harvest operations, and the processing and manufacturing methods. Thus the need for uniformity and standardization

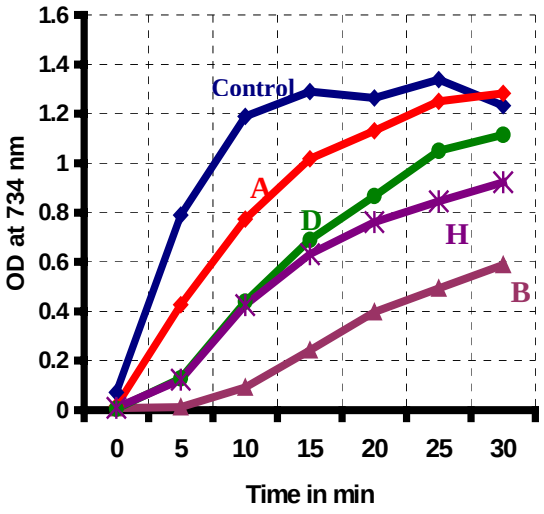

Figure 3.1. Comparison of the antioxidant abilities of four samples of Ashwagandha monitored by the ABTS assay. Ashwagandha samples were 2 mg/ml in water; The change in absorbance of ABTS at 734 nm was monitored over time.

guidelines in regulatory frameworks that is in vogue or contemplated in natural health products.

3.2.2. *Salacia oblonga* Extract

Much of the research on the *Salacia oblonga* extract has focused on understanding its role in treating diabetes. Its applications in the treatment of diabetes are well characterized and the biological mechanisms of its compounds have been studied (matsuda *et al.,* 1999; Heacock *et al.,* 2005). Here we report on its anti-oxidant properties and the effect of this extract on human lens epithelial cell lines.

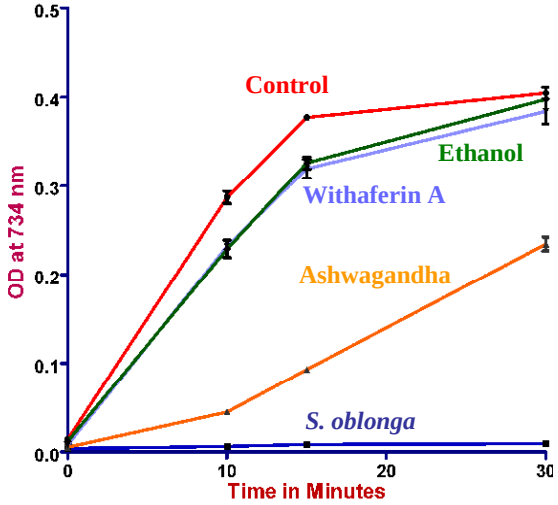

Figure 3.2. ABTS assay of Ashwagandha and *Salacia oblonga* (0.1 mg/ml final concentration)

Turning to antioxidant agents, addition of *Salacia oblonga* extract (0.1 mg/ml) led to a rapid drop in the ABTS absorption at 734 nm within minutes, this drop is much higher in comparison to Ashwagandha at similar concentration, as evident in figure 3.2. It is also far more potent as an antioxidant than Withaferin A which has very little such ability.

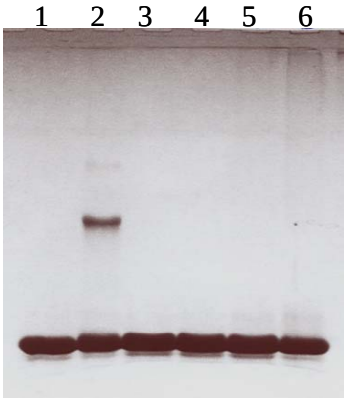

Figure 3.3. SDS/PAGE of oxidized proteins (1 mg/ml). Protection offered by Ashwagandha and *Salacia oblonga to* ***riboflavin-induced photo-oxidation.*** Lane 1 = Control RNase A,, lane 2 = RNase A +20 mM riboflavin, lane 3 = RNase A + 0.1 mg/ml Ashwagandha – irradiated, lane 4 = RNase A +20 mM riboflavin + 0.1 mg/ml Ashwagandha – irradiated, lane 5 = RNase A 0.1 mg/ml *S.oblonga* – irradiated, lane 6 = RNase A +20 mM riboflavin + 0.1 mg/ml *S.oblonga* - irradiated

Figure 3.3 shows the electrophoresis pattern of test protein RNase A subjected to oxidative stress by riboflavin. Both Ashwagandha and *S. oblonga* are equally efficient in protecting the damage to the protein caused due to $^1O_2$ generated by photo-sensitizer riboflavin.

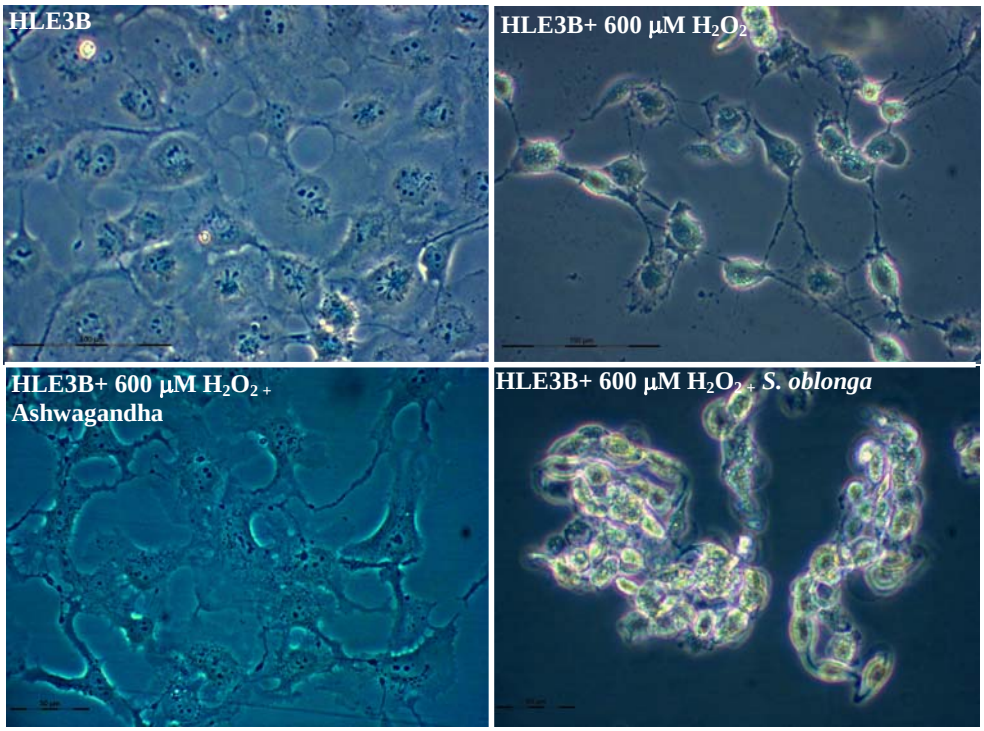

Figure 3.4. Phase contrast microscopic images showing the morphological features of HLE3B cell lines after treatments with various plant extracts and H_2O_2. Images were magnified 400 times.

While the anti-oxidant activities and the protection offered to the proteins against oxidative stress induced damage is better than Ashwagandha, the *Salacia oblonga* extract showed marked cellular toxicity to HLE3B cells even at a low concentrations (0.1 mg/ml) as shown in Figure 3.4, while Ashwagandha extract shows a marked protection against H_2O_2 induced cell death. The protection offered by the Ashwagandha extract has been earlier shown to be dose dependent (Thiagarajan *et al.,* 2003).

3.2.3. Molecular features of the Catechin (+) hydrate, Epigallocatechin gallate, Quercetin and Witheferin A

Figure 3.5 shows the potent antioxidant properties of the various compounds tested. While Quercetin, Catechin and EGCG are found to have potent anti-oxidant properties, Witheferin A did not show any. The anti-oxidant properties of the compounds tested are found to be in the order Quercetin > Catechin > Epigallocatechin gallate. We then proceeded to monitor their cyto-protective abilities using human lens epithelial cell lines.

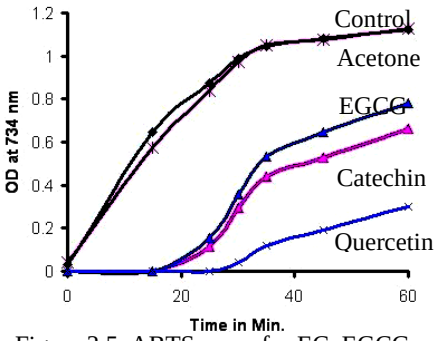

Figure 3.5. ABTS assay for EC, EGCG, Quercetin and Witheferin A

It was earlier shown that crude extracts of the plants which are rich in these compounds are able to protect cells from oxidative stress induced cell death (Thiagarajan *et al.,* 2001, 2002, 2003). This prompted us to look at whether the constituent individual compound can offer the same protection as that of the crude extract. This will give an indication about whether the observed activity in the crude extract is because of the particular individual compound or due to a combination of compounds in that extract.

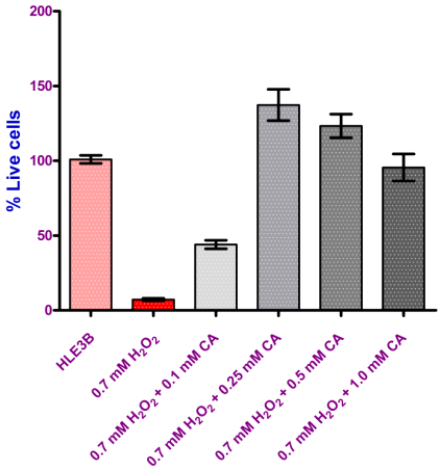

Figure 3.6. MTT cell viability assay for HLE3B, oxidized with H_2O_2 and tested for various concentrations of Catechin

We thus subjected HLE3B cells to H2O2-induced stress in the absence

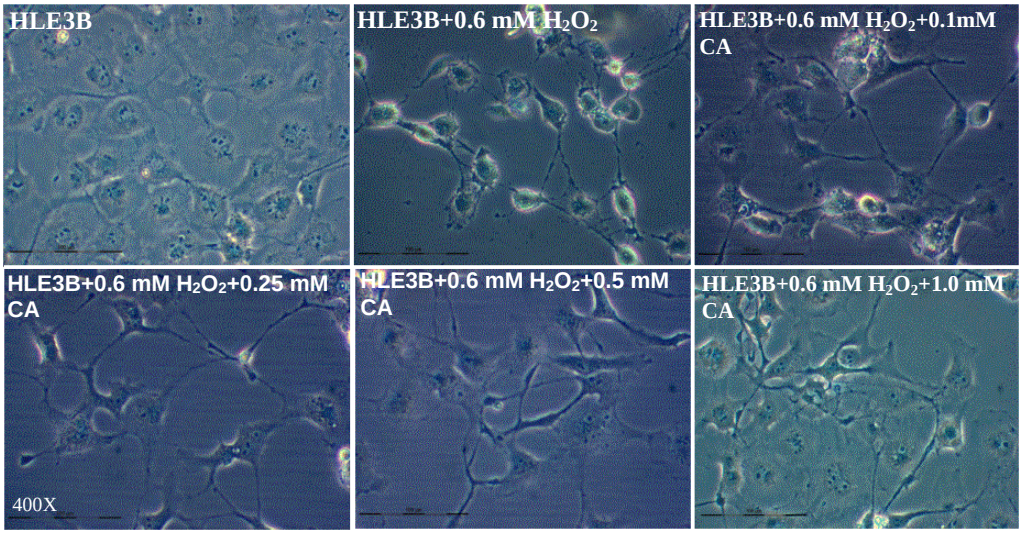

Figure 3.7. Phase contrast microscopic images showing the morphological features of HLE3B cell lines after treatments with various concentrations of catechin and H_2O_2.

and presence of the compounds, and assayed the viability of cells using the MTT method. Figure 3.6 shows that (+) Catechin protects HLE3B cells from permanent damage and keeps them viable. This protection is dose dependent manner, i.e. the higher the dose higher the protection. Catechin does not show any cellular toxicity even at 1mM, as shown in Figure 3.7. While Catechin is found to have potent cellular protection against oxidative damage, Quercetin did not do so, while EGCG was found to be cyto-toxic.

Russo *et al.* (2001) investigated the free radical scavenging capacity of methanolic extracts of *Withania somnifera* and the effect on DNA cleavage induced by H_2O_2 UV-photolysis and whether this extract was capable of reducing cytotoxicity and DNA damage in human non-immortalized fibroblasts. In our earlier studies (Thiagarajan *et al.,* 2003) we could show similar effects of the extract, using HLE3B cells. But we found that the endogenous compound withaferin A does not offer any cellular protection to HLE3B cell lines against oxidative stress.

Earlier studies on tea extract from our laboratory (Thiagarajan *et al.,* 2001) had shown potent cataractostatic ability in HLE3B cell lines and in oxidative stress induced cataract models in the rat pups. Based on these, we have now analyzed the ability of catechin and EGCG to do so. Though catechin showed protection against oxidative stress induced cell death in human lens epithelial cell lines, its functionality in the oxidative models of cataract yet to be tested. The other component of tea extract, EGCG, is cytotoxic to HLE3B. Our present results thus suggest that the cataractostatic properties observed earlier (Thiagarajan *et al.,* 2001) is due to the presence of the abundant amount of catechin in the extract. Before attributing

cataractostatic abilities to the catechin, it is essential to check the activity of catechin in oxidative cataract models. Such a comparative analysis of the crude extract and the catechin will also provide the necessary information about the use of single compounds in treating the diseases and the avoidance of several side effects which might arise due to other components in the crude extract.

Finally, the issue of toxicology and safety of these compounds and the doses to humans needs to be addressed. A remarkably low rate of adverse drug events associated with the use of EGb761-containing products from G*inkgo biloba* has been reported (De Feudis, 1998). Rhee *et al*. (2001), commenting about the use of complementary and alternative medicine for glaucoma, have worried about possible toxicities of ginkgo and other herbal remedies. The second issue is that the material available over the counter in drug stores and nature food shops is not a standardized extract, since phytochemical variations occur based on locality specific and strain specific factors.

STUDY OF SOME NEUROPROTECTIVE COMPOUNDS FROM PLANTS AND THEIR POTENTIAL THERAPEUTIC VALUE IN GLAUCOMA

4.0. INTRODUCTION

Glaucoma is a major cause of irreversible blindness in the world, and is estimated 6.8 million people are bilaterally blind due to glaucoma (Quigley *et al.,* 1996). The disease is characterized by slow progressive degeneration of retinal ganglion cells and their axons. Elevated intraocular pressure (IOP) is a major risk factor associated with the disease. The current therapeutic management of glaucoma aims to halt the disease progression by altering the IOP by several means. While lowering the IOP helps in retarding the disease progression, it is not always sufficient to fully prevent disease progression. Also, IOP is not elevated in all patients exhibiting the characteristics of glaucomatous neurodegeneration. The similarity in clinical and histopathological finding in patients with normal as well as in elevated IOP indicates that there exists IOP-independent neuronal damage mechanisms in glaucoma. It is because of these reasons that recent efforts have focused on understanding other possible risk factors and mechanisms involved in glaucomatous degeneration. Tissue hypoxia, oxidative stress and glutamate-mediated excitotoxicity have been identified as some of these pathogenic mechanisms.

4.0.1. Hypoxic component of glaucomatous tissue stress

The major evidence for the role of tissue hypoxia in glaucoma pathogenesis has come from blood flow studies. Clinical evidence for vascular abnormalities

in glaucoma patients include vasospasm, systemic hypertension, antigenic vascular perfusion defects, and alterations in blood flow parameters, which may result in reduced vascular perfusion in the optic nerve and retina (Chung *et al.,* 1999; Cioffi and Wang, 1999; Flammer, 1994; Flammer *et al.,* 2002; Hayreh, 1978; Osborne *et al.,* 1999). Hypoxic tissue stress in glaucomatous eyes, which is thought to develop secondary to, or independent from, elevated IOP, may adversely affect neuronal survival by inducing cell death (Gross *et al.,* 1999; Kitano *et al.,* 1996; Osborne *et al.,* 2004; Rosenbaum *et al.,* 1997; Tezel and Wax, 1999; Tezel and Wax, 2000a).

Molecular evidence for the role of tissue hypoxia in glaucoma came from the identification of some hypoxia inducible genes, mainly hypoxia inducible factor-1 α (HIF-1α). This gene expression is tightly regulated by cellular O_2 concentration and increases as cells are exposed to decreasing O_2 concentration. Under hypoxic conditions, HIF-1α activates the transcription of several genes, including vascular endothelial growth factor (VEGF) and inducible nitric oxide synthetase (iNOS) whose presence increases the O_2 delivery or facilitate the metabolic adoption to hypoxia (Guillemin and Krasnow, 1997; Iyer *et al.,* 1998; Semenza, 1999; Wang *et al.,* 1995). A study by Tezel and Wax (2004) showed histopathalogically that the glaucomatous optic nerve and retina express significantly higher amounts of HIF-1α than age matched controls.

4.0.2. Oxidative component of glaucomatous tissue stress

Increasing evidence shows that the glaucomatous stress induced by elevated IOP and / tissue hypoxia also involves an oxidative component. Several experimental animal models support the role of oxidative stress in

glaucomatous damage. Experimental elevation of IOP induces oxidative stress in the retina; this is in consistent with retinal ischemia models as well as with moderate and chronic elevation of IOP (Bonne *et al.,* 1998; Muller *et al.,* 1997). Ko *et al.,* (2005) showed that cauterization of episcleral veins results in an increase in reactive oxygen species or ROS, generation and increased lipid peroxidation in the ocular hypertensive rat retina. Another supportive evidence for oxidative stress during glaucomatous degeneration comes from the detection of autoantibodies against glutathione S-transferase (GST) in the serum of glaucomatous patients (Yang *et al.,* 2001). GST is a major group of detoxification enzymes regulated *in vivo* by ROS, and its induction by ROS appears to be an adaptive response, since this enzyme detoxifies toxic metabolites produced by oxidative stress (Hayes and Strange, 1995).

Histopathological studies on human donors (Kerrigan *et al.,* 1997; Wax *et al.,* 1998), and studies using various experimental animal models of glaucoma (Garcia-Valenzuela *et al.,* 1995; Li *et al.,* 1999; Quigley *et al.,* 1995) have demonstrated that glaucomatous optic nerve axons and RGCs die through apoptosis. Figure 4.1 shows the multiple pathogenic mechanisms triggered by elevated IOP and/or tissue hypoxia, associated with optic nerve degeneration and RGC apoptosis in glaucoma.

Oxidative stress induced death of RGC soma, dendrite, axon, or synapse appears to be coupled with mitochondrial dysfunction, which is importantly associated with ROS generation. Increasing evidence suggests mitochondrial dysfunction in glaucoma (Mittag *et al.,* 2000; Tatton *et al.,* 2001; Tezel and Yang, 2004). Abu-Amero *et al.,* (2006) demonstrated mitochondrial DNA abnormalities in patients and suggested that mitochondrial dysfunction-associated oxidative stress as a risk factor for glaucoma patients.

Another series of findings demonstrate oxidative injury through the involvement of TNF death receptor signaling. TNF-α is upregulated in the glaucomatous optic nerve head and retina (Tezel *et al.,* 2001b; Yan *et al.,* 2000; Yuan and Neufeld, 2000), and is identified to be a mediator of RGC death (Tezel, 2006).

4.0.3. Excitotoxic component of glaucomatous tissue stress

Excitotoxicity is a process which describes the neuronal injury due to the excessive stimulation of neurotransmitter receptors. Early in 1957 Lucas and Newhouse hypothesized, and showed, the loss of neurons in the inner retina after subcutaneous administration of glutamate. Subsequently it has been observed in several other CNS disorders. A decade later, Onley (Onley *et al*., 1967) described brain lesions in mice treated with monosodium glutamate, and coined the term 'excitotoxicity' to describe the process of neuronal death caused by excessive or prolonged activation of receptors for excitatory amino acid neurotransmitters. Subsequently a large body of evidence has accumulated that excessive extracellular glutamate levels can be toxic to neurons including those in the retina.

The role of excitotoxicity in glaucoma is circumstantial and speculative, but derived from several sources: I) The fact that excitatory amino acid glutamate acts as a neurotransmitter in the retina; ii) the observation that elevated vitreous glutamate levels in experimental as well as in clinical glaucoma (Dreyer *et al.,* 1996); iii) evidence from neuroprotection based animal studies, (el-Asrar *et al.,* 1992; Weber *et al.,*

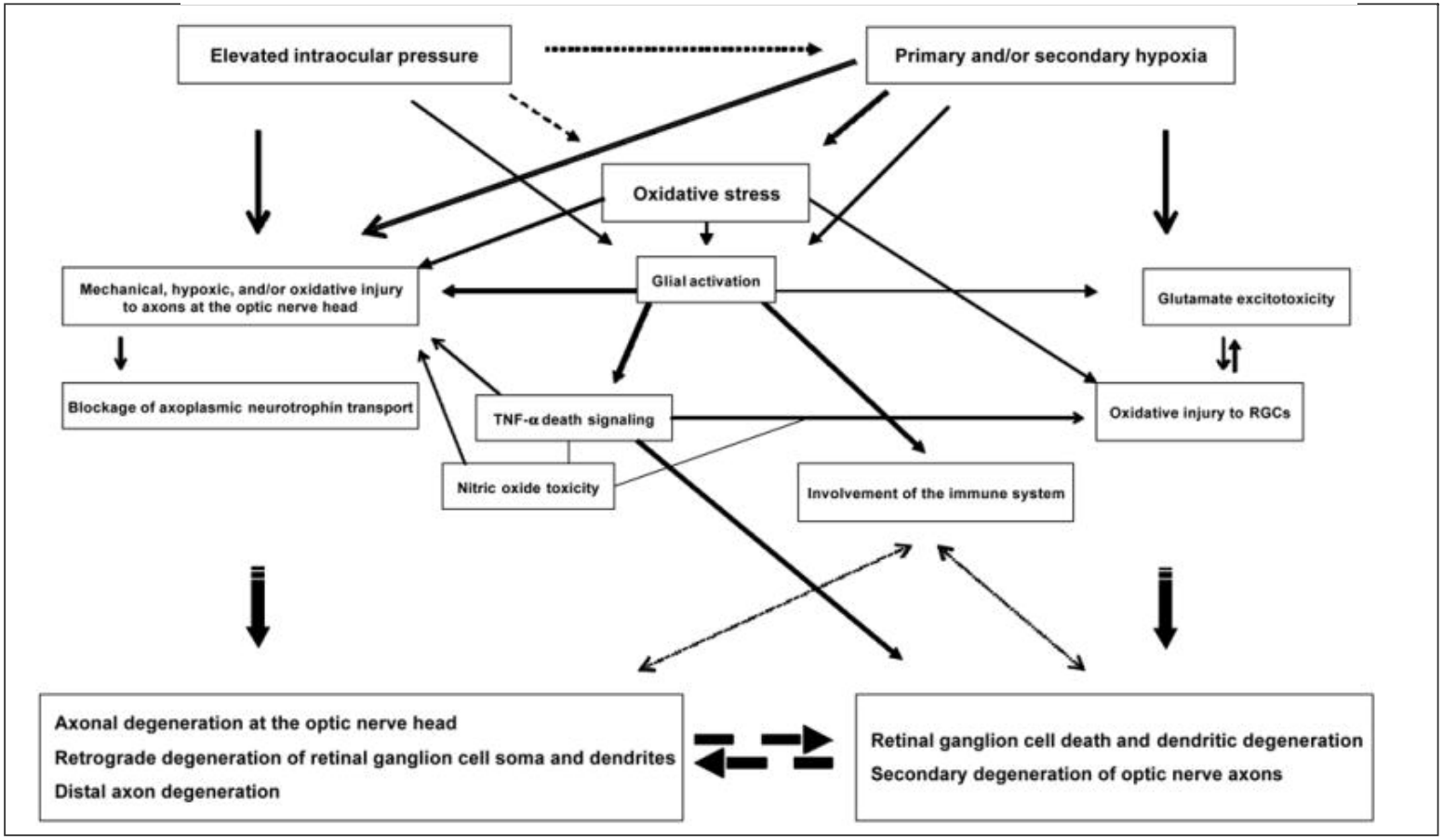

Figure 4.1. Multiple pathogenic mechanisms have been proposed for glaucomatous neurodegeneration. Most of these mechanisms appear to be associated with a common pathway of oxidative injury (Tazel, 2006)

1995; Lam *et al.,* 1997; Kim et al., 2002); iv) evidence that ischemia plays a role in glaucoma (Lam *et al.,* 1997), and v) evidence that secondary degeneration of RGCs after optic nerve injury (Levkovitch-Verbin et al., 2001).

Mechanistic insights into excitotoxicity are well worked out and they involve the loss of ionic homeostasis and ultimately cell death. The principal ionic changes include the influx of Na+ ions, and an increase in Ca2+ ion. These changes occur in parallel and result in ongoing depolarization, amplification and continuation of the injury by further release of glutamate, and calcium induced cell death.

Understanding these factors has provided the much needed impetus to the development of alternative treatment strategies for neuroprotection. This prompted several researchers to look for compounds which can retard glaucomatous neuronal damage induced by ischemia, oxidative stress and excitotoxicity. Several studies have focused using either the elevated IOP model or axotomy model individually. Screening for a compound which can be effective in more than one pathway is important. In this connection we have aimed to look at some of the antioxidant molecules isolated from plant extracts and their ability to retard the oxidative stress-induced as well as excitotoxicity-induced neuronal cell death using rat retinal ganglion cell lines (RGC5) as a model system. The molecules tested include Catechin, Epigallocatechin gallate, Quercetin and Witheferin A.

4.1. MATERIAL AND METHODS

4.1.1. Materials

(+) Catechin hydrate, Epigallocatechin gallate, Quercetin and Withaferin A were purchased from Sigma-Aldrich. Rat Retinal Ganglion Cell lines (RGC5) were a kind gift of Prof. Niraj Aggarwal of university of North Texas.

4.1.2. Preparation of standard stock solutions

Stock concentrations of 1 mM were prepared for catechin (in 10% ethanol), epigallocatechin gallate (in water) and quercetin (in acetone). Hydrogen peroxide, in concentration ranging from 100 to 600 μM, was tested for its ability to induce oxidative stress-related cell death in RGC5. In a similar way, glutamate mediated excitotoxicity was also induced in RGC5 cell lines by incubating the cells with various concentrations of sodium glutamate for various lengths of time period, and used to analyze the cyto-protective functions of the compounds mentioned above.

4.1.3. Phase contrast microscopic examination and morphological assessment

RGC5 cells (50,000 cells per well) were seeded in a 24 well culture plate and incubated at 37 ºC in a humidified 5% CO_2 incubator for 24 hrs. The medium was changed and the cells were treated with either H_2O_2 or glutamate, with or without the test compound, and incubated further for 12-16 h in a humidified CO_2 incubator at 37 ºC. The cells were observed under an Olympus CK40 microscope and phase contrast images were taken using a ProgResC3 camera (Jenoptik, Germany) integrated with microscope.

4.1.4. Assay of cytoprotective ability

The cytoprotective ability of test compounds was studied using the MTT assay (Hansen *et al.,* 1989). This assay is based on the ability of living cells to reduce MTT to form formazon products, which can be quantified at 540 nm, by the intensity of blue color. RGC5 cells (50,000 cells per well in 0.5 ml medium) were seeded in a 24-well tissue culture plate and incubated at 37°C, 5% CO_2. After 22 h of incubation, when cells were about 75 % confluent, oxidative stress was induced using H_2O_2 (100 - 600 μM), in the presence or absence of test compound 12-16 h at 37°C and 5% CO_2. Media was removed and fresh DMEM with 5% FCS was added to each well and after which 50 μl of 5 mg/ml MTT in PBS was added to each well. The cells were further incubated for 4 hours at 37°C in a humidified 5% CO_2 incubator. The medium was removed and 500 μl of 40 mM HCl / isopropanol was added to stop MTT reduction. The blue color developed was read at 590 nm using an ELISA reader from Bio-Rad.

Glutamate mediated excitotoxicity was also induced when the cells were 70% confluent using 30 mM glutamate in DMEM with 5% FCS. The effect of test compounds on glutamate-mediated excitotoxicity was tested by adding the test compound in various concentrations to the cell at the time of induction of excitotoxicity. All the other procedure was fallowed as mentioned above.

4.1.5. Annexin V assay

The assay was performed using the Vybrant Apoptosis Assay kit, Alexa Fluor 488 annexin V/ Propidium iodide (Molecular probes, Invitrogen), and was performed according to the manufacturers instructions. Briefly, 1 X 10^5 RGC5 cells were seeded in a 6-well culture plate and treated with oxidative or excitooxic stress given as above. The cells were trypsinized from the plate and washed twice with ice cold PBS. They were then resuspended in Annexin V binding buffer and the cell density was adjusted to 1X10^6 cells per ml, using a sufficient volume, 100 μl, per assay. 5μl of Alexa Fluor 488 annexin V and 1μl of the 100 μg/ ml PI working solution were added to each 100 μl of cell suspension and incubated for 15 minute at room temparature. After incubation 400 μl of Annexin V binding buffer was added and the samples were kept on ice. The stained cells were analyzed by flow cytometry (BD FACS Aria) by measuring the fluorescence emission at 530 nm and >575 nm. The population separated into three groups: live cells showing only a low level of fluorescence, apoptotic cells showing green fluorescence, and dead cells showing both red and green fluorescence.

4.2. RESULTS AND DISCUSION

Here we present our results on the three compounds tested and their usefulness in retarding the oxidative stress as well as glutamate-mediated excitotoxicity induced RGC5 cell death.

Catechin retards the oxidative stress as well as glutamate excitotoxicity induced cell death in RGC5 lines, in a dose dependent manner as shown by MTT assay results (Figure 4.2a and 4.2b respectively).

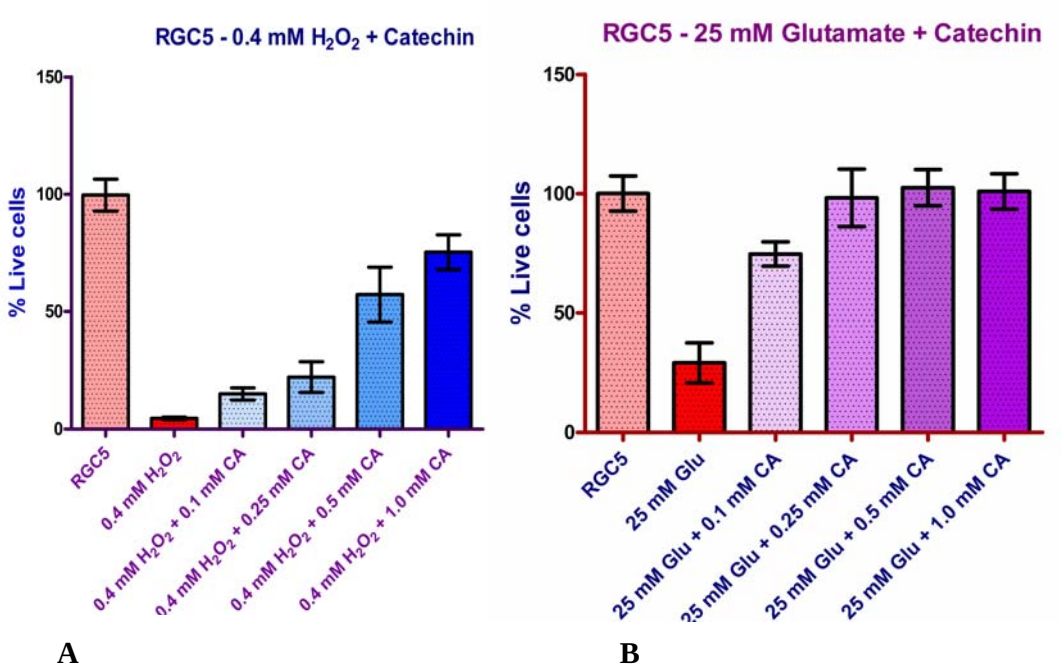

Figure 4.2. MTT cell viability assay for RGC5, oxidized with H_2O_2 (Panel A) and glutamate (panel B) and tested for various concentrations of Catechin. Y-axis indicates the % live cells with $\pm$ slandered deviation (SD)

Figure 4.3 shows the cellular morphology of RGC5 cells after treating with H_2O_2, in the presence of the various concentration of catechin.

Even at 1mM concentrations as high as 1 mM, we find that catechin does not show any cellular toxicity and efficiently inhibits cell death induced by hydrogen peroxide. Figure 4.4 shows similar results obtained with catechin in the glutamate-mediated excitotoxicity as well.

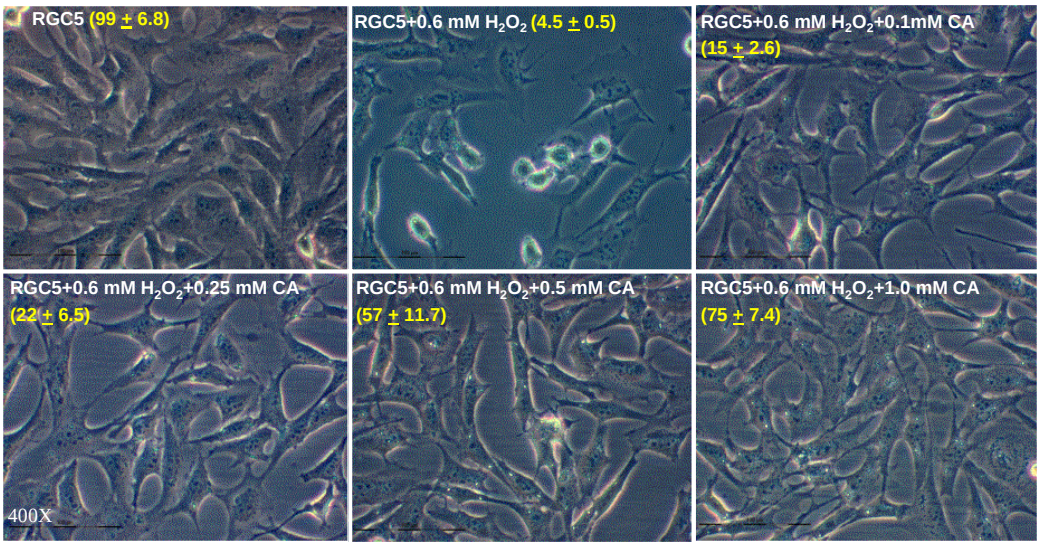

Figure 4.3. Phase contrast microscopic images showing the morphological features of RGC5 cell lines after treatments with various concentrations of Catechin (+) and H_2O_2 (% live cells ± SD).

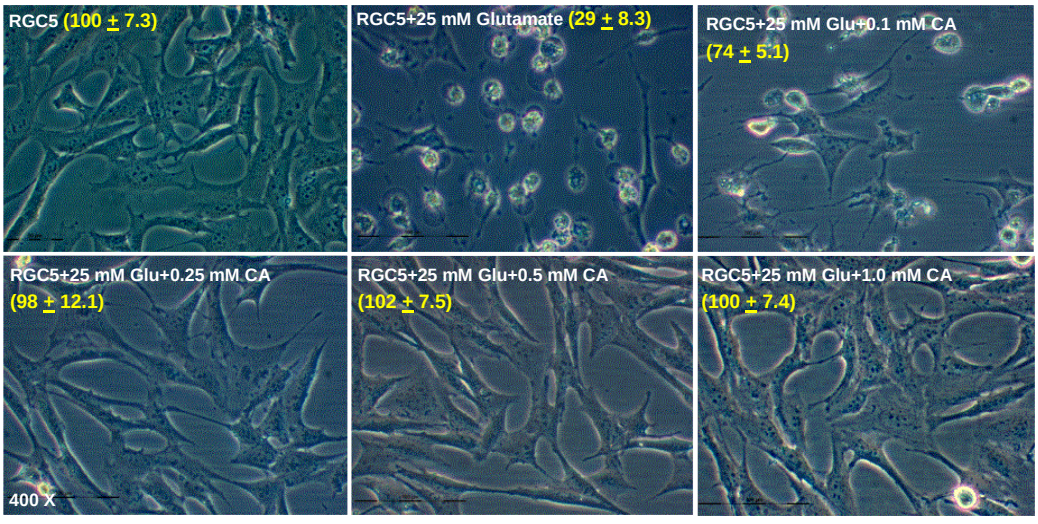

Figure 4.4. Phase contrast microscopic images showing the morphological features of RGC5 cell lines after treatments with various concentrations of Catechin (+) and glutamate (% live cells ± SD)

The results of Anesin V assay reconfirm the results of MTT assay and suggest that glutamate induced cell death can be inhibited by catechin. The percentage of cells undergoing apoptosis in cells grown in normal media is 7.2% (Figure 4.5B). Upon induction of excitotoxicity the number of cells undergoing apoptosis reaches to 32% (Figure 4.5C). Treatment with 1 mM catechin brings down the number of cells undergoing apoptosis back to 11.6% (Figure 4.5D), indicating that catechin protects excitotoxicity induced apoptosis of the cells.

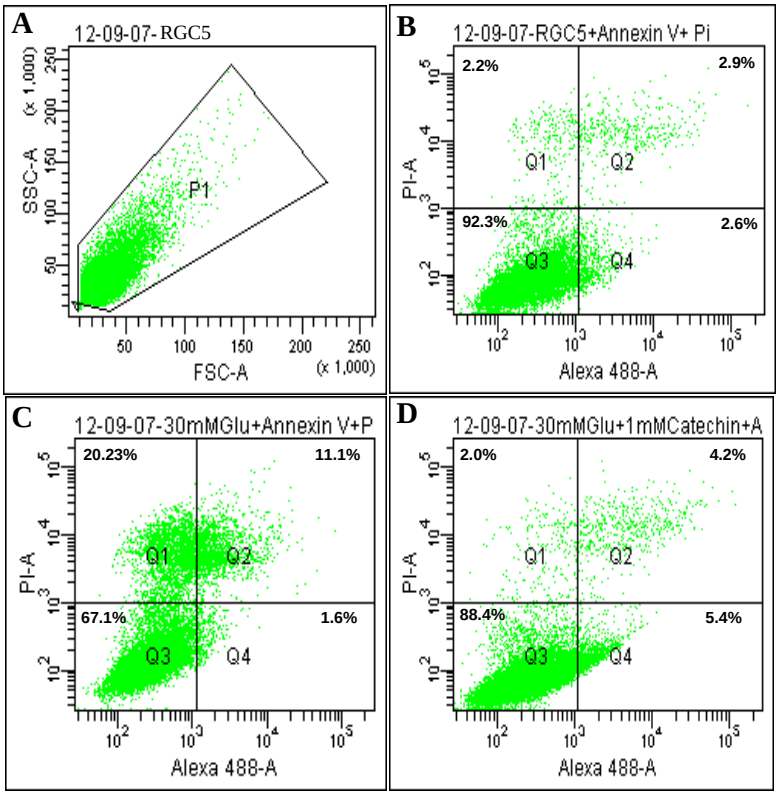

Figure 4.5. FACS analysis of the annexin V assayed RGC5 cells, **Panel A** shows the side scatter vs forward scatter pattern. **Panel B** shows the distribution of the normal cells labeled with annexin V and PI. **Panel C** shows the Aneexin V and PI labeled cells after inducing the apoptosis with glutamate. Panel D shows the Annexin V and PI labeled RGC5 cells treated with 30 mM glutamate and 1 mM catechin.

Figure 4.6 shows that quercetin prevents cell death induced by glutamate, but it reveals that it does not show much protection against oxidative stress induced death. In comparison with catechin, the protection offered by quercetin against glutamate-induced excitotoxicity is significantly less. However, while the protection offered by quercetin is less, it did not show any cellular toxicity.

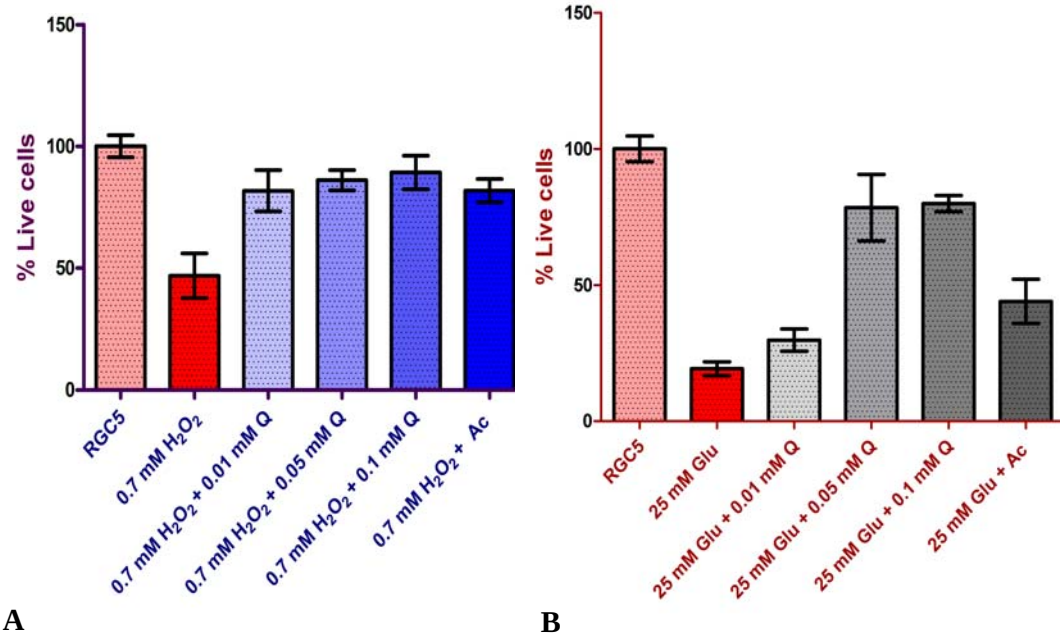

A **B**

Figure 4.6. MTT cell viability assay for RGC5, oxidized with H_2O_2 (Panel A) and glutamate (panel B) and tested for various concentrations of Catechin. Y-axis indicates the % live cells with $\pm$ SD.

While catechin and quercetin show protection against cell death induced by glutamate and also some extent to oxidative stress, epigallocatechin gallate is found to be toxic to the RGC5 cells, as shown in the Figure 4.7. This indicates that there are molecule specific effects, which need to be investigated.

Our results suggest that of the three compounds, catechin appears to be the best towards neuroprotection of retinal ganglion cells. It will be interesting to check whether a similar kind of neuroprotection is seen in experimental models for glaucoma. Further studies should also be directed to find out the mechanism of action of this molecule in neuroprotection. Finally, while several studies, including the present one, point to the usefulness of antioxidants and cytoprotective agents in cataract and glaucoma, the issue of the concentration required *in situ* at the target site cannot be ignored. Daily systemic administration through diet or supplementation, while good, it is not certain how much reaches the relevant parts of the eye. How to deliver the necessary dose in a targeted and sustained mode is an issue that is important and challenging.

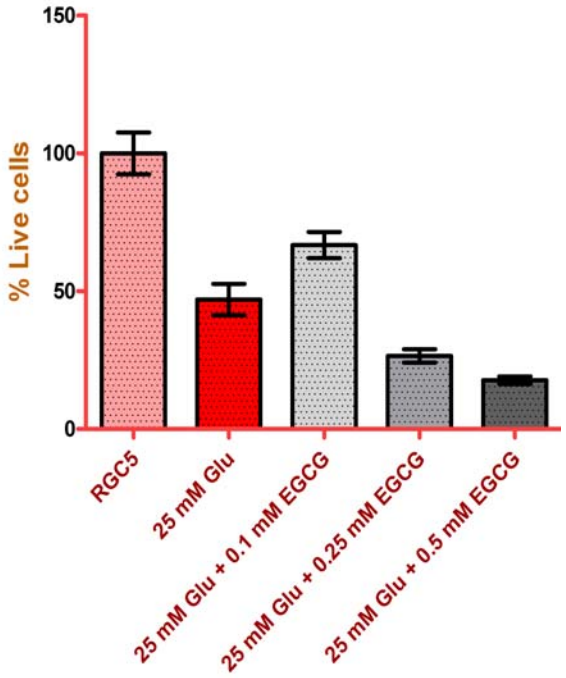

Figure 4.7. MTT cell viability assay for RGC5 treated with glutamate and with various concentrations of EGCG.

SUMMARY

Blindness is one of the most devastating disabilities of people across the world. The personal, social and economic consequence of blindness has become an important public health issue, especially in underdeveloped and developing countries. A recent estimate by the WHO, released in 2004, has claimed that nearly 37 million people around the world were blind that includes 1.4 million children under the age of 15 years (Resnikoff *et al.,* 2004). The WHO report also suggests that 75% of blindness is caused by four specific age-related conditions such as cataract, glaucoma, age-related macular degeneration and diabetic retinopathy. Cataract is a leading cause of blindness, which accounts for 47.8% of total blindness, followed by glaucoma (12.3%), age-related macular degeneration (8.7%) and diabetic retinopathy (4.8%).

Childhood blindness accounts for 3.9% of global blindness (Resnikoff *et al.,* 2004). Though it looks less in comparison to other adult blindness, it is the second largest cause of blind-person years, following cataract. Children who are born blind or who become blind are blind for lifetime, with all the associated emotional, social, and economic costs to the child, the family, and society. Hence childhood blindness also seeks immediate attention.

In this context, we have focused our study on the two leading causes of global blindness, namely, cataract including congenital cataract and glaucoma, which together contribute to ~60% of global blindness.

In this thesis we have addressed different aspects of cataract and glaucoma which include:

1. Molecular phenotyping of γ-crystallins associated with autosomal dominant congenital cataract. We have studied this by cloning, expression, and solution state, *in silico* and *in situ* (in cell cultures) structural characterization of some mutant γ-crystallins, associated with autosomal dominant congenital cataract.
2. Evaluation of the anti-oxidant and cytoprotective activity of active constituents of various plant extracts such as catechin, epigallocatechin gallate, quercetin, and withaferin A, and their ability to retard damage and death of human lens epithelial cells induced by oxidative stress.
3. Evaluation of the neuroprotective actions of catechin, epigallocatechin gallate and quercetin, by inducing glaucomatous retinal ganglion cells (RGC) degeneration in rat retinal ganglion cell lines (RGC5) by excitotoxicity and oxidative stress.

I. Molecular phenotyping of γ-crystallins associated with autosomal dominant congenital cataract.

Congenital cataract is the common cause of blindness in children which accounts for nearly 10-30% of childhood blindness. The prevalence of congenital cataract in India varies from 1-6 per 10,000 (Lambert and Drack 1996). Genetic etiology accounts fro 30-50% of congenital cataract (Lund *et al.,* 1992). γ-Crystallins are a set of the majorproteins constituting the human eye lens While there are 7 genes in humans which code for various γ-crystallins, only γC and D crystallins (CRYC and CRYD, respectively) are abundantly expressed. A large number of mutations in γC and D-crystallins

are known to be associated with congenital cataract. Hence the understanding of the role of these mutations in cataract formation is important.

A few such mutations studied in the present thesis include a) A 5-base insertion in the γC-crystallin gene, associated with autosomal dominant variable zonular pulverulent cataract (Ren *et al.,* 2000): b) R168W, a point mutation (502 C → T) in exon 3 of γC-crystallin, leading to a protein chain truncated at position 156, associated with congenital lamellar cataract (Santhiya *et al.,* 2002); c) A novel nonsense mutation (W157X) in CRYGC associated with autosomal dominant congenital nuclear cataract and microcornea (Zang *et al.,* 2007), and d) A homologous mutation in the third exon of CRYGD (470G → A), resulting in termination of the chain after residue 157 (W157X), associated with congenital central nuclear cataract (Santhiya *et al.,* 2002).

We have thus gone ahead to study the structural properties of these protein in three ways: by cloning and expressing the protein and analyzing its solution state structural properties, homology modeling, and by transfecting into the cell lines HLE 3B, RGC5 and COS1.

Salient findings

(i) On the 5-base insertion mutant of human γC-crystallin

1. Molecular modeling of this mutant crystallin has suggested a random coil structure to the protein, as only the N-terminal 38 amino acid sequence shows homology with wild type γC-crystallin and the rest of

the sequence does not match with any other protein in the protein databank.

2. CD spectroscopic analysis of the cloned, isolated and purified protein confirmed that it does not adopt any ordered chain conformation, but only a random coiled structure.

(ii) On the R168W mutant of human γC-crystallin

1. Homology modeling of this protein showed a significant increase in the hydrophobic surface area exposed to solvent, in comparison to the normal wild type γC-crystallin.
2. Overexpression of this protein found it to be quite soluble; the solution state structural properties of this protein do not show any significant difference from those of the wild type. Surface hydrophobicity analysis, using an extrinsic nonpolar fluorescent probe, showed it to have a somewhat greater exposure of nonpolar side chains; the mutant also exhibited an increased tendency to self-aggregate upon heating to 65 °C, in contrast to the wild type molecule.
3. Transfection of the mutant cDNA construct into Human Lens Epithelial Cell lines (HLE3B), rat Retinal Ganglion Cell (RGC5) lines and into COS1 cell lines did not show any protein aggregation, *in situ*, in the cells, quite similar to the behavior of the wild type construct.

Note: Detailed studies on these two mutants have been published; see Talla *et al*. (2006), attached as annexure 1.

(iii) On the W157X mutant of human γC-crystallin

1. Homology modeling of this protein showed an exposure of several hydrophobic residues, which are otherwise buried inside the core of the wild type molecule.
2. Overexpression of the mutant by cloning and expressing in *E. coli* resulted in the formation of inclusion bodies. Attempts to solubilize the protein were not very successful; the protein is seen to have very low solubility, which prevented us from pursuing any solution state structural studies.
3. Transfection of the mutant construct into HLE3B, RGC5 and COS1 cell lines showed intracellular, *in situ,* aggregates; it was also seen not to enter the cell nuclei, quite in contrast to the behavior of the wild type construct, which was seen to be uniformly present in the soluble form in the cytoplasm and nucleus.

(iv) On the homologous W156X mutant of human γD-crystallin

1. Homology modeling of this protein revealed the exposure of several hydrophobic residues which are otherwise buried inside the wild type molecule.
2. a) Over-expression of this protein in *E.coli* resulted in the formation of inclusion bodies, in contrast to wild type molecule; b) solubility of the mutant was found to be only 0.2 mg /m, while the wild type molecule is

soluble up to 200 mg/ml; c) the secondary structure of the mutant protein is similar to that of the wild type molecule; d) thermal and chemical denaturation and renaturation studies revealed the structural stability of the mutant protein to be far less than that of the wild type molecule, and e) the mutant protein aggregates much faster and to a higher extent than the wild type molecule does, when heated to 65 °C.

4. Transfection of the mutant construct into HLE3B, RGC5 and COS1 cell lines showed punctuate intracellular aggregates; it also was not seen to enter into the nuclei, which is in contrast to the wild type construct.

Note: Detailed studies on these mutants are being published (Talla *et al*., manuscript submitted; see annexure 2)

2. Evaluation of the anti-oxidant and cytoprotective activity of plant extracts and their active constituents - their ability to retard oxidative stress induced damage to the human lens epithelial cells

From congential catarcts in newborns and children, we move to cataract that affects the elderly and aged. Age related cataract is a common cause of blindness in the world, accounting for nearly 48% of the total blindness burden in the world (Resnikoff *et al.,* 2004). One of the major etiological factors

associated with this type of cataract is found to be aging and accumulated oxidative stress, and resultant damage to the lens proteins. Administration of antioxidants on a regular basis is hypothesized to be beneficial in this situation. It is for this reason that a large number of studies have concentrated on identifying affordable, accessible and acceptable antioxidants. In this connection, we have looked at the properties of some plant extracts (such as those of tea, fruit skins, *withania somnifera* or *ashwagandha, salacia oblonga*) that have been reported to be useful in this regard, as well as their active constituents such as (+) Catechin and epigallocatechin gallate (EGCG) from tea, quercetin from certain fruits skins and withaferin A (from *Withania somnifera*) and have studied their ability to retard oxidative stress and cellular damage, using the human lens epithelial cell line HLE3B as the model.

Salient findings

1. Extracts of *ashwagandha* and *salacia oblonga* were found to have very potent antioxidant properties. However, while *ashwagandha* extract was seen to protect against oxidative stress- induced cell death in HLE3B, *salacia oblonga* extract was found to be cytotoxic.
2. (+) catechin from the tea extract was been found to be protect against oxidative stress- induced damage in HLE3B, whereas epigallocatechin gallate from the same extract, while a good antioxidant, was seen to have a cytotoxic effect on this cell line.
3. Quercetin was also found to offer protection against oxidative stress-induced damage, but the protection offered here is significantly less than that of catechin

4. Withaferin A, the withanolide from *ashwagandha* or *withania somnifera*, while reported to display anti-cancer activity, was not seen to be as effective as an antioxidant as the others studied.

III. Evaluation of the neuroprotective actions of catechin, epigallocatechin gallate and quercetin, by inducing glaucomatous RGC degeneration in rat retinal ganglion cell lines (RGC5) by excitotoxicity and oxidative stress.

From cataract, we now turn to glaucoma. Glaucoma is a form of irreversible blindness, accounting for 12.3% of total global blindness burden, next only to cataract.. An estimated 6.8 million people are bilaterally blind due to glaucoma (Quigley, 1996). The disease is characterized by a slow progressive degeneration of retinal ganglion cells and their axons. Elevated intraocular pressure (IOP) is a major risk factor associated with the disease. The current therapeutic management of glaucoma is aim to halt the disease progression by altering the IOP by several means. However, while lowering the IOP helps in retarding the disease progression, it does not prevent it. Also, IOP is not elevated in all patients exhibiting the characteristics of glaucomatous neurodegenaration. Similar clinical and histopathological findings in patients with normal, as well as with elevated IOP, indicate that there exist IOP-independent mechanisms of neuronal damage in glaucoma. Hence, recent efforts have focused on the understanding of the other possible risk factors and mechanisms involved in glaucomatous degeneration. Some of these are tissue hypoxia, oxidative stress, and glutamate-mediated excitotoxicity. This has resulted in studies aimed at finding neuroprotective agents that might be

of use against glaucoma. It is with this in view that we have studied the neuroprotective abilities of catechin, epigallocatechin gallate and quercetin on glutamate mediated excitotoxicity, as well as oxidative stress- induced cell death in the rat Retinal Ganglion Cell (RGC5) lines.

Salient findings

1. Catechin was seen to offer the maximum neuro-protection to the RGC5 cells against glutamate mediated excitotoxicity induced cell death, as well as against oxidative stress- induced cell death. This neuroprotection offered by catechin is dose dependent. Also, catechin was found not toxic to RGC5 cells, even at concentrations as high as 1 mM.
2. Quercetin does not offer much of the neuro-protection to the RGC5 cell lines treated with oxidative as well as glutamate mediated cell death but it does not show any cytotoxic effects.
3. Epigallocatechin gallate does not offer any neuroprotection to either of these stress conditions; indeed, it was found to be cytotoxic to RGC5 cell lines

REFERENCES

1. Abu-Amero KK., Morales J., Bosley TM. Mitochondrial abnormalities in patients with primary open-angle glaucoma. *Invest Ophthalmol Vis Sci.* 2006;47:2533-2541.
2. Agarwal R., Diwanay S., Patki P., Patwardhan B. Studies on immunomodulatory activity of withania somnifera (Ashwagandha) extracts in experimental immune inflammation. *J Ethnopharmacol.* 1999;67:27-35.
3. Al-Ghoul KJ. Costello MJ. Light microscopic variation of fiber cell size, shape and ordering in the equatorial plane of bovine and human lenses. *Mol Vis.* 1997;3:2.
4. Alizadeh A., Clark, JI., Seeberger T., Hess J., Blankenship T., Spicer A., FitzGerald PG. Targeted genomic deletion of the lens-specific intermediate filament protein CP49. *Invest Ophthalmol Vis Sci.* 2002;43: 3722-3727.
5. Altschul SF., Madden TL., Schaffer AA., Zhang J., Zhang Z., Miller W., and Lipman DJ. Gapped and PSI-BLAST: A new generation of protein database search program. *Nucleic Acids Res.* 1997;25:3389-3402.
6. Andley UP., Song Z., Wawrousek E.F., Bassnett S. The molecular chaperone alphaA-crystallin enhances lens epithelial cell growth and resistance to UVA stress. *J Biol Chem.* 1998;273**:**31252-31261.
7. Andley UP., Song Z., Wawrousek EF., Fleming TP. Bassnett S. Differential protective activity of alphaA- and alphaB-crystallin in lens epithelial cells. *J Biol Chem.* 2000;275:36823-36831.

8. Arai H., Atomi Y. Chaperone activity of alpha B-crystallin suppresses tubulin aggregation through complex formation. *Cell Struct. Funct.* 1997;22:539-544.

9. Arend O., Plange N., Sponsel WE., Remky A. Pathogenetic aspects of the glaucomatous optic neuropathy: fluorescein angiographic findings in patients with primary open angle glaucoma. *Brain Res Bull*. 2004;62:517-522.

10. Asherie N., Pande J., Pande A., Zarutskie J A., Lomakin J., Lomakin A., Ogun O., Stern LJ., King J. Benedek GB. Enhanced crystallization of the Cys18 to Ser mutant of bovine gammaB crystallin. *J Mol Biol.* 2001;314:663-669.

11. Balasubramanian D., Kanwar R. Molecular pathology of dityrosine cross-links in proteins: structural and functional analysis of four proteins. *Mol Cell Biochem.* 2002;234-235(1-2):27-38.

12. Basak A., Bateman O., Slingsby C., Pande A., Asherie N., Ogun O., Benedek GB., Pande J. High-resolution X-ray crystal structures of human gammaD crystallin (1.25 A) and the R58H mutant (1.15 A) associated with aculeiform cataract. *J Mol Biol.* 2003;328:1137-1147.

13. Bassnett S., Winzenburger PA. Morphometric analysis of fibre cell growth in the developing chicken lens. *Exper Eye Res.* 2003;76: 291-302.

14. Bateman A., Birney E., Durbin R., Eddy SR., Howe KL., Sonnhammer E L. The Protein families database. *Nucleic Acids Res.* 2000;32:D138-141.

15. Beebe DC. Vasiliev O. Guo J., Shui YB., Bassnett S. Changes in adhesion complexes define stages in the differentiation of lens fiber cells. *Invest. Ophthalmol Vis Sci.* 2001;42:727-734.

16. Benedek GB. Cataract as a protein condensation disease: the proctor lecture. *Invest Ophthalmol Vis Sci.* 1997; 38:1911-1921.

17. Benedek GB. Theory of transparency of the eye. *Appl Opt.* 1971;10: 459-473.

18. Berbers GA., Hoekman WA., Bloemendal H., de Jong WW., Kleinschmidt T., Braunitzer G. Homology between the primary structures of the major bovine beta-crystallin chains. *Eur J Biochem.* 1984;139:467-479.

19. Bhat SP. Crystallins, genes and cataract. *Prog Drug Res*. 2003;60**:** 205-262.

20. Bhattacharya SK., Satyan KS. and Ghosal S. Antioxidant activity of glycowithanolides from Withania somnifera. *Indian J Exp Biol.* 1997;35: 236-239.

21. Bloemendal H., de Jong W., Jaenicke R., Lubsen NH., Slingsby C., Tardieu A. Ageing and vision: structure, stability and function of lens crystallins. *Prog Biophys Mol Biol.* 2004;86:407-485.

22. Bloemendal H., de Jong WW. Lens proteins and their genes. *Prog Nucleic Acid Res Mol Biol.* 1991;41:259-281.

23. Boelens WC., Croes Y., de Jong WW. Interaction between *α*B-crystallin and the human 20S proteasomal subunit C8/alpha7. *Biochim Biophys Acta,* 2001;1544:311-319.

24. Bonne C., Muller A., Villain M. Free radicals in retinal ischemia. *Gen Pharmacol.* 1998;30:275-280.

25. Brodsky LI., Ivanov VV., Kalai dzidis Ya.L., Leontovich AM., Nikolaev VK., Feranchuk SI., Drachev VA. GeneBee-NET:Internet-based server for analyzing biopolymers structure. *Biochem.* 1995;60(8):923-928.

26. Brodsky LI., Vasiliev AV., Kalaidzidis Ya L., Osipov Yu S., Tatuzov RL., Feranchuk SI. GeneBee: the program package for biopolymer structure analysis. *Dimacs*, 1992;8:127-139.

27. Bron AJ., Vrensen GF., Koretz J., Maraini G., Harding JJ. The ageing lens. *Ophthalmologica.* 2000;214:86-104.

28. Cardamone M., Puri NK. Spectrofluorimetric assessment of the surface hydrophobicity of proteins. *Biochem J.* 1992;282:589-593.

29. Carter JM., Hutcheson AM., Quinlan RA. In vitro studies on the assembly properties of the lens proteins CP49, CP115: coassembly with alpha-crystallin but not with vimentin. *Exp Eye Res.* 1995;60:181-192.

30. Casson RJ. Possible role of excitotoxicity in the pathogenesis of glaucoma. *Clin Exp Ophthalmol.* 2006;34:54-63.

31. Chalfie M., Tu Y., Euskirchen G., ward WW., Prasher DC. Green fluorescent protein as a marker for gene expression. *Science* 1994;263:802-805.

32. Chung HS., Harris A., Evans DW., Kagemann L., Garzozi HJ., Martin B. Vascular aspects in the pathophysiology of glaucomatous optic neuropathy. *Surv Ophthalmol.* 1999;43:S43-50. Suppl 1.

33. Chylack LT Jr., Brown NP, Bron A, Hurst M, Köpcke W, Thien U, Schalch W. The Roche European American Cataract Trial (REACT): a randomized clinical trial to investigate the efficacy of an oral antioxidant

micronutrient mixture to slow progression of age-related cataract. *Ophthalmic Epidemiol.* 2002;9(1):49-80.

34. Cioffi GA. Ischemic model of optic nerve injury. *Trans American Ophthalmol Society,* 2005;103:592-613.

35. Cioffi GA., Wang L. Optic nerve blood flow in glaucoma. *Semin Ophthalmol.* 1999;14:164-170.

36. Clark JI., Muchowski PJ. Small heat-shock proteins and their potential role in human disease. *Curr Opin Struct Biol.* 2000;10:52-59.

37. Cohen AI. The electron microscopy of the normal human lens. *Invest Ophthalmol.* 1965;4:433-446.

38. Cordeiro MF., Guo L., Luong V., Harding G., Wang W., Jones HE., Moss SE., Sillito AM., Fitzke FW. Real-time imaging of single nerve cell apoptosis in retinal neurodegenaration. *Proc Natl Acad Sci*. U S A. 2004;101(36):13352-13356.

39. Cumming RG., Mitchell P. Alcohol, smoking and cataracts: the Blue Mountains Eye Study. *Arch of Ophthalmol*.1997;115:1296-1303.

40. Dandona L., Williams JD., Williams BC., Rao GN. Population based assessment of childhood blindness in Southern India. *Arch Ophthalmol*. 1998;116:545-546.

41. Davis L., Kuttan G. Effect of withania somnifera on cyclophosphamide-induced urotoxicity. *Cancer Lett.* 2000;148:9-17.

42. Davis L., Kuttan G. Effect of withania somnifera on cytokine production in normal and cyclophosphamide treated mice. *Immunopharmacol Immunotoxicol.* 1999;21:695-703.

43. De Feudis FV. *Ginkgo biloba* extract (EGb761): from chemistry to the clinic. Weisbaden, Germany: Ullstein Medical Verlagssgesellschaft mbH & Co. 1998.

44. Delaye M., Tardieu A. Short-range order of crystallin proteins accounts for eye lens transparency. *Nature,* 1983;302:415-417.

45. den Engelsman J., Keijsers V., de Jong WW., Boelens WW. The small heat-shock protein *α*B-crystallin promotes FBX4-dependent ubiquitination. *J Biol Chem.* 2003;278:4699-4704.

46. Derham BK., Harding JJ. Alpha-crystallin as a molecular chaperone. *Prog Retin Eye Res.* 1999;18:463-509.

47. Devi PU, Sharada AC, Solomon FE. In vivo growth inhibitory and radiosensitizing effects of withaferin A on mouse Ehrlich ascites carcinoma. *Cancer Lett.* 1995;95(1-2):189-193.

48. Devi U P., Kamath R. Radiosensitizing effect of withaferin A combined with hyperthermia on mouse fibrosarcoma and melanoma. *J Radiat Res.* (Tokyo). 2003;44(1):1-6.

49. Dhuley JN. Adaptogenic and cardioprotective action of ashwagandha in rats and frogs. *J Ethnopharmacol.* 2000;70:57-63.

50. Dreyer EB., Zurakowski D., Schumer RA., Podos SM., Lipton SA. Elevated glutamate levels in the vitreous body of humans and monkeys with glaucoma. *Arch Ophthalmol.* 1996;114:299-305.

51. Dufresne CJ., Farnworth ER. A review of latest research findings on the health promotion properties of tea. *J Nutri Biochem.* 2001;12(7):404-421.

52. Eddy SR. Profile hidden Markov models. *Bioinformatics* 1998;14:755-763.

53. el-Asrar AM., Morse PH., Maimone D., Torczynski E., Reder AT. MK-801 protects retinal neurons from hypoxia and the toxicity of glutamate and aspartate. *Invest Ophthalmol Vis Sci*. 1992;33:3463-3468.

54. Evans J R. *Ginkgo biloba* extract for age-related macular degeneration. *Cochrane Database Syst Rev.* 2000; 2:CD001775

55. Evans SV. SETOR: Hardware lighted three-dimensional solid model representations of macromolecules. *J. Mol. Graphics* 1993; 11**,** 134-138.

56. Fisher J., Levkovitch-Verbin H., Schori H., Yoles E., Butovsky O., Kaye JF., Ben-Nun A., Schwartz M. Vaccination for neuroprotection in the mouse optic nerve: implications for optic neuropathies. *J Neurosci.* 2001;21,136-142.

57. Flammer J. The vascular concept of glaucoma. *Surv Ophthalmol.* 1994;38 Suppl:S3-6.

58. Flammer J., Orgul S., Costa VP., Orzalesi N., Krieglstein GK., Serra LM., Renard JP., Stefansson E. The impact of ocular blood flow in glaucoma. *Prog Retin Eye Res.* 2002;21:359-393.

59. Forrester JV., Dick AD., McMenamin PG., Lee WR. The Eye : Basic sciences in practice. 2nd ed. Saunders: Elsevier Limited; 2002: p15.

60. Foster A., Gilbert C., Rahi J. Epidemiology of cataract in childhood: a global perspective. *J Cataract Refract Surg.* 1997;23:601-604.

61. Francis PJ., Berry V., Moore AT., Bhattacharya S. Lens biology: development and human cataractogenesis. *Trends Genet.* 1999;5:191-196.

62. Franz GH., Joachim Stephanie C., Hoffmann Esther M., Pfeiffer Norbert. Complex autoantibody repertoires in patients with glaucoma. *Mol Vis.* 2004;10:132-137.

63. Fu L., Liang JJ. Conformational change and destabilization of cataract gammaC-crystallin T5P mutant. *FEBS Lett.* 2002;513:213-216.

64. Fujita Y., Ohto E., Katayama E., Atomi Y. alphaB-crystallin-coated MAP microtubule resists nocodazole and calcium-induced disassembly. *J Cell Sci.* 2004;117:1719-1726.

65. Garcia-Valenzuela E., Shareef S., Walsh J., Sharma SC. Programmed cell death of retinal ganglion cells during experimental glaucoma. *Exp Eye Res.* 1995;61:33-44.

66. Garland D., Russell P., Zigler JS. Jr. in Oxygen Radicals in Biology and Medicine, eds. Simic, M. G., Taylor KA., Ward JF., & von Sonntag C. 1988;pp571-577.

67. Giersing OM. En kataraktos Bondefamilie. Ugeskr Laeger 3 1878; XXVI:273-277, Cited in ref. X chitra and balu.

68. Goldbohm RA., Hertog MG., Brants HA., van Poppel G., van den Brandt PA. Consumption of black tea and cancer risk: a prospective cohort study. *JNCI* 1996;88(2):93-100.

69. Graw J. Cataract mutations and lens development. *Prog Retin Eye Res.* 1999;18:235-267.

70. Graw J., Loster J. Developmental genetics in ophthalmology. *Ophthalmic Genet.* 2003;24:1-33.

71. Gross RL., Hensley SH., Gao F., Wu SM. Retinal ganglion cell dysfunction induced by hypoxia and glutamate: potential

neuroprotective effects of beta-blockers. *Surv Ophthalmol.* 1999;43:S162-170. Suppl 1.

72. Guardia T., Rotelli AE., Juarez AO., Pelzer LE. Anti-inflammatory properties of plant flavonoids. Effects of rutin, quercetin, and hesperidin on adjuvant arthritis in rat. *Farmaco*. 2001;56(9):683-687.
73. Guillemin K., Krasnow MA. The hypoxic response: huffing and HIFing. *Cell,* 1997;89:9-12.
74. Gupta PD., Johar K., Vasavada A. Causative and preventive action of calcium in cataractogenesis. *Acta Pharmacol Sin.* 2004;25(10):1250-1256.
75. Gupta R., Srivastava OP. Effect of deamidation of asparagine 146 on functional and structural properties of human lens alphaB-crystallin. *Invest Ophthalmol Vis Sci.* 2004;45(1):206-214.
76. Hammond CJ., Hammond CJ., Snieder H., Spector TD., Gilbert CE. Genetic and environmental factors in age-related nuclear cataracts in monozygotic and dizygotic twins. *N Engl J Med.* 2000;342:1786-1790.
77. Hamza A., Zhan CG. How can (-)-epigallocatechin gallate from green tea prevent HIV-1 infection? Mechanistic insights from computational modeling and the implication for rational design of anti-HIV-1 entry inhibitors. *J Phys Chem* . 2006;110(6):2910-2917.
78. Hansen MB., Nielsen SE.and Berg K. Re-examination and further development of a precise and rapid dye method for measuring cell growth/cell kill. *J Immunol Methods,* 1989;119:203-210.
79. Harding JJ. Viewing molecular mechanisms of ageing through a lens. *Ageing Research Reviews* 2002;1:465-479.

80. Hayes JD., Strange RC. Potential contribution of the glutathione S-transferase supergene family to resistance to oxidative stress. *Free Radic Res.* 1995;22:193-207.

81. Hayreh SS. Pathogenesis of optic nerve damage and visual field defects. In: Heilman K, Richardson KT., editors. Glaucoma, conceptions of a disease. WB Saunders; Philadelphia: 1978. pp.104-180.

82. Heacock P M. *et al*., Effect of a medical food containing an herbal α-glucosidase inhibitor on postprandial glycemia and insulinemia in healthy adults. *J American dibetic association.* 2005;105(1):65-71.

83. Hejtmancik FJ., Marc Kantorow. Molecular genetics of age-related cataract. *Exp Eye Res.* 2004;79(1):3-9.

84. Hejtmancik JF. The genetics of cataract: Our vision becomes clearer. *Am J Hum* Genet. 1998;62:520-525.

85. Heon E., Priston M., Schorderet DF., Billingsley GD., Girard PO., Lubsen N., Munier FL. The gamma-crystallins and human cataracts: a puzzle made clearer. *Am J Hum Genet.* 1999;65:1261-1267.

86. Herbrink P., van Westreenen H., Bloemendal H. Further studies on the polypeptide chains of beta-crystallin. *Exp Eye Res.* 1975;20:541-548.

87. Hope JN., Chen HC., Hejtmancik JF. Aggregation of βA3-crystallin is independent of the specific sequence of the domain connecting peptide. *J Biol Chem.* 1994;269:21141-21145.

88. Horwitz J. Alpha-crystallin can function as a molecular chaperone. *Proc Natl Acad Sci. USA,* 1992;89:10449-10453.

89. http://catalog.nucleusinc.com /displaymonograph.php?MID=42

90. Hung L., Estrada R., Yappert MC., Borchman D. oxidation-induced changes in human lens epithelial cells. *Free Radic Biol Med.* 2006;41:1425-1432.

91. Inouye S., Tsuji FI. Evidence for redox forms of the Aequorea green fluorescent protein. *FEBS Lett.* 1994;341:277-280.

92. Iyer NV., Kotch LE., Agani F., Leung SW., Laughner E., Wenger RH., Gassmann M., Gearhart JD., Lawler AM., Yu AY., Semenza GL. Cellular and developmental control of O_2 homeostasis by hypoxia-inducible factor 1 alpha. *Genes Dev.* 1998;12:149-162.

93. Jobby MK., Sharma Y. Calcium-binding to lens betaB2- and betaA3-crystallins suggests that all beta-crystallins are calcium-binding proteins. *FEBS J.* 2007;274(16):4135-4147.

94. John SWM. Mechanistic Insights into Glaucoma Provided by Experimental Genetics. *Invest Ophthalmol Vis Sci.* 2005;46:2650-2661.

95. Katiyar S., Elmets CA., Katiyar SK. "Green tea and skin cancer: photoimmunology, angiogenesis and DNA repair". *J Nutr Biochem.* 2007; 18(5):287-296.

96. Kelly LA., Maccallum R., Sternberg MJE. Recognition of remote homologies using three-dimensional information to generate a position-specific scoring matrix in the program 3D-PSSM. RECOMB 99. *Proceedings of the Third Annual Conference on Computational Molecular Biology*, 1999;218-225.

97. Kermer P., Ankerhold R., Klocker N., Krajewski S., Reed JC., Bahr M. Caspase-9: involvement in secondary death of axotomized rat retinal ganglion cells in vivo. *Brain Res Mol Brain Res.* 2000;85:144-150.

98. Kerrigan LA., Zack DJ., Quigley HA., Smith SD., Pease ME. TUNEL-positive ganglion cells in human primary open-angle glaucoma. *Arch Ophthalmol.* 1997;115:1031-1035.

99. Khaw PT., Shah P., Elkington AR. Glaucoma-1: Diagnosis. *B Med J.* 2004;328:97-99.

100. Kim KK., Kim R., Kim SH. Crystal structure of a small heat-shock protein. *Nature,* 1998;394:595-599.

101. Kim TW., Kim DM., Park KH., Kim H. Neuroprotective effect of memantine in a rabbit model of optic nerve ischemia. *Korean J Ophthalmol.* 2002;16:1-7.

102. Kitano S., Morgan J., Caprioli J. Hypoxic and excitotoxic damage to cultured rat retinal ganglion cells. *Exp Eye Res.* 1996;63:105-112.

103. Kmoch S., Brynda J., Asfaw B., Bezouska K., Novak P., Rezacova P., Ondrova L., Filipec M., Sedlacek J., Elleder M. Link between a novel human gammaD-crystallin allele and a unique cataract phenotype explained by protein crystallography. *Hum Mol Genet.* 2000;9:1779-1786.

104. Ko ML., Hu DN., Ritch R., Sharma SC. The combined effect of brain-derived neurotrophic factor and a free radical scavenger in experimental glaucoma. *Invest Ophthalmol Vis Sci.* 2000;41:2967-2971.

105. Kosinski-Collins MS., King J. In vitro unfolding, refolding, and polymerization of human gamma D crystallin, a protein involved in cataract formation. *Protein Sci.* 2003;12(3):480-490.

106. Krishnaiah S., Vilas K., Shamanna BR., Rao GN., Thomas R., Balasubramanian D. Smoking and its association with cataract: results

of the Andhra Pradesh eye disease study from India. *Invest Ophthalmol Vis Sci.* 2005;46(1): 58-65.

107. Kundu B., Shukla A., Guptasarma P. Peptide scanning-based identification of regions of gamma-II crystallin involved in thermal aggregation: evidence of the involvement of structurally analogous, helix-containing loops from the two double Greek key domains of the molecule. *Arch Biochem Biophys.* 2003;410:69-75.

108. Kupfer C. The conquest of cataract: a global challenge. *Trans Ophthalmol Soc.* UK 1984;104: 1-10.

109. Kurup PA. The antibacterial principle of Withania somnifera. I. Isolation and antibacterial activity. *Antibiotics and Chemotherapy,* 1958;8:511-515.

110. Kuszak JR., Rae JL. Scanning electron microscopy of the frog lens. *Exper Eye Res.* 1982;35:499-519.

111. Kuszak JR., Macsai MS., Bloom KJ., Rae JL., Weinstein RS. Cell-to-cell fusion of lens fiber cells in situ: correlative light,scanning electron microscopic, and freeze-fracture studies. *J Ultrastruct Res.* 1985;93:144-160.

112. Kuszak JR., Peterson KL.,Brown HG. Electron microscopic observations of the crystalline lens. *Microsc Res Tech*. 1996;33:441-479.

113. Lam TT., Abler AS., Kwong JM., Tso MO. N-methyl-D-aspartate (NMDA)--induced apoptosis in rat retina. *Invest Ophthalmol Vis Sci.* 1999;40:2391-2397.

114. Lam TT., Kwong JM., Tso MO. Early glial responses after acute elevated intraocular pressure in rats. *Invest Ophthalmol Vis Sci.* 2003;44:638-645.

115. Lam TT., Siew E., Chu R., Tso MO. Ameliorative effect of MK-801 on retinal ischemia. *J Ocul Pharmacol Ther*. 1997;13:129-137.

116. Lambert SR., Drack AV. Infantile cataracts. *Surv Ophthalmol*. 1996;40:427-458.

117. Lampi KJ., Ma Z., Shih M., Shearer TR., Smith JB., Smith DL., David LL. Sequence analysis of betaA3, betaB3, and betaA4 crystallins completes the identification of the major proteins in young human lens. *J Biol Chem.* 1997;272:2268-2275.

118. Lamson DW., Brignall MS. Antioxidants and cancer III: quercetin. *Alt Med Rev.* 2000;5(3):196-208.

119. Lapatto R., Nalini V., Bax B., Driessen H., Lindley PF., Blundell TL., Slingsby C. High resolution structure of an oligomeric eye lens beta-crystallin. Loops, arches, linkers and interfaces in beta B2 dimer compared to a monomeric gamma-crystallin. *J Mol Biol.* 1991;222:1067-1083.

120. Lebuisson DA., Leroy L., Rigal G. Treatment of senile macular degeneration with *Ginkgo biloba* extract. Preliminary double-blind drug *vs* placebo study. *Press Med.* 1986;15:1556-1558.

121. Levkovitch-Verbin H., Quigley HA., Kerrigan-Baumrind LA., D'Anna SA., Kerrigan D., Pease ME. Optic nerve transection in monkeys may result in secondary degeneration of retinal ganglion cells. *Invest Ophthalmol Vis Sci.* 2001;42:975-982.

122. Li Y., Schlamp CL., Nickells RW. Experimental induction of retinal ganglion cell death in adult mice. *Invest Ophthalmol Vis Sci.* 1999;40:1004-1008.

123. Liang JN. Interactions and chaperone function of αA-crystallin with T5P γC-crystallin mutant. *Protein Sci.* 2004;3:2476-2482.

124. Libby RT., Gould DB., Anderson MG., John SW. Complex genetics of glaucoma susceptibility. *Annu Rev Genomics Hum Genet.* 2005;6:15-44. Review.

125. Libby RT., Li Y., Savinova OV., Barter J., Smith RS., Nickells RW., John SW. Susceptibility to neurodegeneration in glaucoma is modified by Bax gene dosage. *PLoS Genet*. 2005;1(1):17-26.

126. Lindley PF., Najmuddin S., Bateman O., *et al.* Structure of the bovine gamma-B crystallin at 150K. *J Chem Soc., Faraday Trans*. 1993;89: 2677.

127. Lipton SA. Possible role for memantine in protecting retinal ganglion cells from glaucomatous damage. *Surv Ophthalmol.* 2003;48:S38-46. (Suppl. 1).

128. Loster J., Pretsch W., Sandulache R., Schmitt-John T., Lyon MF., Graw J. Close linkage of the dominant cataract mutations (Cat-2) with Idh-1 and cryge on mouse chromosome 1. *Genomics*, 1994;23:240-242.

129. Lucas DR., Newhouse JP. The toxic effect of sodium L-glutamate on the inner layers of the retina. *AMA Arch Ophthalmol.* 1957;58(2):193-201.

130. Lund AM, Eiberg H, Rosenberg T, Warburg M. Autosomal dominant congenital cataract; linkage relations; clinical and genetic heterogeneity. *Clin Genet.* 1992;41(2): 65-69.

131. Maher P., Hanneken A. The molecular basis of oxidative stress-induced cell death in an immortalized retinal ganglion cell line. *Invest Ophthalmol Vis Sci.* 2005;46(2):749-757.

132. Maisel H., Perry MM. Electron microscope observations on some structural proteins of the chick lens. *Exp Eye Res.* 1972;14:7-12.

133. Mandal K., Kono M., Bose SK., Thomson J., Chakrabarti B. Structure and stability of gamma-crystallins--IV. Aggregation and structural destabilization in photosensitized reactions. *Photochem Photobiol.* 1988;47:583-591.

134. Marner E., Rosenberg T., Eiberg H. Autosomal dominant congenital cataract: morphology and genetic mapping. *Acta Ophthalmol*. 1989;67:151-158.

135. Marner EA. family with eight generations of hereditary cataract. *Acta Ophthalmol.* 1949;27:537-551.

136. Matsuda H., Murakami T., Yashiro K., Yamahara J., Yoshikawa M. Antidiabetic principles of natural medicines. IV. Aldose reductase and qlpha-glucosidase inhibitors from the roots of Salacia oblonga Wall. (Celastraceae): structure of a new friedelane-type triterpene, kotalagenin 16-acetate. *Chem Pharm Bull* (Tokyo). 1999;47(12):1725-1729.

137. McCarty CA. The importance of epidemiology in the effort of reducing world blindness due to cataract. *Ophthal Res.* 2003;35(S1):264.

138. McCarty CA., Nanjan BM., Taylor HR. Attributable risk estimates for cataract to prioritize medical and public health action. *Invest Ophthalmol Vis Sci*. 2000;41:3720-3725.

139. McCay PB. Vitamin E: interactions with free radicals and ascorbate. *Ann Rev Nutr*.1985;5:323-340.

140. Miller NJ., Rice-Evans C., Davies MJ., Gopinathan V. and Milner A. A novel method for measuring antioxidative capacity and its application to monitoring the antioxidant status in premature neonates. *Clin Sci. (Colch.)* 1993;84:407-412.

141. Mishra LC., Singh BB., Dagenais S. Scientific basis for the therapeutic use of Withania somnifera (ashwagandha): a review. *Altern Med Rev.* 2000;5:334-346.

142. Mittag TW., Danias J., Pohorenec G., Yuan HM., Burakgazi E., Chalmers-Redman R., Podos SM., Tatton WG. Retinal damage after 3 to 4 months of elevated intraocular pressure in a rat glaucoma model. *Invest Ophthalmol Vis Sci.* 2000;41:3451-3459.

143. Mizuguchi K., Deane CM., Blundell TL., Johnson MS., Overington JP. JOY: protein sequence-structure representation and analysis. *Bioinformatics,* 1998;14:617-623.

144. Mohan R., Hammers HJ., Bargagna-Mohan P., Zhan XH., Herbstritt CJ., Ruiz A., Zhang L., Hanson AD., Conner BP., Rougas J., Pribluda VS. Withaferin A is a potent inhibitor of angiogenesis. *Angiogenesis.* 2004;7(2):115-122.

145. Morimoto RI., Santoro MG. Stress-inducible responses and heat shock proteins: new pharmacologic targets for cytoprotection. *Nat Biotechnol.* 1998;16:833-838.

146. Muller A., Pietri S., Villain M., Frejaville C., Bonne C., Culcas M. Free radicals in rabbit retina under ocular hyperpressure and functional consequences. *Exp Eye Res.* 1997;64:637-643.

147. Murali Krishna C., Uppuluri S., Riesz P., Zigler JS., Jr, Balasubramanian D. A study of the photodynamic efficiencies of some eye lens constituents. *Photochem Photobiol.* 1991;54:51-58.

148. Naskar R., Wissing M., Thanos S. Detection of early neuron degeneration and accompanying microglial responses in the retina of a rat model of glaucoma. *Invest Ophthalmol Vis Sci.* 2002;43:2962-2968.

149. Nicolls A., Sharp KA., Honig B. Protein Folding and Association: Insights from the interfacial and thermodynamic properties of Hydrocarbons. *Proteins Struc Func Genet.* 1991;11:281-296.

150. Olney JW. Brain lesions, obesity, and other disturbances in mice treated with monosodium glutamate. *Science,* 1969; 164:719-721.

151. Osborne NN. Ganglion cell death in glaucoma: what do we really know?. *Br J Ophthalmol.* 1999;83:980-986.

152. Osborne NN., Casson RJ., Wood JP., Chidlow G., Graham M., Melena J. Retinal ischemia: mechanisms of damage and potential therapeutic strategies. *Prog Retin Eye Res.* 2004;23:91-147.

153. Paliwal S., Sundaram J., Mitragotri S. "Induction of cancer-specific cytotoxicity towards human prostate and skin cells using quercetin and ultrasound". *Br J Canc.* 2005;92 (3):499-502.

154. Panda S., Kar A. Evidence for free-radical scavenging activity of Ashwagandha root powder in mice. *Indian J Physiol Pharmacol*. 1997;41: 424-426.

155. Pande A., Annunziata O., Asherie N., Ogun O., Benedek GB., Pande J. Decrease in protein solubility and cataract formation caused by the Pro23 to Thr mutation in human gamma D-crystallin. *Biochemistry* 2005;44:2491-2500.

156. Pande A., Pande J., Asherie N., Lomakin A., Ogun O., King J., Benedek GB. Crystal cataracts: human genetic cataract caused by protein crystallization. *Proc Natl Acad Sci.,* USA. 2001;98:6116-6120.

157. Pande A., Pande J., Asherie N., Lomakin A., Ogun O., King JA., Lubsen NH., Walton D., Benedek GB. Molecular basis of a progressive juvenile-onset hereditary cataract. *Proc Natl Acad Sci.,* USA. 2000;97:993-1998.

158. Patil C., Walter P. Intracellular signaling from the endoplasmic reticulum to the nucleus: the unfolded protein response in yeast and mammals. *Curr Opin Cell Biol.* 2001;13:349-355.

159. Pigaga V., Quinlan RA. Lenticular chaperones suppress the aggregation of the cataract-causing mutant T5P gamma C-crystallin. *Exp Cell Res*. 2006;312(1):51-62.

160. Plenum Press, New York; Berman ER. Biochemistry of the Eye. *New York: Plenum Press*, 1991;210-308.

161. Prasher DC., Eckenvode VK., Ward WW., Prendergast FG., Cormier MJ. Primary structure of the Aequorea Victoria green-fluorescent protein. *Gene,* 1992;111:229–233.

162. Quigley HA. Number of people with glaucoma worldwide. *Br J Ophthalmol.* 1996;80(5):389-393. Review.

163. Quigley HA., McKinnon SJ., Zack DJ. *et al.* Retrograde axonal transport of BDNF in retinal ganglion cells is blocked by acute IOP elevation in rats. *Invest Ophthalmol Vis Sci.* 2000;41:3460-3466.

164. Quigley HA., Nickells RW., Kerrigan LA., Pease ME., Thibault DJ., Zack DJ. Retinal ganglion cell death in experimental glaucoma and after axotomy occurs by apoptosis. *Invest Ophthalmol Vis Sci.* 1995;36:774-786.

165. Rae JL., Truitt KD., Kuszak JR. A simple fluorescence technique for light microscopy of the crystalline lens. *Curr Eye Res.* 1982;2:1-5.

166. Rae JL., Truitt KD., Kuszak JR. The use of procion dyes for light microscopy of the frog lens. *Invest Ophthal Vis Sci.* 1983;24:1167-1171.

167. Rajini B., Shridas P., Sundari CS., Muralidhar D., Chandani S., Thomas F., Sharma Y. Calcium binding properties of gamma-crystallin: calcium ion binds at the Greek key beta gamma-crystallin fold. *J Biol Chem.* 2001;276(42):38464-38471.

168. Raman B., Rao CM. Chaperone-like activity and quaternary structure of alpha crystalline. *J Biol Chem.* 1994;269:27264-27268.

169. Ren Z., Li A., Shastry BS., Padma T., Ayyagari R., Scott MH., Parks M M., Kaiser-Kupfer MI., Hejtmancik JF. A 5-base insertion in the γC-crystallin gene is associated with autosomal dominant variable zonular pulverulent cataract. *Hum Genet.* 2000;106:531-537.

170. Renwick JH., Laweler SD. Probable linkage between a congenital cataract locus and the duffy blood group locus. *Ann Hum Genet.* 1963;27:67-84.

171. Resnikoff S., Pascolini D., Etya'ale D., Kocur I., Pararajasegaram R., Pokharel GP., Mariotti SP. Global data on visual impairment in the year 2002. *Bull World Health Organ.* 2004;82(11):844-851.

172. Rhee DJ., Katz LJ., Spaeth GL., Myers JS. Complementary and alternative medicine for glaucoma. Surv Ophthalmol. 2001;46:43-55.

173. Rosenbaum DM., Rosenbaum PS., Gupta A., Michaelson MD., Hall DH., Kessler JA. Retinal ischemia leads to apoptosis which is ameliorated by aurintricarboxylic acid. *Vision Res.* 1997;37:3445-3451.

174. Rudzinski M., Saragovi HU. Glaucoma: Validated and Facile In Vivo Experimental Models of a Chronic Neurodegenerative Disease for Drug Development. *Curr Med Chem Central Nervous System Agents*, 2005;5:43-49.

175. Russo A., Izzo AA, Cardile V, Borrelli F, Vanella A. Indian medicinal plants as antiradicals and DNA cleavage protectors. *Phytomedicine* 2001;8(2):125-132.

176. Sali A., Blundell TL. Comparative protein modeling by satisfaction of spatial constraints. *J Mol Biol.* 1993;339:1103-1113.

177. Sangwan RS., Chaurasiya ND., Misra LN., Lal P., Uniyal GC., Sharma R., Sangwan NS., Suri KA., Qazi GN., Tuli R. Phytochemical variability in commercial herbal products and preparations of *Withania somnifera* (Ashwagandha). *Curr Sci.* 2004;86:461-465.

178. Santhiya ST., Shyam Manohar M., Rawlley D., Vijayalakshmi P., Namperumalsamy P., Gopinath PM., Loster J., Graw J. Novel mutations in the γ-crystallin genes cause autosomal dominant congenital cataracts. *J Med Genet.* 2002;39:352-358.

179. Schwartz M., Yoles E. Optic nerve degeneration and potential neuroprotection: implications for glaucoma. *Eur J Ophthalmol.* 1999;9:S9-11 (Suppl 1).

180. Semenza GL. Perspectives on oxygen sensing. *Cell,* 1999;98:281-284.

181. Shi J., Blundell TL., Mizuguchi K. FUGUE: Sequence-structure homology recognition using environment-specific substitution tables and structure-dependent gap penalties. *J Mol Biol.* 2001;310:243-257.

182. Shields MB., Allingham RR., Damji K., Freedman S., Moroi S., Shafranov G. Textbook of glaucoma. 5th ed. Philadelphia, PA.Lippincott Williams & Wilkins; 2005.

183. Singh S., Kumar S. Withania somnifera: The Indian Ginseng Ashwagandha. Central Institute of Medicinal and Aromatic Plants, P. O. CIMAP, Lucknow 226015, India 1998.

184. Sinha D., Esumi N., Jaworski C., Kozak CA., Pierce E., Wistow G. Cloning and mapping of the mouse Crygc gene and non-lens expression of γS-crystallin. *Mol Vis.* 1998;4:8.

185. Sinha D., Wyatt MK., Sarra R., Jaworski C., Slingsby C., Thaung C., Pannell L., Robison WG., Favor J., Lyon M., Wistow G. A temperature-sensitive mutation of Crygs in the murine Opj cataract. *J Biol Chem.* 2001;276(12):9308-9315.

186. Smelser GK. Embryology and morphology of the lens. In Symposium on the lens (Harris JE, ed), 1965;pp 22-34. Saint Louis: C.V. Mosby Co.

187. Sonna LA., Fujita J., Gaffin SL., Lilly CM. Invited review: effects of heat and cold stress on mammalian gene expression. *J Appl Physiol.* 2002;92:1725-1742.

188. Spector A. oxidative stress-induced cataract: mechanism of action. *FASEB J*. 1995;9:1173-1182.

189. Srivastava OP., Srivastava K. Existence of deamidated alphaB-crystallin fragments in normal and cataractous human lenses. *Mol Vis.* 2003;9:110-118.

190. Stadtman ER., Berlett BS. Reactive oxygen-mediated protein oxidation in aging and disease. *Drug Metab Rev.* 1998;30(2):225-243. Review.

191. Stephan DA., Gillanders E., Vanderveen D., Freas-Lutz D., Wistow G., Baxevanis AD., Robbins CM., VanAuken A., Quesenberry MI., Bailey-Wilson J., Juo SH., Trent JM., Smith L., Brownstein MJ. Progressive juvenile-onset punctate cataracts caused by mutation of the gammaD-crystallin gene. *Proc Natl Acad Sci.,* USA. 1999;96:1008-1012.

192. Sun TX., Das BK., Liang JJ. Conformational and functional differences between recombinant human lens alphaA- and alphaB-crystallin. *J Biol Chem.* 1997;272:6220-6225.

193. Tatton WG., Chalmers-Redman RM., Sud A., Podos SM., Mittag TW. Maintaining mitochondrial membrane impermeability. an opportunity for new therapy in glaucoma?. *Surv Ophthalmol.* 2001;45:S277-283. Suppl 3 discussuin S295-276.

194. Tezel G. Oxidative stress in glaucomatous neurodegeneration: mechanisms and consequences. *Prog Retin Eye Res.* 2006;25(5):490-513.

195. Tezel G., Li LY., Patil RV., Wax MB. Tumor necrosis factor-alpha and its receptor-1 in the retina of normal and glaucomatous eyes. *Invest Ophthalmol Vis Sci.* 2001a;42:1787-1794.

196. Tezel G., Li LY., Patil RV., Wax MB. Tumor necrosis factor-alpha and its receptor-1 in the retina of normal and glaucomatous eyes. *Invest Ophthalmol Vis Sci.* 2001b;42:1787-1794.

197. Tezel G., Wax MB. Increased production of tumor necrosis factor-alpha by glial cells exposed to simulated ischemia or elevated hydrostatic pressure induces apoptosis in cocultured retinal ganglion cells. *J Neurosci.* 2000;20:8693-8700.

198. Tezel G., Wax MB. Inhibition of caspase activity in retinal cell apoptosis induced by various stimuli in vitro. *Invest Ophthalmol Vis Sci.* 1999;40:2660-2667.

199. Tezel G., Yang X. Caspase-independent component of retinal ganglion cell death, in vitro. *Invest Ophthalmol Vis Sci.* 2004;45:4049-4059.

200. Thampi P., Zarina S., Abraham EC. alpha-Crystallin chaperone function in diabetic rat and human lenses. *Mol Cell Biochem.* 2002;229(1-2):113-118.

201. Thiagarajan G., Chandani S., Rao SH., Samuni AM., Chandrasekaran K., Balasubramanian D. Molecular and cellular assessment of *ginkgo biloba* extract as a possible ophthalmic drug. *Exp Eye Res.* 2002;75(4):421-430.

202. Thiagarajan G., Chandani S., Sundari CS., Rao SH., Kulkarni AV., Balasubramanian D. Antioxidant properties of green and black tea, and their potential ability to retard the progression of eye lens cataract. *Exp Eye Res.* 2001;73(3):393-401.

203. Thiagarajan G., Venu T., Balasubramanian D. Approaches to relieve the burden of cataract blindness through natural antioxidants: use of Ashwagandha (Withania somnifera). *Curr Sci.* 2003;85:1065-1071.

204. Tomarev SI. Eyeing a new route along an old pathway. *Nat Med.* 2001;7(3):294-295.

205. Trokel S. The physical basis for transparency of the crystalline lens. *Invest Ophthalmol.* 1962;1:493-501.

206. van den Ijssel P., Norman DG., Quinlan RA. Molecular chaperones: small heat shock proteins in the limelight. *Curr Biol.* 1999;9:R103-105.

207. van Montfort RL., Basha E., Friedrich K.L., Slingsby C., Vierling E. Crystal structure and assembly of a eukaryotic small heat shock protein. *Nat Struct Biol.* 2001;8:1025-1030.

208. Varma SD., Chand D., Sharma YR., Kuck JF. Jr. & Richards RD., *Curr Eye Res*. 1984;3:35-37.

209. Veretout F., Delaye M., Tardieu A. Molecular basis of eye lens transparency. Osmotic pressure and X-ray analysis of alpha-crystallin solutions. *J Mol Biol.* 1989;205:713-728.

210. Vorwerk CK., Gorla MS., Dreyer EB. An experimental basis for implicating excitotoxicity in glaucomatous optic neuropathy. *Surv Ophthalmol.* 1999;43:S142-50.

211. Wang GL., Jiang BH., Rue EA., Semenza GL. Hypoxia-inducible factor 1 is a basic-helix-loop-helix-PAS heterodimer regulated by cellular O2 tension. *Proc Natl Acad Sci.* U S A. 1995;92:5510-5514.

212. Wang K., Cheng C., Li L., *et al.* γD-crystallin-associated protein aggregation and lens fiber cell denucleation. *Invest Ophthalmol Vis Sci*. 2007;48:3719-3728.

213. Wang X., Garcia CM., Shui Y-B., Beebe DC. Expression and regulation of α-, β- and γ-crystallins in mammalian lens epithelial cells. *Invest Ophthalmol Vis Sci*. 2004;45:3608-3619.

214. Wax MB., Tezel G., Edward PD. Clinical and ocular histopathological findings in a patient with normal-pressure glaucoma [see comments]. *Arch Ophthalmol.* 1998;116:993-1001.

215. Weber M., Bonaventure N., Sahel JA. Protective role of excitatory amino acid antagonists in experimental retinal ischemia. *Graefes Arch Clin Exp Ophthalmol*. 1995;233:360-365.

216. Weiner SJ., Kollmann PA., Case DA., Singh UC., Ghio C., Alagona G., Profeta SJ., Weiner PA new forcefield for molecular mechanical simulations of nucleic acids and proteins. *J Am Chem Soc.* 1984;106:765-784.

217. Wistow G., Slingsby C., Blundell T., Driessen H., de Jong W., Bloemendal H. Eye-lens proteins: the three-dimensional structure of beta-crystallin predicted from monomeric gamma-crystallin. *FEBS Lett.* 1981;133:9-16.

218. Xi JH., Bai F., Andley UP. Reduced survival of lens epithelial cells in the alphaA-crystallin-knockout mouse. *J Cell Sci.* 2003;116:1073-1085.

219. Yan X., Tezel G., Wax MB., Edward DP. Matrix metalloproteinases and tumor necrosis factor alpha in glaucomatous optic nerve head. *Arch Ophthalmol.* 2000;118:666-673.

220. Yang J., Tezel G., Patil RV., Romano C., Wax MB. Serum autoantibody against glutathione S-transferase in patients with glaucoma. *Invest Ophthalmol Vis Sci.* 2001;42:1273-1276.

221. Yoles E., Schwartz M. Degeneration of spared axons following partial white matter lesion: implications for optic nerve neuropathies. *Exp Neurol.* 1998a;153:1-7.

222. Yoles E., Schwartz M. Elevation of intraocular glutamate levels in rats with partial lesion of the optic nerve. *Arch Ophthalmol.* 1998c;116:906-910.

223. Yoles E., Schwartz M. Degeneration of spared axons following partial white matter lesion: implications for optic nerve neuropathies. *Exp Neurol.* 1998b; 153:1-7.

224. Yoles E., Schwartz M. Potential neuroprotective therapy for glaucomatous optic neuropathy. *Surv Ophthalmol.* 1998b;42(4):367-72.

225. Yuan L., Neufeld AH. Tumor necrosis factor-alpha: A potentially neurodestructive cytokine produced by glia in the human glaucomatous optic nerve head. *Glia.* 2000;32:42-50.

226. Zhang L., Liu P. A novel nonsense mutation in *cry*g*c* associated with autosomal dominant congenital nuclear cataract and Microcornea. *Invest Ophthalmol Vis Sci.* 2007;48: e-abstract 2443.

227. Zigman S., Datiles M., Torczynski E. Sunlight and human cataracts. *Invest Ophthalmol Vis Sci.* 1979;18:462-467.

LIST OF PUBLICATIONS

1. Geetha Thiagarajan, **Talla Venu** and Dorairajan Balasubramanian. Approaches to relieve the burden of cataract blindness through natural antioxidants: use of Ashwagandha (*Withania somnifera*) *Curr.sci.* 2003;85 (7):1065-71.
2. **Talla Venu** and D. Balasubramanian. Phytochemical variability. *Curr Sci.* 2004;86(8):1054-1054.
3. **T. Venu** and D. Balasubramanian. Cataract as a Protein Disease. In Protein Structure-Function Relationship. Atiya Abbasi, Syed Abid Ali eds., 2005 pp. 245-259.
4. **Venu Talla**, Chitra Narayanan, Narayanaswamy Srinivasan and Dorairajan Balasubramanian. Mutation causing self-aggregation in human γC-crystallin leads to congenital cataract. *Invest Ophthalmol Vis Sci*. 2006;47(12):5212-5217.
5. **Venu Talla** and Dorairajan Balasubramanian. Cataract: A Protein-folding Disease in the Eye. In Protein Structure-Function Relationship. Atiya Abbasi, Syed Abid Ali eds., (in press).
6. **Venu Talla**, Narayanaswamy Srinivasan and Dorairajan Balasubramanian. Visualization of *in situ* intracellular aggregation of two cataract-associated human γ-Crystallin mutants: lose a tail, lose transparency. (accepted in *Invest. Ophthalmol. Vis. Sci.* 2008).
7. **Venu Talla** and Dorairajan Balasubramanian. Neuroprotective Activity of Catechin and its Relevance to Glaucoma Treatment (Manuscript under preparation).

LIST OF PRESENTATIONS

1. Presented a poster entitled "Neuroprotective Activity of Catechin - Relevance to Glaucoma Treatment" at the 76th annual meeting of **Society for Biological Chemists India (SBCI)**, held at the Sri Venkateswara University, Tirupati, India, during 25-27th Nov, 2007.
3. Presented a poster entitled *"Reduced protein solubility caused by W156X mutation in human γd-crystallin is associated with cataract."* at the 75th annual meeting of **Society for Biological Chemists India (SBCI)**, held at the Jawaharlal Nehru University, New Delhi, India, during 7-11th Dec, 2006.
4. Presented a poster entitled *"Mutation Leading to Quaternary Structural Change in Human c-Crystallin Causes Congenital Cataract"* at the 21st congress of the **Asia-Pacific Academy of Ophthalmology (APAO-2006)** held at Singapore, during 10-14th June 2006.
5. Presented a poster entitled *"Molecular Structural Phenotyping of γ-Crystallins Involved in Autosomal Dominant Congenital Cataract"* at the 74th annual meeting of **Society for Biological Chemists India (SBCI)**, held at the Central Drug Research Institute, Lucknow, India, during 7-10th Nov, 2005.
6. Presented a paper entitled *"Structural Characterization of the Mutant Protein, (R168w) C-crystallin, Associated With Autosomal Dominant Congenital Lamellar Cataract"* in the 14th Annual meeting of the **Indian Eye Research Group (IERG),** held at the LV Prasad Eye Institute, Hyderabad on 30-31st July 2005.

7. Presented a poster entitled *"Structural Characterization of Mutant C-Crystallins: Role in Autosomal Dominant Congenital Lamellar Cataract"* at the 73rd annual meeting of **Society for Biological Chemists India (SBCI)**, held at the GB Pant Agricultural University, Pantnagar, India, during 17-20th Nov, 2004.
8. Presented a poster entitled *"Antioxidant Properties of Withania Somnifera (Ashwagandha) and its Ability to Retard the Progression of Cataract"* at the 10th **Asian and Oceanian Biochemists and Molecular Biologists (FAOBMB) Congress**, held at the Indian Institute of Science, Bangalore, India, during 7-11th Dec 2003.
9. Participated in a workshop on *"Internet Applications in Biological Research"* at Bioinformatics Center, Indian Institute of Spices Research (IISR) Calicut, Kerala from 16th Jan'2002 to 18th Jan'2002.

AWARDS AND FELLOWSHIPS

1. Won a **Best Poster award** in 75th annual meeting of Society for Biological Chemists India (SBCI), held at the Jawaharlal Nehru University, New Delhi, India, during 8-11th Dec, 2006.
2. Won a **Best Poster award** in Structural Biology category in 74th annual meeting of Society for Biological Chemists India (SBCI), held at the Central Drug Research Institute, Lucknow, India, during 7-11th Nov, 2005.
3. Awarded a **Senior Research Fellowship** for the period of 2004-2007 by the Council of Scientific and Industrial Research (CSIR), INDIA.
4. Awarded a **Junior Research Fellowship** for the period of 2002-2004 by Council of Scientific and Industrial Research (CSIR), INDIA.

5. Qualified for **GATE-2002 Fellowship.**
6. Awarded the **Meritorious Fellowship** from **Department of Biotechnology**, Govt. Of India for the years 2000 -2002 for the masters degree.